Mass spectrometric methods for characterization of protein aggregation and antigen recognition structures

Dissertation submitted for the degree of
Doctor of Natural Sciences

Presented by
Iurașcu, Marius Ionuț
at the

Universität
Konstanz

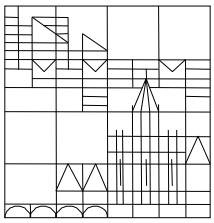

Faculty of Mathematics and Natural Sciences
Department of Chemistry

Date of the oral examination: November 10th 2015
First referee: Prof. Dr. Dr. h. c. Michael Przybylski
Second referee: Prof. Dr. Malte Drescher

Acknowledgements

The present work has been performed between January 2008 and March 2013 in the Laboratory of Analytical Chemistry and Biopolymer Structure Analysis, Department of Chemistry at the University of Konstanz, under the supervision of Prof. Dr. Dr. h. c. Michael Przybylsk

I would like to thank to:

Prof. Dr. Dr. h.c. Michael Przybylski for offering me the opportunity to perform my PhD work in his laboratory, for his guidance and kind advice throughout the years;

Dr. Malte Drescher for helping me to understand the secrets of electron paramagnetic resonance and for writing the second review of this thesis;

Prof. Dr. Michael Gross and Dr. Henry Rohrs (Washington University, Saint Louis) and Prof. Dr. Alina Zamfir (Aurel Vlaicu University, Arad, Romania) for their hospitality and the experience gained in their laboratories;

All members of the group for their help, advice and inspiring atmosphere.

This dissertation has been published in part, and presented at the following conferences:

Publications

1. **Iurascu, M.I.**, C. Cozma, N. Tomczyk, J. Rontree, M. Desor, M. Drescher and M. Przybylski, *Structural characterization of beta-amyloid oligomer-aggregates by ion mobility mass spectrometry and electron spin resonance spectroscopy.* Anal Bioanal Chem, 2009. **395**(8): p. 2509-19.

2. **Iurascu, M.I**., C. Cozma, J. Langridge, N. Tomczyk, M. Desor and M. Przybylski, *Structural Characterization of Oligomer-Aggregates of β-Amyloid Polypeptide Using Ion Mobility Mass Spectrometry*, in *Ion Mobility Spectrometry - Mass Spectrometry*. 2010, CRC Press. p. 313-325

3. Cozma, C., D. Sebastian, **M.I. Iurascu**, C. Mosoarca, M. Galusca, A. Zamfir, T. Fritz, M. März, S. Petersohn and M. Przybylski, *Klinische Diagnostik von Lysosomalen Speicherkrankheiten*. Transfer: das Steinbeis-Magazin, 2010. **2**: p. 22-23.

4. Vlad, C., **M.I. Iurascu**, S. Slamnoiu, B. Hengerer and M. Przybylski, *Characterization of oligomerization-aggregation products of neurodegenerative target proteins by ion mobility mass spectrometry.* Methods Mol Biol, 2012. **896**: p. 399-412.

5. **Iurascu, M.I.**, O. Marroquin-Belaunzanar, C. Cozma, C. Renner and M. Przybylski, Discontinuous mixed-disulfide epitope of Ankylosing Spondylitis related Human Leukocyte Antigen B27 identified by affinity-mass spectrometry, *in press*

Publications in Conference Proceedindgs

1. **Iurascu, M.I.**, C. Cozma, N. Tomczyk, M. Desor, M. Drescher and M. Przybylski, *Structure, reaction intermediates and topographical characterization of ß-amyloid oligomerisation revealed by electrospray-ion mobility mass spectrometry and electron spin resonance spectroscopy.* IMSC proceedings, 2009, Bremen, Germany

2. Paraschiv G., A. Almeida, P. Juszczyk, M. Dragusanu, **M.I. Iurascu**, A. Szymanska, Z. Grzonka and M. Przybylski, *Structural characterization and binding affinities of neuroprotective β-amyloid (Aβ) epitopes recognized by the protease inhibitor cystatin C.* IMSC proceedings, 2009, Bremen, Germany

3. **Iurascu M.I.**, C. Cozma, M. Desor, M. Drescher and M. Przybylski, *Structure, reaction intermediates and topographical characterization of ß-amyloid oligomerisation revealed by ion mobility mass spectrometry and electron paramagnetic resonance spectroscopy*, ASMS 2010, Salt Lake City, USA. Journal of the American Society for Mass Spectrometry, 2010. 21(5, Supplement): p. S92-S121.

4. **Iurascu M.I.**, C. Cozma, M. Gross, D. Clemme and M. Przybylski, *Mass spectrometric and bioaffinity MS investigations of proteins involved in metabolic and age related diseases*. IMSC proceedings, 2012, Kyoto, Japan

Conference Oral Presentations:

1. **Iurascu, M.I.**, C. Cozma, N. Tomczyk, M. Desor, M. Drescher and M. Przybylski, *Reaction intermediates and topography of β–amyloid oligomerisation revealed by ion mobility mass spectrometry and electron paramagnetic resonance spectroscopy.* RSMS 2010, Sinaia, Romania

2. **Iurascu, M.I.**, C. Cozma, N. Tomczyk, M. Desor and M. Przybylski, *Structural characterization of ß-amyloid peptide and aggregates revealed by Fourier transform – ion cyclotron resonance and ion mobility mass spectrometry*. FTMS Workshop 2010, Mülheim/Ruhr, Germany

3. **Iurascu, M.I.**, O. Marroquin-Belaunzanar, C. Cozma, C. Renner and M. Przybylski, *Investigations of a mixed disulfide epitope of spondyloarthritides related HLA-B27 by proteolytic excision mass spectrometry*. Affinity-MS Workshop 2014, Rostock, Germany

Conference Poster Presentations:

1. **Iurascu, M.I.**, C. Cozma, G. Paraschiv and M. Przybylski, *In vitro preparation and mass spectrometric characterization of ß-amyloid (Aß)- oligomers and fibrils relevant to Alzheimer's disease*. DGMS 2008, Giessen, Germany

2. **Iurascu, M.I.**, C. Cozma, M. Drescher and M. Przybylski, Characterization of Beta-Amyloid oligomerization by electrospray mass spectrometry and electron spin resonance spectroscopy. DGMS 2009, Konstanz, Germany

3. **Iurascu, M.I.**, C. Cozma, M. Drescher and M. Przybylski *Characterization of Beta-Amyloid oligomerization by electrospray mass spectrometry and electron spin resonance spectroscopy.* Afinity-MS Workshop 2009, Konstanz, Germany

4. **Iurascu, M.I.**, C. Cozma, M. Desor, M. Drescher and M. Przybylski, *Structure, reaction intermediates and topographical characterization of ß-amyloid oligomerisation revealed by ion mobility mass spectrometry and electron paramagnetic resonance spectroscopy*. DGMS 2010, Halle, Germany

5. **Iurascu, M.I.**, C. Cozma, M. Desor, M. Drescher and M. Przybylski, *Structural characterization of ß-amyloid peptide and aggregates revealed by FT-ICR and ion mobility mass spectrometry and electron paramagnetic resonance spectroscopy.* DGMS 2011, Dortmund, Germany

6. **Iurascu, M.I.**, C. Cozma, N. Tomczyk, M. Desor and M. Przybylski *Structural characterization of ß-amyloid peptide and aggregates revealed by Fourier transform – ion cyclotron resonance and ion mobility mass spectrometry.* RSMS 2011, Timisoara, Romania

7. **Iurascu, M.I.**, C. Cozma, M. Desor, M. Drescher and M. Przybylski, *Oligomerisation studies of modified A-beta peptides using mass spectrometry*. DGMS 2012, Poznan, Poland

8. **Iurascu, M.I.**, O. Marroquin Belaunzanar, C. Cozma and M. Przybylski, *Mass spectrometric and bioaffinity epitope investigations of spondyloarthritides related HLA-B27.* DGMS 2014, Frankfurt, Germany

9. **Iurascu, M.I.**, O. Marroquin Belaunzanar, C. Cozma and M. Przybylski, *Mass spectrometric and bioaffinity epitope investigations of spondyloarthritides related HLA-B27.* Mass-Spec Forum 2014, Vienna, Austria

TABLE OF CONTENTS

TABLE OF CONTENTS

1 INTRODUCTION

1.1 Mass spectrometric methods for protein analysis and proteomics

As initially coined by Mark Wilkins in 1996 [1], the proteome was termed as the total number of proteins expressed by a genome, however, unlike the genome which is specific for a certain organism, the proteome can be considered a snapshot of a cell, an organ or an organism, at a particular point in time. The proteome evolves during the life of an organism within complex biological mechanisms, particularly via post- translational modifications of proteins. The study of proteomes led to the development of the proteomics field [2-7], that has comprised a growing number of analytical and bioanalytical methods for protein investigation and characterization, which may be classified in two major classes: separation techniques and analytical methods. The high complexity of the human proteome has led to slow pace advancements, compared to the Human Genome Project; recently a draft map of a human proteome was discussed by Kim and collaborators [8].

There are 20 different amino acids genetically encoded (Appendix 2), representing the building blocks of proteins. Amino acids are small organic molecules with an amino functional group attached to the α-carbon of a carboxylic acid. The rest of the molecule is variable though different side-chains. Peptides and proteins resulted from gene translation are formed only from L-amino acids. Amino acids can form polymer chains via peptide bonds and the length of the peptidic chain varies largely, according to the functionality of proteins in the organism. However, there are smaller peptides and polypeptides with a functional role, e.g. in cell signaling.

In order to become biologically active, the polypeptide chains synthesized on ribosomes are subject to a series of modifications [9-13]. These post- translational modifications define the structure and function of a protein and may involve folding and formation of non-covalent bonds, formation of covalent bonds such as disulfide bridges, excision of

unnecessary sequence parts after folding (inteins and exteins) [14-16], and major chemical modifications (e.g. nitration, glycation, acetylation, alkylation, phosphorylation etc.). The amino acid sequence forms the primary structure of a protein or peptide; while there are another three levels of protein structure and folding (Figure 1).

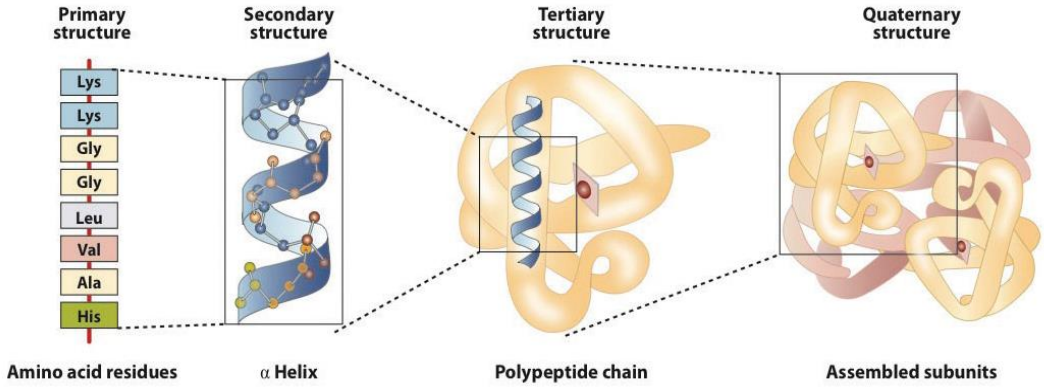

Figure 1. Protein structure levels: primary structure, the sequence of amino acids; secondary structure, three-dimensional form of the amino acid chain given by hydrogen bonds (α-helix, β-sheet); tertiary structure, spatial position of each atom in the molecule; and quaternary structure, interaction between chains of amino acids [17]

The chemical bonds along the amino acid chain are free to rotate making the protein's backbone flexible. This enables proteins to fold and bring different parts of the chain in close proximity to each other. For example, CO and NH_2 groups from the backbone of a protein form hydrogen bonds forcing the chain to adopt complex 3D geometries. These specific shapes define the secondary structure of a protein. When the folding occurs randomly [18] the resulting shape is called a random coil. When the hydrogen bonds form along the polypeptide chain, 3 to 4 amino acids apart, the chain adopts a spiral structure termed alpha helix. When hydrogen bonds form between two sequences of amino acids, the protein folds and the two chains align one to another forming a β-sheet. The alignment of the chains is either parallel, pointing to the same direction from C-terminal to N-terminal, or antiparallel, pointing in opposite directions. Beta sheets can be formed by a minimum of two chains but can include any number of parallel chains. A protein typically

consists of a mixture of all or some of these secondary structure subunits in different ratios and motifs depending on the type of protein (e.g. membrane proteins contain mainly α-helix, immunoglobulins structure is dominated by β-sheet bound by short random coil regions, etc.).

Hydrogen bonds are strong enough to maintain the local structure of a protein but are not enough to sustain its overall shape. Brownian movement of the chain combined with ions and water interactions may perturb the 3D structure of a protein. Often, after a high degree of folding, proteins are stabilized by covalent bonds across the amino acid chain. The most common example are disulfide bridges between -SH groups of cysteins [19-21]. This prevents proteins from unfolding and preserves their biological function. The final structure of a protein, with exact spatial position for each atom, forms the tertiary structure. The quaternary structure of a protein describes protein complexes formed by two or more polypeptide chains that act as a single protein. During their life time proteins are subjected to different types of modifications with importance for their biological activity and later on for their inactivation and removal. This increases even more the complexity of proteomics with ancillary fields such as glycoproteomics and lipoproteomics.

Unnecessary (redundant, inactive, degraded) proteins are eliminated by various biological mechanisms (e.g. the proteasome pathway [22-24]). In certain proteopathies [25], automatic removal mechanisms are disrupted, mainly due to unusual chemical modifications. Detection of certain types of modifications can be of importance in the detection and diagnosis of several diseases. One of the most common alterations of proteins is misfolding [26]. When misfolding of proteins prevents their elimination, this could lead to large scale peptides or protein accumulation which may harm the cells. The most exposed cells in the organism to this impairment are neuronal cells which are unable to regenerate. Misfolding proteins often lead to neurodegenerative diseases such as Parkinson’s Disease, Alzheimer’s and Huntington’s Disease [27, 28].

Initially developed for small molecules, mass spectrometry proved to be a highly efficient tool for investigating proteins and peptides due to the development of “soft”- ionization techniques, particularly electrospray (ESI) ionization and matrix assisted laser desorption (MALDI) ionization. Mass spectrometry, as a standalone technique or combined with separation techniques (e.g. liquid chromatography, gas chromatography, ion mobility, affinity chromatography, biosensor etc), was employed in structural studies, but also used with success in studies of protein folding, interactions with ligands and other proteins. Other studies employ combinations of mass spectrometry with in vitro chemical treatment of proteins to obtain insights into their functions, topography (e.g. protein foot-printing, H/D exchange in combination with affinity- mass spectrometry to characterize epitope-paratope locations and surface exposure [29-31]).

In “soft” ionization mass spectrometry, the analyte is transferred in gaseous ionic form with limited or without in-source fragmentation. Matrix assisted laser desorption ionization (MALDI) and electrospray ionization (ESI) are based on fundamentally different physical principles and have led to the development of many additional ionization methods, including combinations of the ESI and MALDI. MALDI-MS is a preferred technique for the analysis of biological samples and complex mixtures, due to its high sensitivity and relative tolerance of salt-based buffers used in biological studies. The sample is typically co-crystallized with the matrix on the target and desorbed by a radiation burst produced with a laser [32-35]. Most matrices are organic acids in order to provide a proton needed for positive ion formation; however MALDI measurements in negative ion mode is also possible [36]. Upon the laser burst, molecules of matrix and analyte are spread in a cloud in the front of the metal plate on which they are co-crystallized. The matrix/analyte clusters rapidly decay to produce a cationic form of the analyte molecule (Figure 2) [37]. The desorbed ions are moved through an electric field and directed by ion optics to the analyzer (e.g. ToF, FT-ICR). Characteristic for MALDI mass spectrum are the predominance of singly charged ions and the presence of matrix clusters that renders low masses difficult to analyze. For the

development of the MALDI method Koichi Tanaka received the Nobel Prize in Chemistry in 2002.

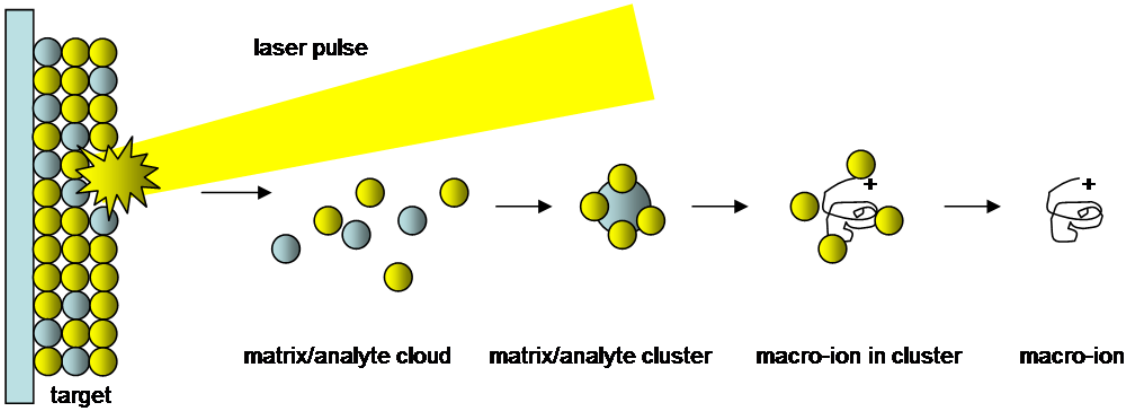

Figure 2. Matrix assisted laser desorption ionization (MALDI). The sample is co-crystallized with an UV absorbent matrix on a steel plate and hit with a laser. The matrix absorbs the radiation and explodes releasing the analyte molecules and providing them with electric charges

In electrospray ionization (ESI), the ionization takes place by converting the analyte solution into a spray under high voltage before the entrance into the mass spectrometer (Figure 3). At the exit of the capillary the liquid surface tension and the electric field forces shape the liquid into a cone known as Taylor cone [38]. At the point where the electric field is higher than the surface tension, a jet of droplets are expelled forming a spray of aerosol droplets containing the analyte [39, 40]. The electrospray is usually accompanied by a jet of dry gas (inert gas) that promotes the evaporation of solvent. The analyte molecule is rapidly dehydrated and retains the electric charges becoming a multiply charged ion. This effect reduces the charge to mass ratio (m/z) increasing the mass range of the mass spectrometer. Because of the liquid input of ESI, it can be combined with other analytical methods such as liquid chromatography. For developing the electrospray ionization method, John B. Fenn [41] received the Nobel Prize for Chemistry in 2002. Analyte molecules retaining their native properties from solution are of special interest since a folded and an unfolded conformation of a molecule may lead to a different surface area and to a different charge state (Figure 3).

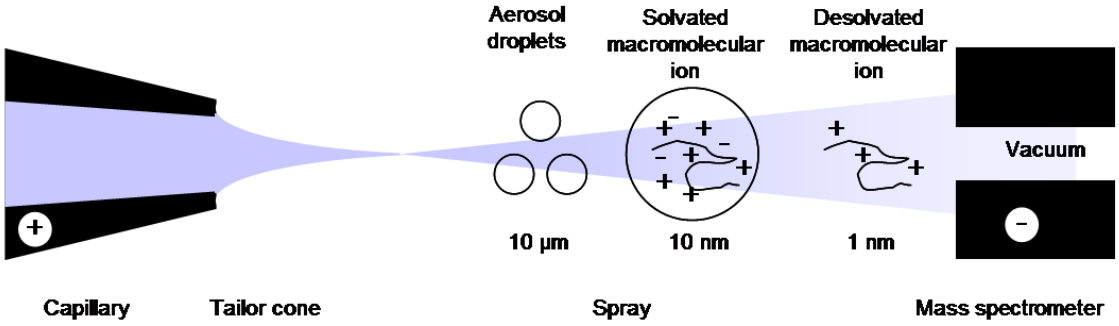

Figure 3. Principle of Electrospray ionization (ESI). The analyte is solubilized in an aqueous solution and sprayed in an electric field in front of the inlet of the MS instrument. When electrostatic repulsion becomes higher than the surface tension the molecules are spread in aerosol droplets. Upon solvent evaporation the electric charges are transferred to the analyte forming multiply charged ions

1.2 Affinity mass spectrometry methods for protein structure identification and characterization

Affinity –mass spectrometry is a combination method based on the capture of biological material with a ligand (mainly coupled to a solid support) and its analysis by mass spectrometry [42-44]. The types of ligands used in affinity purifications include oligonucleotides, glycans, lipids, peptides or proteins, and, most frequently, antibodies. In affinity-MS, a single molecule or a group of compounds of interest from a complex mixture is affinity captured by using in a specific matrix. There are multiple variations of affinity techniques, including immunoprecipitation, affinity chromatography, epitope excision/extraction, biosensor etc.

An antibody (Ab) is a large protein, also known as immunoglobulin, with a key role in the immune system. It is capable of recognizing and binding specific molecules [45] and trigger the immune response. Antibodies are produced by the plasma B cells and may be found in five isotypes (IgA, IgD, IgE, IgG and IgM [46-49]) in mammals. Antibodies have distinct Y shape and

may occur as a monomer (IgD, IgE, IgG), a dimer (IgA) or a pentamer (IgM). The molecule's structure is composed of two identical heavy chains [50] (HC) and two identical light chains (LC) linked by two disulfide bridges in the hinge region. All chains have a constant domain at the C-terminal and a variable domain at the N-terminal ends. The HC constant region may be one of five types (α, δ, ε, γ and μ) and is the one that gives the antibody's isotype. The part of the Ab responsible for recognition and binding the foreign molecules is called paratope and is situated at the N-terminus in the variable region. The paratope comprises of a set of hyper-variable regions or complementarity-determining regions (CDR [51-53]) that gives an antibody its specificity (Figure 4). There are six unique CDRs on each antibody molecule, three on the light chain and three on the heavy chain (CDR1, CDR2 and CDR3) amounting to a total of 12 CDRs for a monomeric antibody and 60 CDRs for a pentameric antibody. CDR3 presents the highest variability among all CDRs.

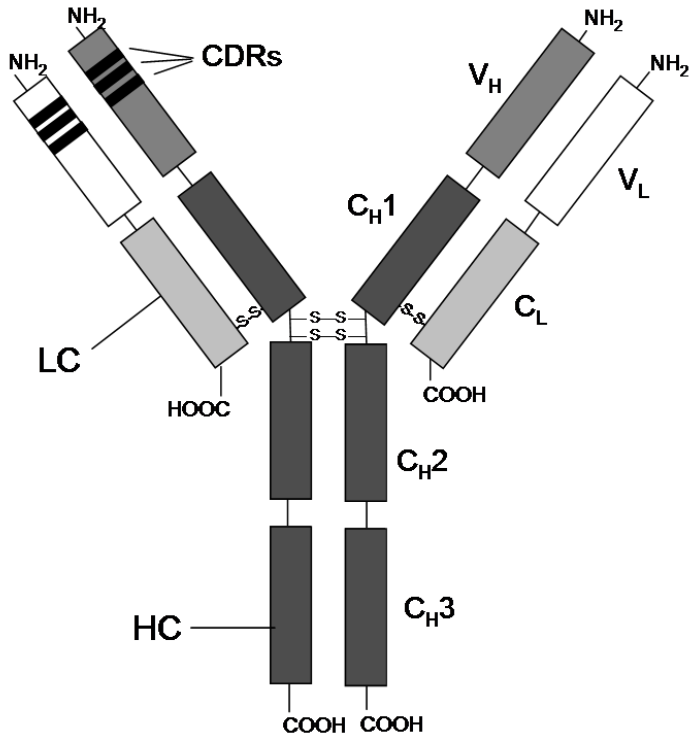

Figure 4. An antibody consists of two pairs of light (LC) and heavy chains (HC) bound together by two disulfide bridges. Each chain has a constant domain (C_H1, C_H2 and C_H3 for HC and C_L for LC) and a variable domain (V_H and V_L) with three hyper variable domains per chain (CDR1, 2 and 3)

In the case when the antigen is a protein, the sequence of amino acids recognized by the immunoglobulin is called an antigenic determinant or epitope. Depending on the structure, epitopes can be linear or discontinuous. Linear epitopes are short, single sequences formed of 5 to 10 amino acids. Discontinuous epitopes [54-57] are formed by two or more separate sequences of amino acids acting as a one epitope.

The understanding and characterization of protein-protein interaction is of high importance for biochemical and biomedical applications such immune system modulation, clinical diagnosis and targeted therapy. Antibody-drug conjugates are used to specifically deliver drugs to organs and tissues. Monoclonal antibody therapy is used to target foreign molecules or cells in order to stimulate the immune response. For example, immune therapies with the use of antibodies are developed against different cancer types [58] and viruses, e.g. Ebola [59]. On the other hand, clinical diagnoses make use of the antibody antigen interaction for the detection of diseases, e.g. malaria [60].

Fabry's Disease (FD) [61] is a rare lysosomal storage disease (LSD) characterized by the deficiency of alpha-galactosidase A. The role of the enzyme is to hydrolyze the terminal alpha-galactosyl groups from glycoproteins and its absence may lead to the accumulation of galactosyl-ceramides (Figure 5) in blood vessels and other organs and tissues. Fabry is an X-chromosome linked genetic disease which can be treated by enzyme replacing therapy [62]. Fabry can be diagnosed by (i) gene sequencing (currently expensive), (ii) alpha-Galactosidase activity determination [63] and (iii) alpha-Galactosidase quantification with the use of an anti-alpha-Galactosidase antibody (investigated in this thesis).

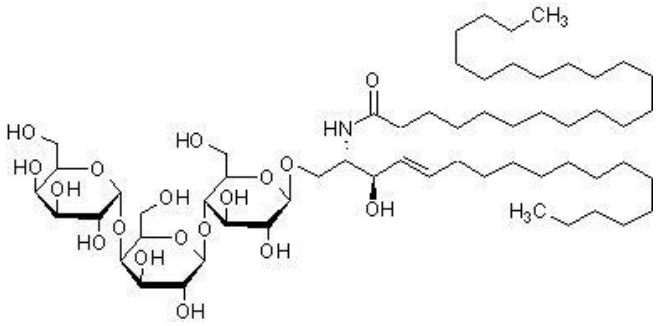

Figure 5. N-Tricosanoyl ceramide trihexoside, a galactosyl-ceramide that typically is accumulating in the tissues of Fabry patients

A second example of antibodies of high recent interest are antibodies against the human leukocyte antigen (HLA). Ankylosing spondylitis [64] is a spondyloarthritides caused by the inactivation of HLA [65, 66]. HLA proteins are located on the cell surface and are responsible for detection and elimination of foreign peptides by exposing them to the immune system through the formation of protein complexes (Figure 6). When HLA loses the beta-2-microglobulin, it forms homodimers which trigger an inflammatory response. HD6 antibody [67] may be used to block the inactivated HLA protein and to decrease the inflammation.

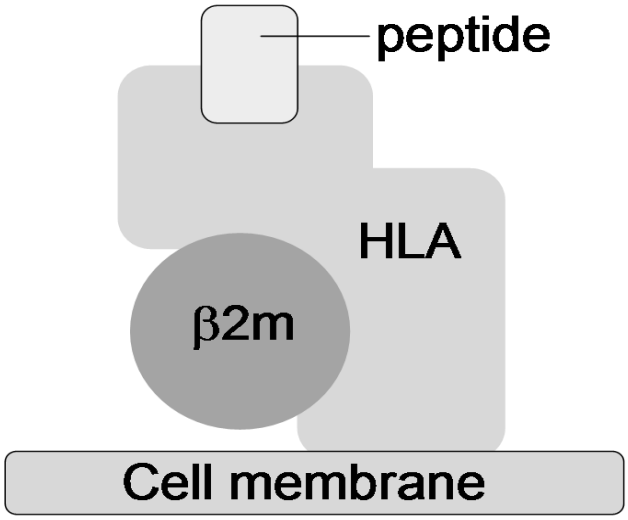

Figure 6. HLA complex with beta-2-microglobulin and a foreign peptide to be eliminated used to activate the immune response.

Antibody-antigen interactions are reversible non-covalent interactions and may comprise Van der Waals interactions, hydrophobic interactions and ionic bonds. In order to characterize the peptide-peptide interaction site, two affinity based methods combined with mass spectrometry have been first described and applied in Przybylski group [68-71] : epitope excision [72] and epitope extraction [73] (Figure 7).

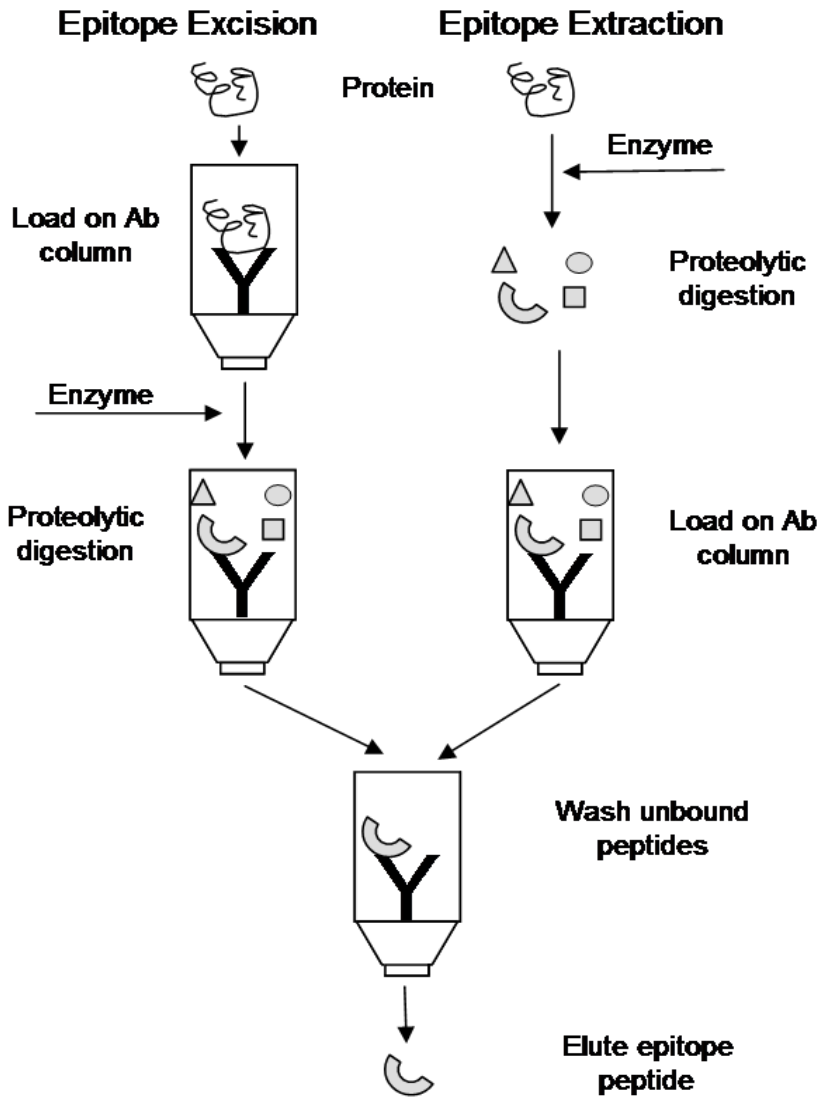

Figure 7. Epitope Excision (left): the protein of interest is bound to the antibody column and subjected to proteolytic digestion in situ; unbound peptide fragments are washed away and the epitope peptide is eluted and identified by mass spectrometry. Epitope Extraction (right): the protein of interest is subjected to proteolytic digestion and the peptide mixture is loaded on the antibody column; unbound peptide fragments are washed away and the epitope peptide is eluted and identified by mass spectrometry.

Epitope excision [74-76] is based on selective proteolysis of an antibody-antigen complex. Mass spectrometric characterization was used to determine the structure of the epitope. The antibody is immobilized on a solid support (e.g. silica beads, agarose) in a micro-column and incubated with the antigen. A specific enzymatic proteolysis is carried out by the addition of a protease to the column. Due to its stability in native form to proteolytic digestion, the antibody creates a shielding effect around the epitope against enzymatic degradation. The region recognized by the antibody will remain undigested and bound to the immobilized antibody. The unbound fragments are removed and collected for mass spectrometric analysis. Finally, the antibody-epitope complex is dissociated and the eluted fragments are identified by mass spectrometry. Antibodies in native state are highly resistant to proteases and the antibody column is typically reusable, depending on the protease employed, the digestion time and the harshness and the elution procedure. Epitope excision combined with mass spectrometry is the a good method of epitope identification for a wide variety of proteins (e.g. prions [77], inhibitors [78, 79] and lectins [80, 81]).

Epitope extraction is based on non-selective proteolysis of an antigen in the absence of the antibody. The antibody is immobilized on a solid support in a micro-column and the proteolytic digestion mixture is added to the column. The epitope peptides recognized by the antibody are retained on the column while the unbound fragments are removed and collected for mass spectrometric analysis. Finally, the antibody-epitope complex is dissociated and the eluted fragments are identified by mass spectrometry. The advantage of epitope extraction is that it can be applied in situations where the protein of interest is not available in free form (such as proteins separated a priori by 2D gel electrophoresis [82]) or when it is unusual resistant to protease attacks (when too large, e.g. Her-2 protein, Troponin T [83]). The major disadvantage is the possible cleavage of a linear epitope.

An antibody is characterized by its specificity, affinity and avidity. The amino acid sequence of an epitope and its 3D structure gives an antibody its specificity. The lower the number of variations allowed in the antigen

sequence, the higher the specificity. The affinity is given by the strength of the interaction with a single antigen while the avidity is the capacity of binding multiple antigen molecules measured by the dissociation constant (K_D). K_D determinations are usually done by immobilizing one of the partners on a solid surface and measuring the interaction with the ligand in solution, at different concentrations. One of the methods capable of determination of binding constants between an Ab and a ligand is the biosensor. Several types of technologies are widely used in biosensors such surface plasmon resonance [84-86] (SPR), surface acoustic wave [87] (SAW) and quartz crystal microbalance [88-90] (QCM).

Due to the analogous procedures between immobilizing an antibody on a chip and immobilizing it on a solid phase column, biosensors can be successfully used in proteolytic epitope extraction experiments. Moreover, due to use of a solution based sample delivery system, a biosensor can be coupled with a mass spectrometer to enable direct MS characterization of the eluted ligads [91-93]. On-line coupling of a biosensor and a mass spectrometer requires the use of a desalting interface.

1.3 Analytical methods for amyloid aggregation characterization

Alzheimer's disease (AD) is a neurodegenerative disease characterized, among other, by the accumulation of beta amyloid (Aβ) fibrils in the intra-neuronal space. The presence of the fibrils was first reported in 1906 by the german neuropathologist Alois Alzheimer [94]. A.A. studied a 51 years old patient, Auguste D., with signs of mental and cognitive degradation accompanied by memory loss and paranoia. Upon her autopsy, he noted the presence of plaque-like deposits around the neurons (Aβ plaques) and filaments inside the neurons (neurofibrillary tangles).

AD is the most common form of dementia affecting an increasing number of the elderly population. In Europe, an estimated 0.8% of persons over 65 have Alzheimer's and the number increases to 28.5% for those over 90 years of age [95]. The diagnosis of the disease is mainly obtained by

cognitive tests, lately completed by computer tomograph investigations. The difficulty of diagnosis makes the average life expectancy less than 7 years [96]. There are several competing hypotheses for the cause of Alzheimer's disease. The genetic heritability hypothesis refers to early onset cases of AD which were associated with certain genetic mutations of APP [97-102]. The cholinergic hypothesis suggests that AD is caused by reduced synthesis of the neurotransmitter acetylcholine [103]. The tau hypothesis proposes that the hyperphosphorylation of the tau protein not only disrupts the microtubules but also has a toxic effect leading to neurons death [104]. The amyloid hypothesis suggests that the extracellular deposits of beta-amyloid aggregates are the main cause of AD [105-108].

Amyloid plaques are formed by the aggregation of a small peptide, 39-43 aa in length, known as beta-amyloid peptide (Aβ). Aβ peptide is formed by the miscleavage of the amyloid precursor transmembrane protein APP [109] (amyloid precursor protein). The normal, non-amyloidogenic, APP pathway involves the α- and γ-secretase [110] that cleave APP in small and soluble peptides. In the amyloidogenic pathway of the APP α-secretase is replaced by the β-secretase which leads to the formation of more hydrophobic amyloid-beta peptides [111]. If the A-beta peptides are not eliminated from the brain, they start to aggregate, forming low molecular weight (MW) oligomers and high molecular weight fibrils. The fibrils further accumulate in the intercellular space forming plaques (Figure 8). Although until now the amyloid plaques were thought to cause the disease, recent studies suggest that the low MW aggregates (oligomers) are the neurotoxic species [112-115].

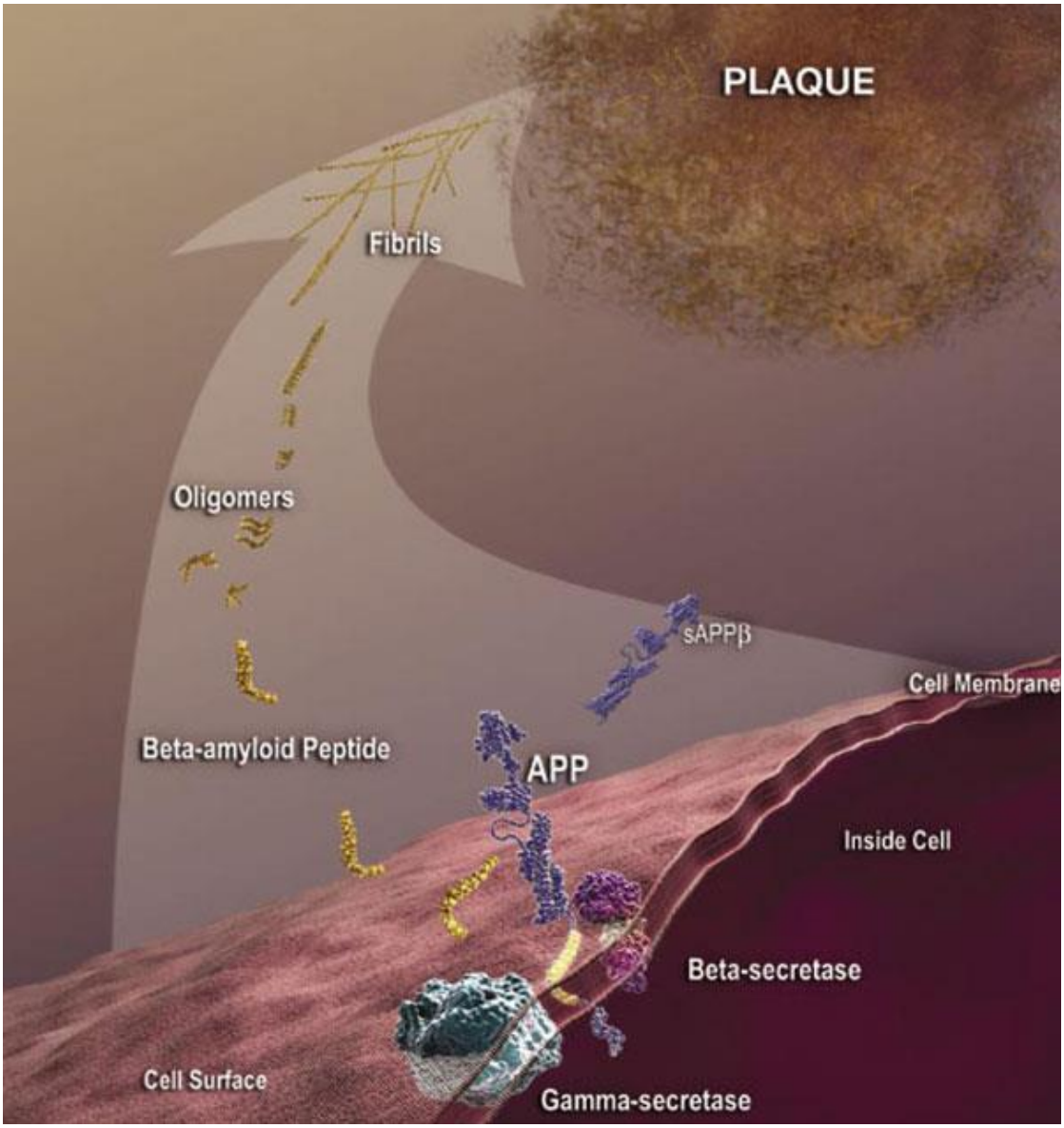

Figure 8. Scheme of beta amyloid pathway: amyloid precursor protein (APP) is cut by the beta- and gamma- secretases resulting in the 40-42 amino acids beta-amyloid peptide prone to form aggregates, fibrils and plaques [116]

The difficulties of *in-vivo* monitoring of beta-amyloid pathways makes the study of AD cause even harder since the Aβ plaques can be evidentiated only by taking a sample of the diseased brain tissue. *In-vitro* aggregation studies offer the possibility of studying the mechanisms of the amyloid fibrils formation. For the analysis of such complex mixtures, an efficient method is the gel electrophoresis. This method was successfully used to identify the oligomerization and degradation degrees in several neurodegenerative diseases, including Alzheimer's disease [117] and Parkinson's disease [118].

One dimensional sodium dodecyl sulfate polyacrylamide gel electrophoresis (1D-SDS-PAGE, GE) is an analysis method based on the separation of molecules according to their migration through a gel through an electric field. The SDS detergent is used to denaturate the proteins and to charge them negatively, proportional to their molecular weight. For complex biological mixtures, two dimensional gel electrophoresis was introduced by O'Farrell and Klose in 1975 [119]. In order to be identified, the proteins are visualized by staining and their migration is compared to a reference molecular weight marker (a mixture of proteins with known molecular weight). Because the precision of GE is low, often mass spectrometric peptide mass fingerprinting is employed for the identification of peptides separated by GE. The protein spots are cut from the gel with a scalpel and the stain is removed by adequate washing. The gel bands are swollen in a buffer containing an enzyme of choice (such as Trypsin) and subjected to *in-gel* proteolytic digestion. The digestion mixture is then analyzed by liquid chromatography - mass spectrometry (LC-MS) creating a map of peptides (proteins fingerprint). Peptide mass fingerprinting [120-122] refers to the identification of a protein based on the map of proteolytic peptides and is done by searching in a database [123].

Ion mobility spectrometry - mass spectrometry (IMS-MS) [124-128] proved to be a powerful method for the analysis of low molecular weight aggregates [117, 129] and peptidic complexes. IMS is a separation and analysis method based on the mobility of ions inside a low pressure gas tube. Ions are accelerated at the beginning of the tube or carried along it by an electric field wave. An inert gas (helium) flows in the opposite sense and slows down the ions with a bigger collision cross-section. After ion mobility separation, the MS section of the instrument identifies the analyses according to their m/z ratio.

1.4 Electron paramagnetic resonance methods for biomolecular characterization

Electron paramagnetic resonance (EPR) is a method of characterization applicable to molecules with an unpaired electron present at one of its atoms. This is a rarely occurring situation in nature, and in most cases there is the need of using corresponding spin labels. In the case of proteins, labeling is a widespread method for preparing a molecule for an EPR measurement and data collection [130-133]. When an unpaired electron found in the outer layer of an atom is placed in an external magnetic field, the magnetic moment of the electron will align itself with this field and will adopt one of the two possible positions: parallel, known as spin-up, or antiparallel, known as spin-down. These positions are characterized by the electronic magnetic moment $m_s = \pm ½$. The energetic gap between the two states is directly proportional to the intensity of the external magnetic field and the electron will naturally tend to occupy the lowest energy level, spin-up. The transition between the two energy levels is called resonance and may occur if an adequate quantity of energy is absorbed (Figure 9) [134].

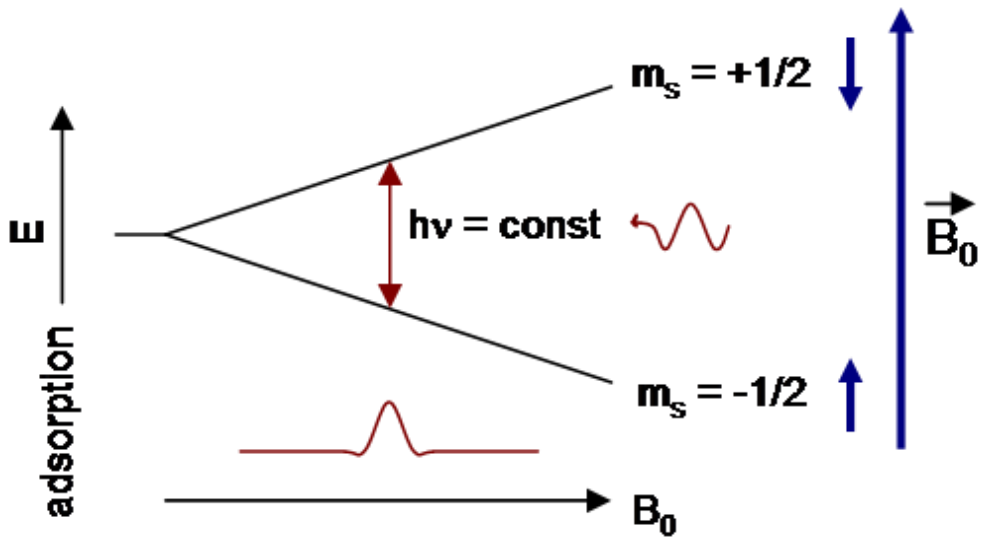

Figure 9. Electron paramagnetic resonance: an unpaired electron aligns its magnetic momentum with an external magnetic field in a spin-up or spin-down position creating two energy levels. The tranzion between the two energy levels is called resonance.

The electron paramagnetic resonance principle is closely related to that of the nuclear magnetic resonance. Thus, closely situated particles may

interfere one with each other through quantum effects. In the case of EPR, two types of interactions may occur: electron-electron coupling, when two unpaired electrons are close to each other, and electron-nucleus coupling, when the electron is coupled with the nucleus of an adjacent atom. When the electron magnetic moment is perturbed by the nuclear magnetic moment of a nearby nucleus, a phenomenon called hyperfine coupling takes place. Hyperfine coupling leads to the multiplication of energy levels. The number of transitions that may occur between these levels depends on the nuclear spin I and is 2I+1. Thus, if the neighboring atom is ^{14}N, with a spin of I=1, then the EPR signal will be split in three (Figure 10) [134].

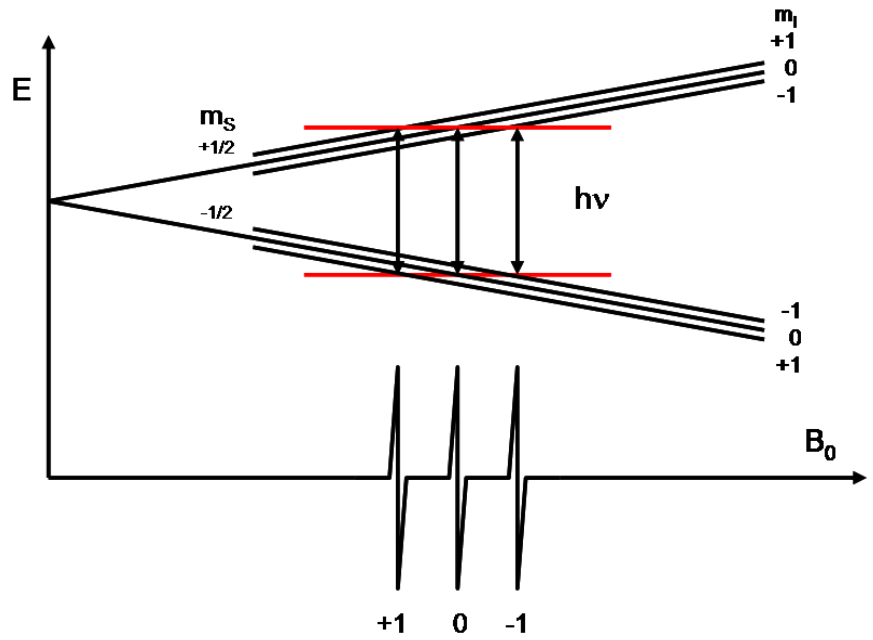

Figure 10. The source of the triple EPR signal is the electron-nucleus coupling when each energetic level splits into 3 new levels allowing for multiple transitions with the same energy difference

When freely moving in solution, the molecules are distributed between the three states and may translate from one state to the other at a very fast rate. The spectra will present very sharp peaks (Figure 11a). If the molecules are cooled, the transition (correlation) time becomes longer and the peaks will loose their sharpness and will become broader (Figure 11b).

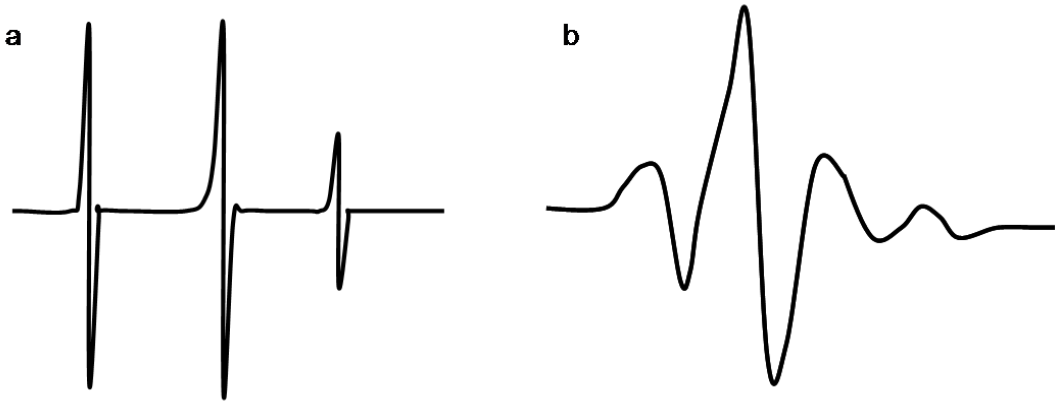

Figure 11. The difference in the EPR spectra shape when the atom is in a fast motion transition (a) and in a slow motion transition (b).

When two unpaired electrons from two separate molecules find themselves in proximity of each other, their magnetic moments will couple. This is known as double electron-electron resonance (DEER) and can be used to determine distances between molecules [135]. EPR measurements provide a useful vision about the topology of molecules. For example, recent applications with neuotoxic aggregates such as β-amyloid peptide from Alzheimers Disease [117] and α-synuclein from Parkinson disease [136, 137].

1.5 Scientific goals of the dissertation

Protein malfunction diseases are found at all levels of the cell, from deep inside the organelle, lysosomal storage diseases, to the outer part of the membrane, neurodegenerative diseases. New protein investigation methods are required to characterize proteins and protein-protein interactions. We present here the development and application of mass spectrometric (MS) and electron paramagnetic resonance (EPR) methods for characterization of protein aggregation and antigen recognition structures. EPR is based on the property of unpaired electrons to absorb and reemit electromagnetic energy under the influence of an external magnetic field. Ion mobility spectrometry (IMS) is an identification method based on the separation of analyte molecules (proteins) carried by an electric field against a counter flowing inert gas. Molecules are separated according to their size and shape. MS is a

powerful analysis method for characterizing molecules according to their mass to charge ratio. The use of multiple ionization methods, matrix assisted laser desorption ionization (MALDI) and electrospray ionization ESI, together with multiple analyzer types, time of flight (ToF), ion trap and Fourier transform - ion cyclotron resonance (FT-ICR), makes MS a versatile analytical method. IMS, MS and EPR were used for protein aggregation characterization related to Alzheimer's disease (AD). AD is a neurodegenerative disorder commonly found in elderly people. It is characterized by memory loss and is caused by the miscleavage of the APP protein and aggregation of the resulting beta amyloid peptides. The aggregates accumulate in the brain forming plaques and hindering the neuronal activity.

Affinity analytical methods are based on the antibody-antigen interactions. When coupled with MS, Affinity-MS can be used for identification and characterization of protein recognition domains (epitopes), with applications in diagnoses of diseases like Fabry disease (FD) and ankylosing spondylitis (AS). FD is a lysosomal storage disease with an onset at a very young age. It is caused by the absence or inactivity of alpha galactosidase which leads to the accumulation of ceramide trihexoside in blood vessels and various organs and tissues. AS is a chronic inflammatory disease of the axial skeleton strongly associated with the expression of human leukocyte antigen (HLA) B27. However, the way in which the antigen triggers the disease is still unclear. While 90% of the people with AS posses the HLA-B27 gene, not all of those who express the protein develop the disease.

The scientific goals of this thesis are:

- *Development of ion mobility mass spectrometric methods for characterization of beta Amyloid aggregates.* This involved synthesis, purification and mass spectrometric characterization of synthetic beta amyloid (1-40) peptides. The aggregation was monitored by gel electrophoresis and Thioflavin T assay. New mass spectrometric and ion mobility mass spectrometric methods of aggregates characterization were developed.

- *Development of electron paramagnetic resonance (EPR) spectroscopy methods of characterization for beta Amyloid aggregates.* This involved synthesis, purification and mass spectrometric characterization of C- and N-terminal cysteinil beta amyloid (1-40) peptides and coupling of 3-(2-iodoacetamido)-2,2,5,5-tetramethyl-1-pyrrolidinyloxy (IPSL) at the cysteine residue. New EPR methods of aggregates characterization were developed based on the influence of aggregation on the freedom of movement of IPSL.

- *Development of affinity proteolytic epitope excision mass spectrometric determination of alpha galactosidase epitope against anti-alpha galactosidase monoclonal antibody with applications in alpha galactosidase deficiency diagnosis in Fabry Disease patients.* This involved determination, synthesis, mass spectrometric and affinity characterization of alpha galactosidase epitope peptide. Biosensor K_D determination for the peptide against the monoclonal antibody.

- *Development of affinity proteolytic epitope excision mass spectrometric determination of HLA-B27 epitope with applications in ankylosing spondylitis diagnosis.* This involved determination, synthesis, mass spectrometric and affinity characterization of HLA-B27 epitope peptides against library selected antibodies. Dimerization of discontinuous epitope and affinity and mass spectrometric characterization. Biosensor K_D determination of the epitope peptides against the library of selected antibodies.

2 RESULTS AND DISCUSSION

2.1 Mass spectrometric methods for characterization of beta amyloid peptide aggregation

Gel electrophoresis (GE) is a separation method used primarily for large biomolecules. GE is commonly used for DNA, RNA and proteins separation. Although very good for samples with a low number of components, the estimation of molecular mass is inaccurate and GE lacks the resolution to solve multi-components samples. Two-dimensional gel electrophoresis is more frequently employed in the characterization of more complex mixtures, such as cell lysates [138]. However, if the mixture is too complex gel electrophoresis alone is not enough to successfully and completely characterize it. In proteomics, due to the large number of peptides and proteins with similar molecular weights, a subsequent mass spectrometric measurement is often used in order to ascertain the identity of an unknown sample. For this purpose, the gel spots of interest are excised and the biological samples recovered, either intact through gel extraction or, more often, by in-gel peptide digestion. The resulting mixture of digested peptides is unique to each protein, forming its fingerprint according to which it can be identified.

Beta amyloid (β-amiloyd, Aβ) peptides are 39 - 43 residues long and have a mass of around 4 kDa. This mass is at the lower limit of detection for gel electrophoresis but it is well feasible for mass spectrometric characterization. Upon aggregation to fibrils, Aβ forms a series of low molecular weight oligomers, as well as high molecular weight protofibrils [139] and fibrils, all of which being subject of high interest due to their biological activity and neurotoxicity [140]. Oligomers are assigned as aggregates with a low number of subunits, usually up to 10. Their molecular weights are in ranges that enable their direct analyses by ESI and MALDI mass spectrometry. For the analysis of Aβ fibrils and high molecular weight aggregates an electrophoretic separation is needed as a first step, followed by an in-gel digestion, prior to mass spectrometric characterization.

2.1.1 Synthesis of β-amyloid peptides

For the study of oligomer formation of the β-amyloid (Aβ) peptides involved in Alzheimer's disease, several peptide fragments of the amyloid precursor protein (APP) were prepared by means of chemical synthesis. To this goal, solid phase peptide synthesis [141] (SPPS) was performed using the 9-Fluorenylmethoxycarbonyl (Fmoc) N-terminal protection strategy, which is suitable for both manual and automated synthesis [142]. The main peptide synthesized was β-amyloid(1-40) with the following primary structure [143-145] (Figure 12).

Aβ(1-40): ^{1}Asp-Ala-Glu-Phe-Arg-His-Asp-Ser-Gly-Tyr^{10}

^{11}Glu-Val-His-His-Gln-Lys-Leu-Val-Phe-Phe^{20}

^{21}Ala-Glu-Asp-Val-Gly-Ser-Asn-Lys-Gly-Ala^{30}

^{31}Ile-Ile-Gly-Leu-Met-Val-Gly-Gly-Val-Val^{40}

Figure 12. Aβ(1-40) aminoacid sequence

In addition to the Aβ(1-40) peptide (**1**), prolonged versions of amyloid-beta peptides were synthesized by the addition of one extra cysteine residue at the N- and C- terminal ends: Cys-Aβ(1-40) (**2**) and Aβ(1-40)-Cys (**3**). The addition of Cysteine was necessary to covalently attach the 3-(2-iodoacetamido)-2,2,5,5-tetramethyl-1-pyrrolidinyloxy (IPSL) radical to the Aβ peptide via a condensation coupling reaction. IPSL is a stable radical with an unpaired electron present at the oxygen atom. The unpaired electron is capable to absorb and reemit electromagnetic energy when placed in a magnetic field in a process called electron spin resonance (ESR) or electron paramagnetic resonance (EPR).

SPPS uses a series of coupling reactions between the carboxyl group of one aminoacid and the amino group of another aminoacid in order to prolong the peptide chain. The yield of peptide synthesis typically decreases with the length of the aa sequence. In order to improve the yield, a double coupling strategy was employed. All peptides were successfully synthesized.

2.1.2 Purification of beta amyloid peptides

After the solid phase peptide synthesis, all peptides were subjected to a purification step. This was necessary in order to increase the purity and to decrease the presence of interfering peptides with truncated or incomplete sequences. Purification was performed by reversed phase high performance liquid chromatography (RP-HPLC) using a C4 Vidaq column. To elute the peptides from the column a gradient of increasing concentration of acidified acetonitrile (ACN) was used. The peptide's distribution between the mobile and stationary phase is highly dependent on the mobile phase composition, thus the retention time is dependent on the organic component concentration in the mobile phase.

All HPLC elution fractions were collected and characterized by MALDI-ToF mass spectrometric measurements in order separate the Aβ from the impurities. The Aβ(1-40) peptide showed a retention time of 21 minutes as shown by the chromatogram and mass spectrum (Figure 13).

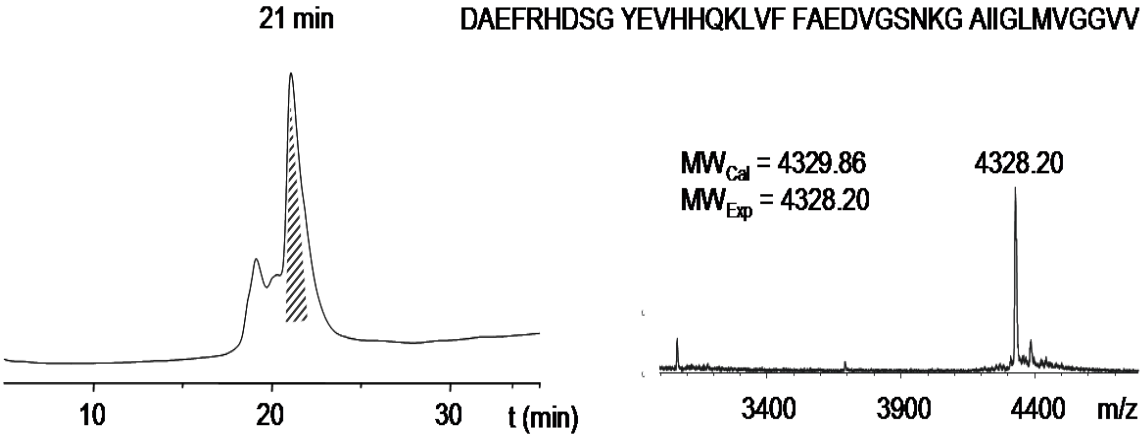

Figure 13. RP-HPLC purification chromatogram profile and the MALDI-ToF mass spectrum of (**1**) peptide

The pure Aβ(1-40) HPLC fractions were combined and lyophilized for better storage and for use in further studies. After various necessary chemical modifications, the peptides were subjected to further purification as shown in par. 2.2.3.

2.1.3 Mass spectrometric characterization of beta amyloid peptides

After synthesis and purification, the Aβ peptides were subjected to mass spectrometric characterization. Low resolution methods such as MALDI-ToF MS were employed during the synthesis and purification steps in order to monitor the status and purity of the products (Figure 13). High resolution MS methods were used for detailed characterization of the structure. Ion Trap and FT-ICR mass spectrometry was performed with ESI and MALDI ionization methods.

Using ESI-MS, the $[M+6H]^{6+}$ and $[M+7H]^{7+}$ ions were observed on the Ion-trap instrument (Figure 14) while predominantly the $[M+5H]^{5+}$ on the FT-ICR-MS (Figure 15). Compared to the soft, ESI ionization mode, MALDI-FT-ICR mass spectrum shows only the singly charged ion (Figure 16).

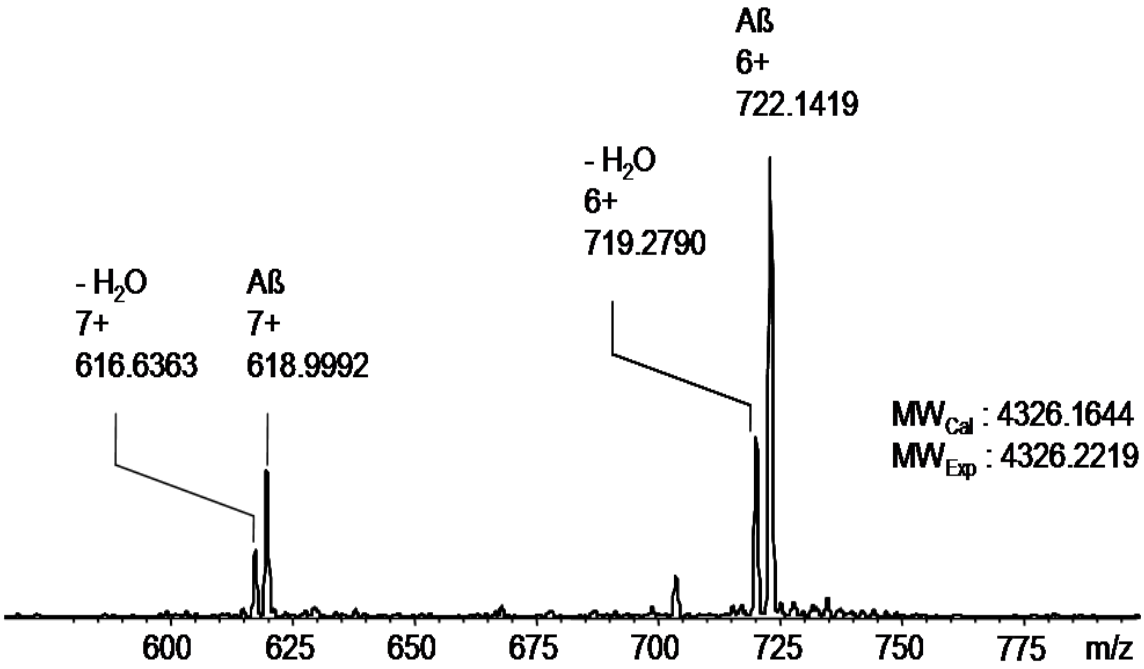

Figure 14. ESI Ion Trap mass spectrum of Aβ(1-40) peptide, showing the $[M+6H]^{6+}$ and $[M+7H]^{7+}$ ions

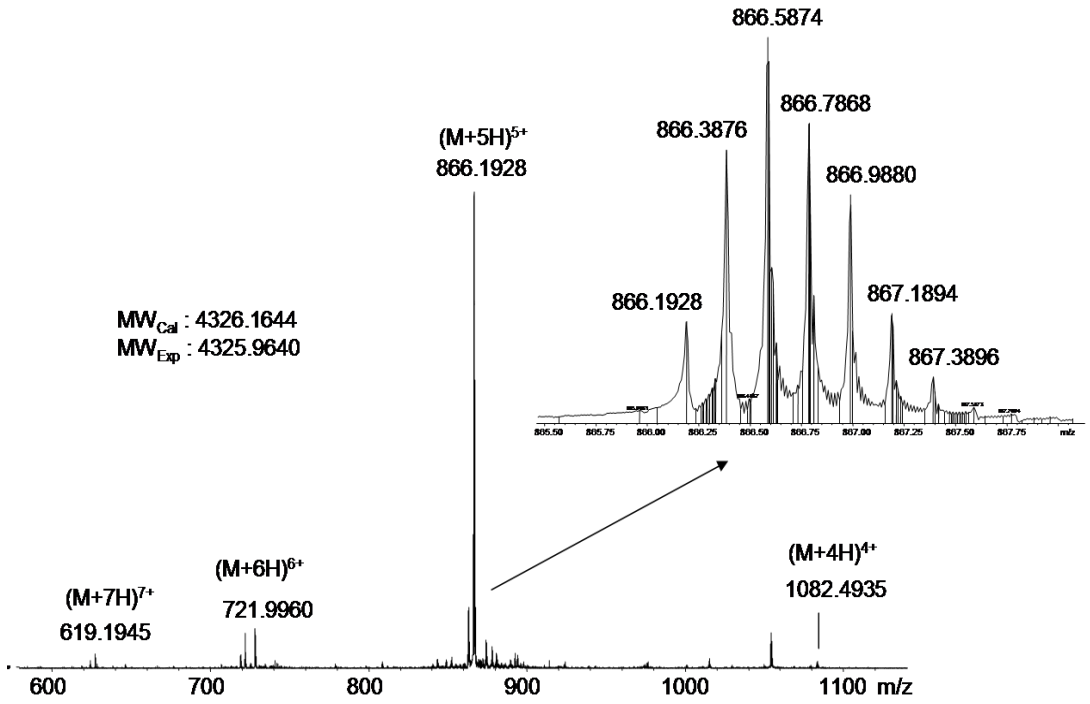

Figure 15. High resolution ESI-FT-ICR mass spectrum of synthetic Aβ(1-40) peptide showing the predominant $[M+5H]^{5+}$ ion and its isotopic distribution.

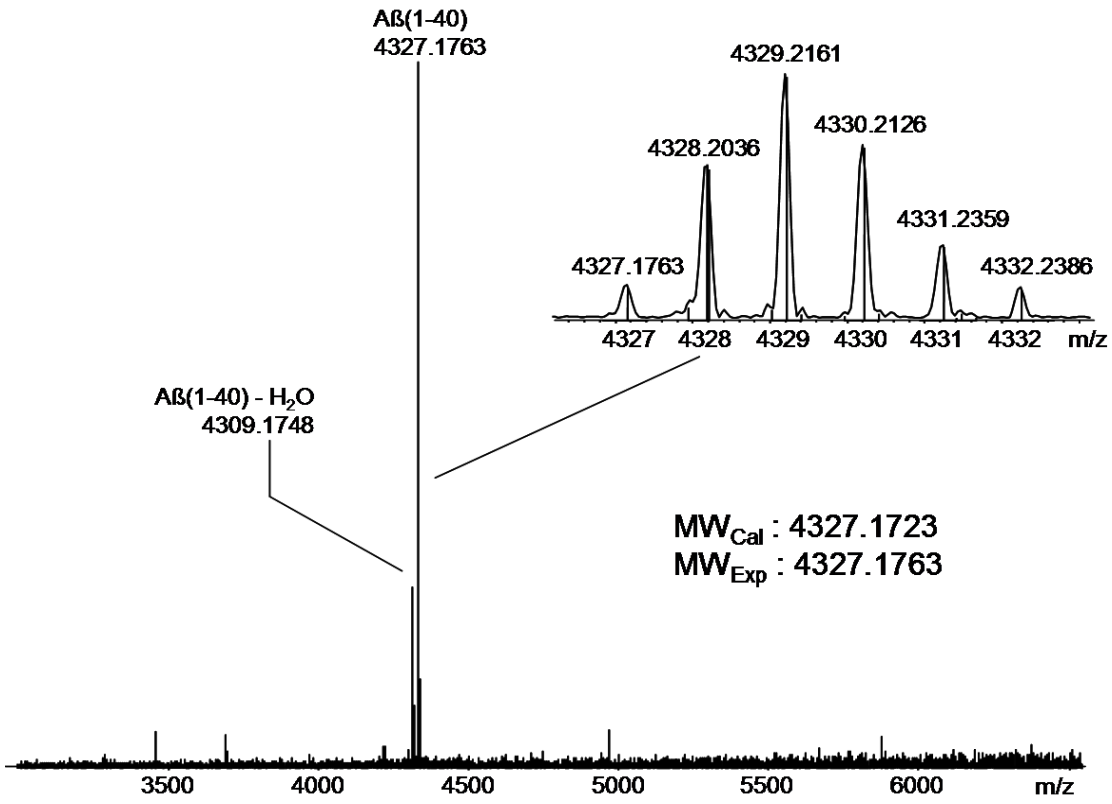

Figure 16. High resolution MALDI-FT-ICR mass spectrum of synthetic Aβ(1-40) peptide (0.92 ppm) showing only the $[M+H]^{1+}$ ion was present and its isotopic distribution.

2.1.4 In-vitro aggregation of β amyloid (1-40) peptide

After the synthesis and purification of the Aβ(1-40) peptide, different oligomerization and fibrilization assays were tested in order to find the optimum conditions for obtaining both low and high molecular weight aggregates. To establish a reproducible method, a series of experiments were conducted under different aggregation conditions.

The incubation buffer and the pH play a key role in the composition of the aggregates. A series of different buffers were chosen and prepared according to Table 1. The second incubation parameter was the incubation time. The incubation time was varied within a wide range from zero (freshly solubilized peptide) and a few minutes to several hours and up to 16 days.

Table 1. Buffers used in A β (1-40) aggregation studies

Buffer composition	pH
10 mM Tris, 150 mM NaCl	8.8
10 mM Tris	8.0
50 mM Na_3PO_4, 150 mM NaCl, 0.02% NaN_3	7.5
10 mM HCl, 150 mM NaCl	2.0

Aβ(1-40) was solubilized at a concentration of 1 µg/µL in fibrillization buffer with the help of several vortex and sonication steps. After solubilisation, the peptide was incubated at 37°C for varying periods of time. The aggregation degree depended on the incubation period yielding an opaque solution or a white precipitate. The aggregates were centrifuged for 15 minutes at 13,000 rpm and the supernatant containing soluble specimens was removed and replaced with an equivalent amount of MilliQ water.

2.1.5 Gel electrophoresis analysis of beta amyloid aggregates

Sodium dodecyl sulfate polyacrylamide gel electrophoresis (SDS-PAGE) is widely used in analytical chemistry to separate synthetic macromolecules and biopolymers. SDS is an anionic detergent used to supply a negative charge to proteins and to unfold them. The charge is usually proportional to the proteins size and proteins mass. A polyacrylamide gel is prepared between two glass plates and the proteins are placed at the top of the gel. By applying an electric field between the top and bottom of the gel, the proteins are forced to migrate across the gel from the negative electrode (cathode) to the positive electrode (anode). The size of the proteins causes them to migrate at different migration rates, the smaller molecules faster and the larger molecules slower, creating the separation (Figure 17).

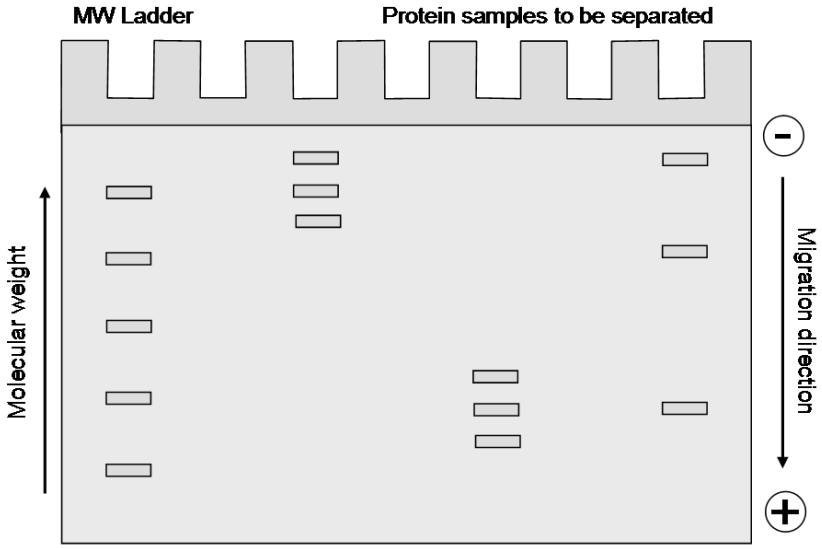

Figure 17. SDS-PAGE: One dimensional gel electrophoresis: proteins are separated according to their molecular weight by loading them at the top of a polyacrylamid gel and applying an electric field

For the electrophoretic analysis of a complex mixture such as the Aβ aggregation study, different types and concentrations of gels were used. In order to ascertain a set of standard conditions through the experiments two methods of SDS-PAGE were chosen for comparison: Tris/Glycine (Laemmli)

and Tris/Tricine (Schägger and von Jagow). Coomassie Brilliant Blue staining was used as a method of visualization for all the PAGE gels during this study.

The most used SDS-PAGE method is the Laemmli Tris/Glycine system, which proved insufficient in separating the low molecular weight oligomers and the high molecular weight aggregates simultaneously (Figure 18.a). By substituting Glycine with Tricine an improuved separation in the low molecular weight region of the gels was obtained (Figure 18.b). Therefore Tris/Tricine-PAGE was used for all subsequent experiments.

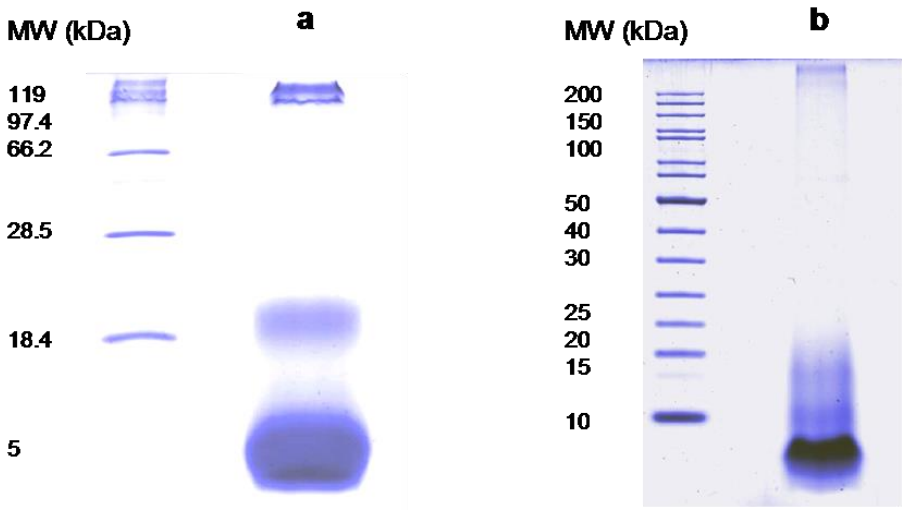

Figure 18. Poly-acrylamide gel tryptic characterization of Aβ(1-40) aggregation after 5 days of incubation at 37 °C by SDS-PAGE Tris/Glycine – Laemmli (a) and Tris-Tricine (b) methods. The second method has a higher power of separation in the low molecular weight range

After selecting the electrophoretic conditions, the aggregates were prepared in the following manner: 1 μg/μL Aβ(1-40) solution was prepared using several aggregation buffers (Table 1). The incubations were carried on at 37 °C for 5 and 16 days, respectively.

As shown in Figure 19, all buffers yielded low and high molecular weight aggregates after prolonged incubation time (16 days). For shorter periods of time however, only the buffer with a pH closer to physiological conditions showed both low and high molecular weight aggregates. Therefore

50 mM Na_3PO_4, 150 mM NaCl, pH 7.5 buffer was chosen for the next set of experiments.

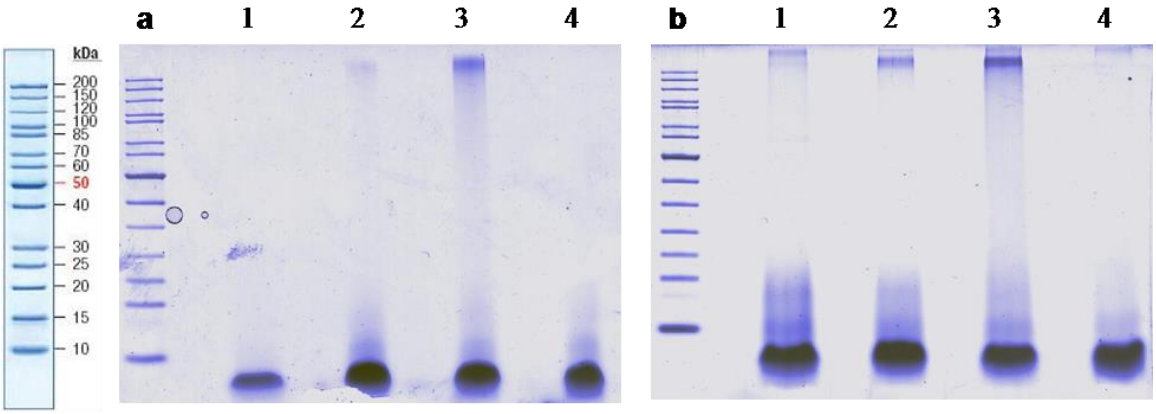

Figure 19. Aβ(1-40) aggregates after 5 (a) and 16 (b) days of incubation at 37 °C in 10 mM Tris, 150 mM NaCl, pH 8.8 (lane 1), 10 mM Tris (lane 2), 50 mM Na3PO4, 150 mM NaCl, pH 7.5 (lane 3) and 10 mM HCl, 150 mM NaCl (lane 4) respectively

2.1.6 In-gel digestion and mass spectrometric characterization of Aβ agreggates

When gel electrophores is not sufficient to determine the composition of a protein mixture, mass spectrometry is the key method for identification. The peptides and proteins are subjected to prior in-gel proteolytic digestion followed by a peptide mass fingerprint performed by MALDI-MS.

After Aβ(1-40) aggregation was carried out by in vitro incubation, the resulting aggregate mixture was subjected to polyacrylamide gel electrophoretic separation. In order to identify the composition of the separated species comprising the Aβ peptide, in-gel tryptic digestion was performed on the gel spots cut from the gel bands. As shown in Figure 18.a four gel bands were identified after gel electrophoresis. After destaining, the gel bands were swollen in a buffer containing Trypsin and incubated overnight at 37 °C. The digestion mixture was concentrated by freeze-drying and subjected to MALDI-ToF-MS analysis. The fragments identified by MS (Table 2) were searched against the National Center for Biotechnology Information

non-redundant protein database (NCBInr) using the MASCOT search engine. All four bands proved to consist only of beta-amyloid (1-40) peptide.

Table 2. Peptides from tryptic digestion of Aβ(1-40) SDS-PAGE gel bands identified by MALDI-MS

Gel band No.	Tryptic peptide masses [M+H]+	Aβ-peptides sequences
1	1084.6	[29 – 40]
	1326.0	[17 – 28]
	1337.0	[6 – 16]
	2393.7	[17 – 40]
	2643.6	[6 – 28]
2	1084.7	[29 – 40]
	1326.0	[6 – 16]
	1337.0	[17 – 40]
3	1085.8	[29 – 40]
	1336.3	[6 – 16]
	2392.6	[17 – 40]
4	1085.6	[29 – 40]
	1326.5	[17 – 28]
	1337.3	[6 – 16]
	2393.4	[17 – 40]
	3709.9	[6 – 40]

2.1.7 Mass spectrometric characterization of aggregated beta-amyloid peptides

The Aβ(1-40) monomer peptide can be characterized by MS using any type of ionization technique. Aβ(1-40) gives singly charged ions under matrix assisted laser desorption ionization and multiple charged ions, between four and seven, in electrospray.

Low molecular weight Aβ aggregates in aqueous solutions are in equilibrium with the monomers. Due to electrostatic repulsions of the hydration sphere, the lower number oligomers are unstable during electrospray ionization and, in contrast, more stable in MALDI-MS. High molecular weight aggregates are insoluble and precipitate making it impossible to detect via mass spectrometry alone.

In order to identify amyloid oligomers via MS, Aβ(1-40) was solubilized at a concentration of 50 µM in 10 mM ammonium acetate. The buffer was chosen in order to avoid salt concentrations that would interfere with matrix formation and desorption/ionization. The Aβ(1-40) peptide was incubated for 5 days at 37 °C, which yielded soluble aggregates. After incubation the Aβ(1-40) aggregates were prepared for MALDI-MS analyses (the sample was mixed with saturated alpha-cyano-4-hydroxycinamic acid (CHCA) matrix solution (1:1, v:v) on a MALDI target and left to dry. The target was introduced into a MALDI mass spectrometer and the sample measured.

As shown in Figure 20, the Aβ(1-40) yielded low molecular weight aggregates upon incubation at physiological pH in ammonium acetate buffer. In addition to the monomer, the Aβ(1-40) dimers and trimers could be observed in the mass spectrum together with traces of the Aβ(1-40) tetramer. Direct mass spectrometric identification of Aβ(1-40) oligomers is a direct proof of the oligomerization.

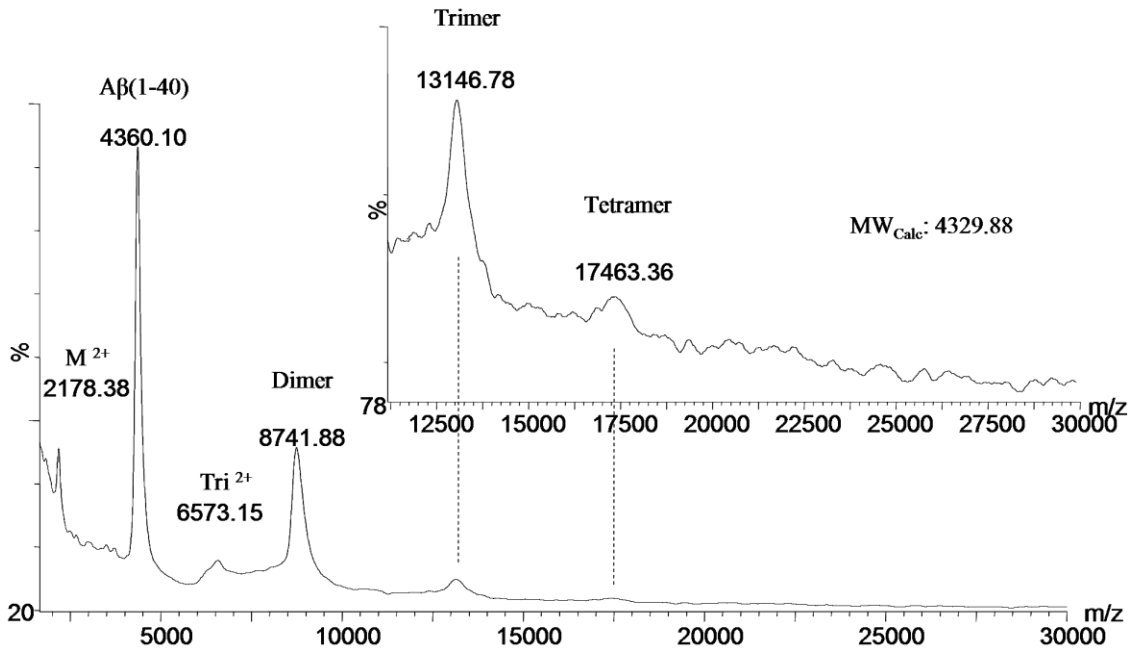

Figure 20. MALDI-TOF mass spectrum of Aβ(1-40) oligomers after 5 days of incubation at 37 °C (50 µM Aβ in 10 mM ammonium acetate buffer): singly charged ions of the dimer, trimer and tetramer and the doubly charged ion of the trimer are detected

.

2.2 Electron paramagnetic resonance and ion mobility mass spectrometry analyses of beta amyloid aggregation

Although mass spectrometry is still the best method for proteomics analysis, new analytical methods like electron paramagnetic resonance and ion mobility mass spectrometry are used in parallel. Electron paramagnetic resonance is an investigation method base on the fact that unpaired electrons are able to absorb and reemit electromagnetic energy when placed in a magnetic field. Unpaired electrons are present only in radical molecules. 3-(2-iodoacetamido)-2,2,5,5-tetramethyl-1-pyrrolidinyloxy (IPSL) is a stable radical with an unpaired electron present at the oxygen atom. IPSL can be attached to a peptide or protein via a condensation reaction with the thiol group of a Cysteine. A cysteinyl residue was inserted at the N- and C-terminal of the Aβ(1-40) sequence in order to make EPR determinations of Aβ oligomers. Ion mobility spectroscopy is an analytical method able to separate molecules according their shape. Molecules are ionized and pushed by an electric field through a neutral gas. The ions are loosing kinetic energy by the collisions with neutral gas molecules and slow down. The higher the collision cross section of an ion is, the higher the chances of a collision are and the slower its speed is. When combined with MS, ion mobility mass spectrometry is able to separate ions both according to their m/z ratio and their size and shape.

2.2.1 Synthesis of cysteine derivates of beta amyloid peptides

In order to attach the IPSL to the backbone of the Aβ(1-40) peptide a cysteine (Cys) had to be inserted in the sequence. In the first part of this study a Cys was attached to the N-terminal of the peptide. Cys-Aβ(1-40) was synthesized by SPPS, Fmoc chemistry, on a 50 μM scale. The raw peptide was purified by RP-HPLC and the composition and purity of the eluted fraction was established by MALDI-ToF-MS investigations (Figure 21).

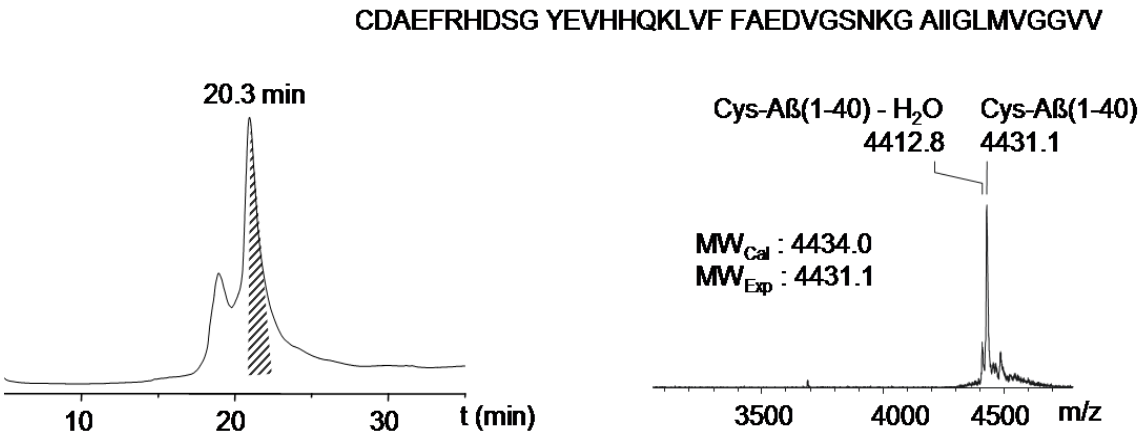

Figure 21. Cys-Aβ(1-40) RP-HPLC purification chromatogram profile and the MALDI-TOF mass spectrum

After synthesis and purification, the N-Cysteinyl-Aβ(1-40) peptide was further characterized by ESI-IonTrap-MS (Figure 22). The peptide proved to be pure, mass spectrum presenting peaks corresponding to both the intact and dehydrated analyte.

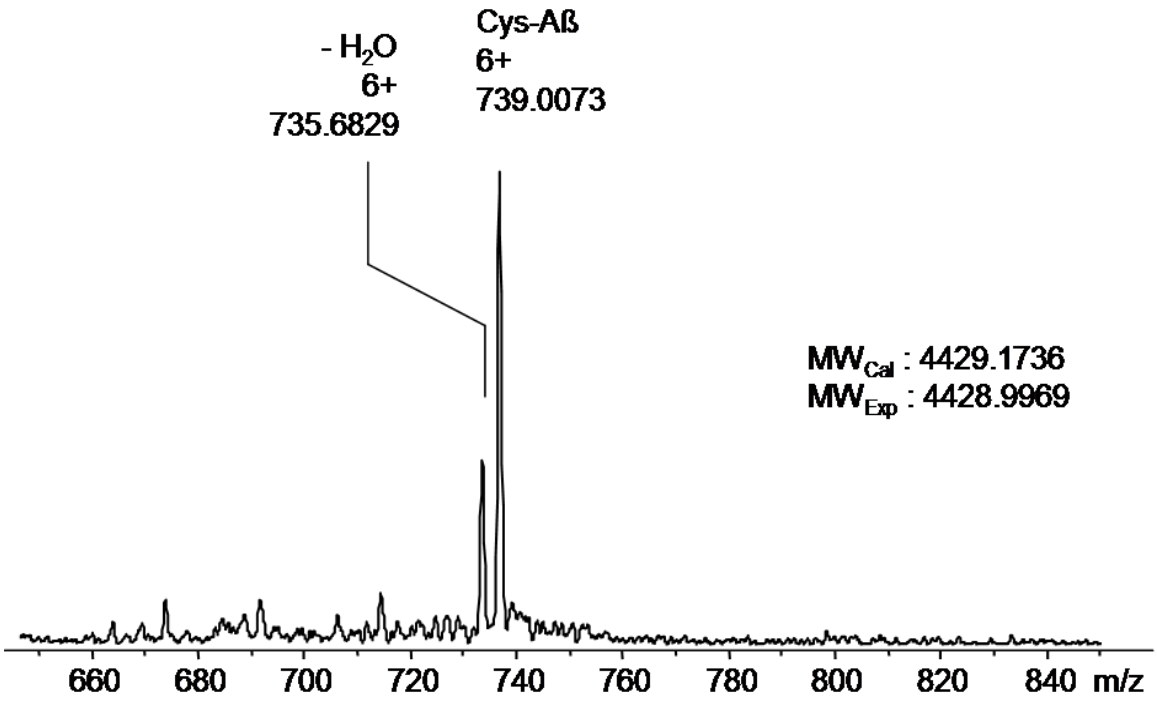

Figure 22. ESI-ion trap-MS spectrum of the Cys-Aβ(1-40) synthetic peptide

2.2.2 Attachment of the spin label

In order to perform electron paramagnetic resonance measurements, a label containing an unpaired electron has to be inserted in the peptide 3-(2-iodoacetamido)-2,2,5,5-tetramethyl-1-pyrolidinyloxy (Figure 23), also know as IPSL (iodo-proxyl spin label), is a stable radical with an unpaired electron present at the oxygen atom. IPSL has an iodoacetamido group that can react with the thiol group of a cysteine. A cysteinyl residue was inserted at the N- and C-terminal of the Aβ(1-40) sequence in order to make the attachment of IPSL to the Aβ(1-40) peptide possible.

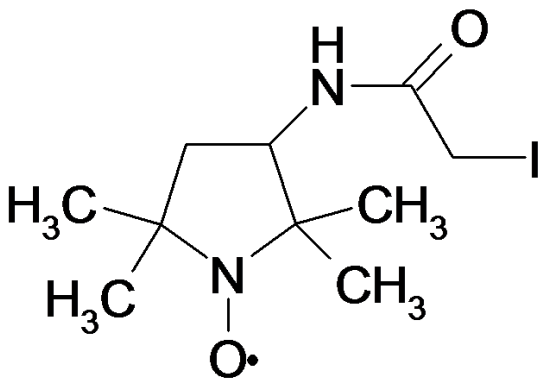

Figure 23. 3-(2-iodoacetamido)-2,2,5,5-tetramethyl-1-pyrolidinyloxy, also knowns as iodo-proxyl spin label (IPSL) has an unpaired electron at the oxygen atom

The coupling of the IPSL label to the Cys-Aβ(1-40) molecule was done through an alkylation reaction of the thiol group (Figure 24). To ensure the complete alkylation of the peptide a 6-fold molar excess of IPSL was used. A solution of 200 µM Cys-Aβ(1-40) and 1200 µM IPLS was prepared in a 25 mM Tris buffer, pH 9, and incubated at 4 °C for 12 h [146].

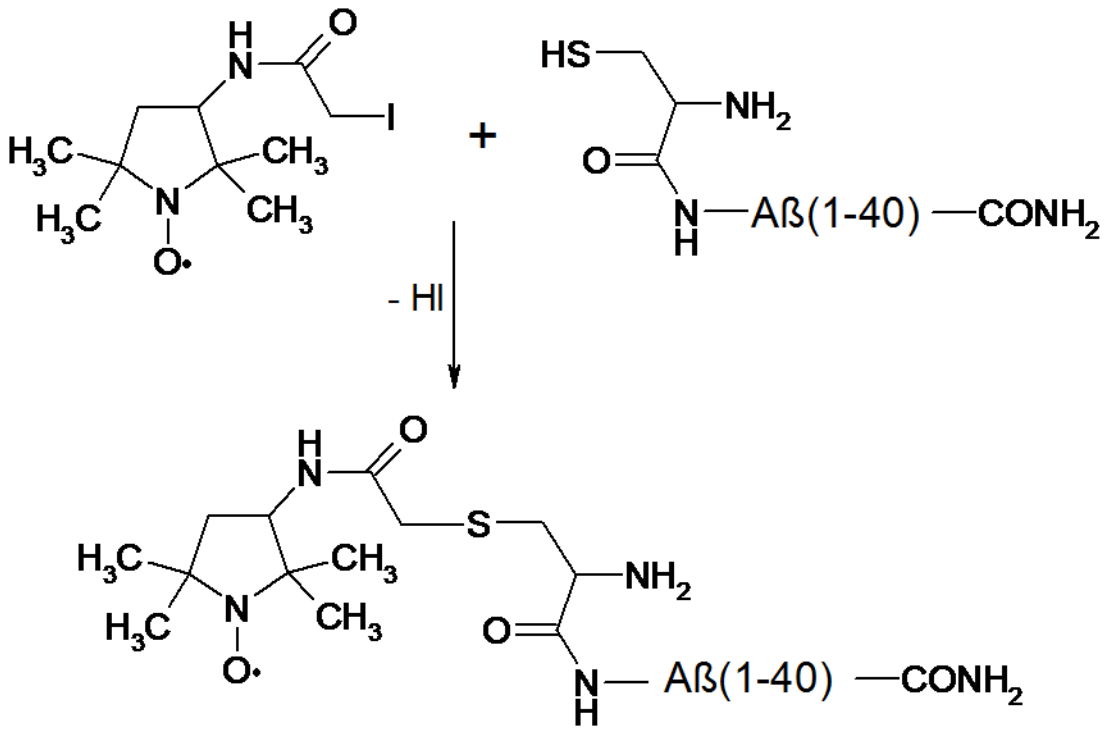

Figure 24. Alkylation reaction between IPSL (1200 µM) and beta amyloid peptide (200 µM) in 25 mM Tris buffer, pH 9 upon incubation at 4 °C for 12 h

2.2.3 Purification and mass spectrometric characterization of IPSL-Cys-Aβ(1-40)

To isolate the pure product after the labeling reaction, the reaction mixture was purified by RP-HPLC. A semi-preparative Vydac C4 column was used as stationary phase and acetonitrile based solvents as mobile phase. The solvents were acidified with 0.1% TFA and the flow rate was set at 4 mL/min. The unreacted IPSL in excess eluted first (RT: 13.6 min), followed by the labeled IPSL-Cys-Aβ(1-40) (RT: 21.5 min). After elution, the fraction of interest was subjected to MALDI-ToF-MS analysis for composition and purity confirmation. The chromatogram and mass spectrum showed that the labeling reaction was total (Figure 25) and no byproducts were observed. The purified IPSL-Cys-Aβ(1-40) was subjected to further mass spectrometric analysis by ESI-IonTrap-MS (Figure 26). The spectrum confirmed the high purity of the analyte.

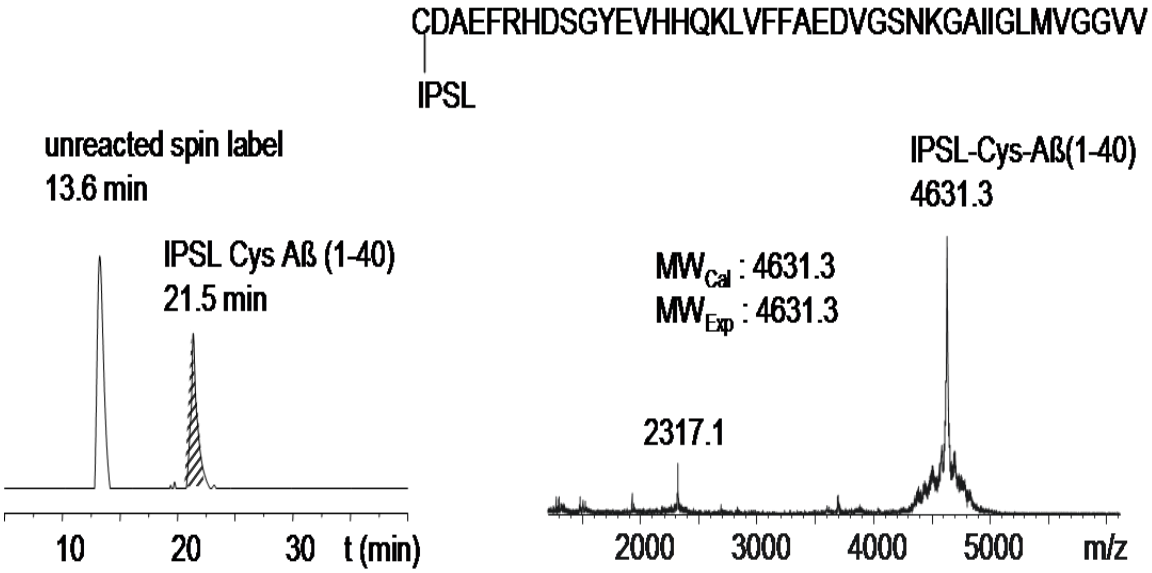

Figure 25. IPSL-Cys-Aβ(1-40) purification chromatogram profile and the MALDI-TOF mass spectrum

.

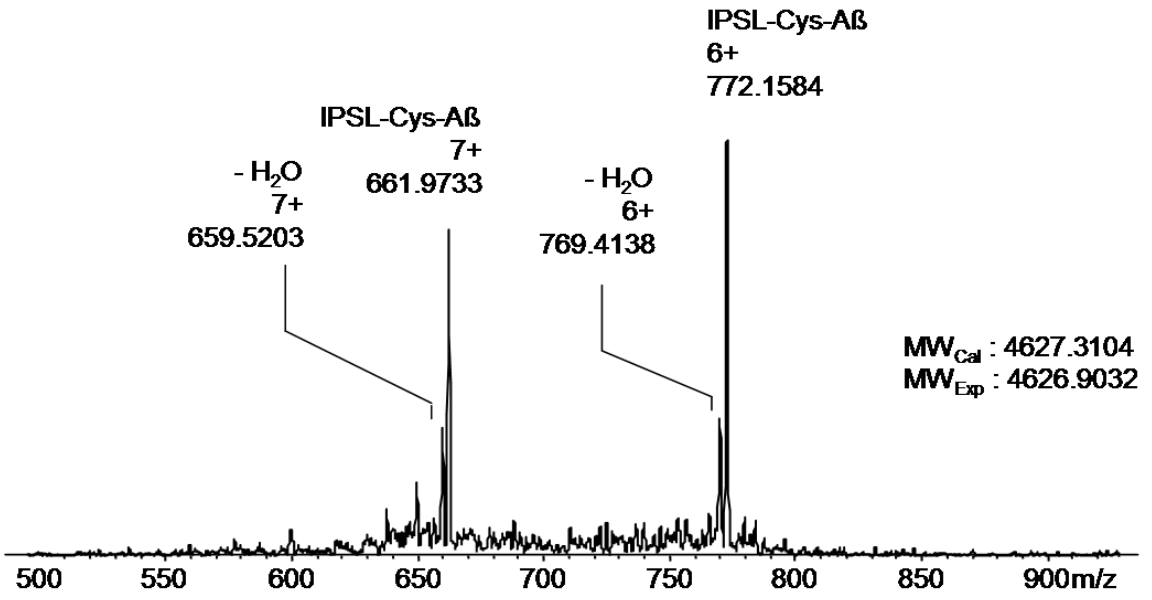

Figure 26. ESI-ion trap-MS spectrum of IPSL-Cys-Aβ(1-40) peptide

2.2.4 Electron paramagnetic resonance characterization of spin labeled beta amyloid (1-40)

To analyze the local mobility of the spin label coupled to the Aβ(1-40) peptide before and after aggregation, an IPSL-Cys-Aβ(1-40) sample was subjected to aggregation as described in 2.1.4. After five days of incubation the labeled amyloid peptide yielded a white opaque solution. High molecular weight components were separated by centrifugation for 15 min at 13000 rpm and a white pellet was separated from the supernatant. A freshly prepared IPSL-Cys-Aβ(1-40) solution was also used for comparison. The insoluble high molecular weight aggregates were suspended in MilliQ water before the samples were loaded into glass capillaries for EPR measurements. After acquirement, the spectra were exported in Matlab (The MathWorks Inc., Natick, Massachusetts, USA) and were fitted against theoretically calculated spectra using the EasySpin [147] package (Figure 27). The fitting experiments were set to simulate a complex composition similar to that observed in the gel electrophoresis in 2.1.5.

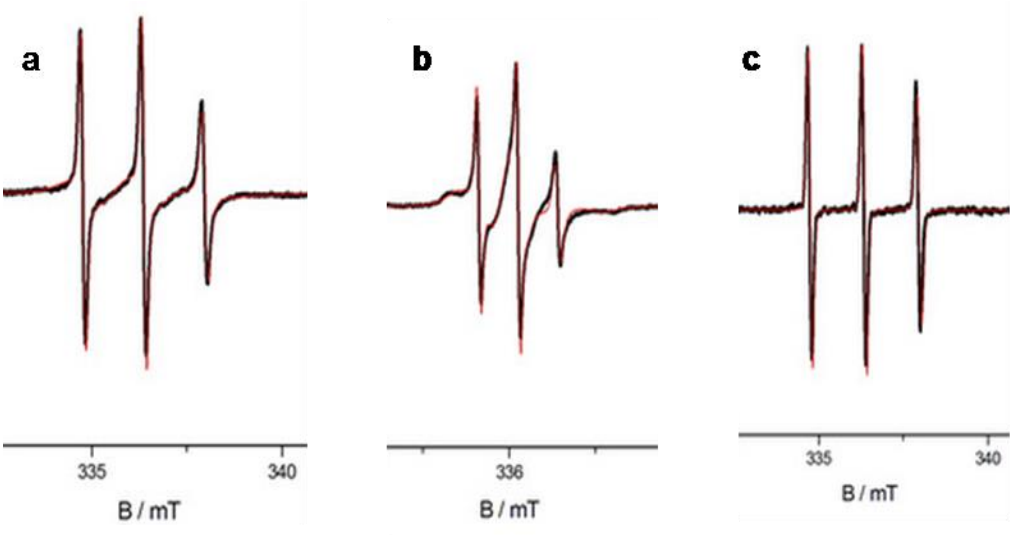

Figure 27. CW-EPR spectra (black) and fitted theoretical curves (red) of freshly solubilized IPSL-Cys-Aβ(1-40) (a) and aggregates after 5 days incubation, centrifuged precipitate (b) and supernatant (c)

Four species could be calculated from the simulations: a fast moving, small component, with a small correlation time of 0.036 ns, a slow moving, large component, with a correlation time of 5.46 ns, and two intermediate species with correlation times of 0.394 and 0.803 ns, respectively (Table 3) [117].

Table 3. Composition of amyloid beta incubation fractions. Four components with different rotational correlation times are contributing to the EPR spectra.

IPSL-Cys-Aβ 0-5 day	Component 1 0.036 ns	Component 2 0.394 ns	Component 3 0.803 ns	Component 4 5.46 ns
Fresh	0.19	0.30	0.51	0.00
Precipitate	0.01	0.02	0.21	0.76
Supernatant	1.00	0.00	0.00	0.00

From the EPR spectra interpretation it was concluded that after five days of incubation and centrifugal separation, the supernatant fraction contains only free, non aggregated peptide, while the precipitate contains high molecular weight aggregates (76%) consistent with fibrils and some lower molecular aggregates (21%) consistent with oligomers. The freshly prepared peptide showed an even composition of monomers (19%) and oligomers (30% and 51%) which indicates that the aggregation process starts instantly during the solubilisation of the peptide.

2.2.5 Aggregation study of modified beta amyloid peptides by Tris-tricine gel electrophoresis

The spin label attachment to the amyloid beta peptide is a perturbing factor for its natural aggregation pattern. To compare to which extent this affects the peptide folding, N-terminal and C-terminal labeled Aβ(1-40) peptides were synthesized by SPPS and purified by RP-HPLC.

Three samples of modified and unmodified peptides, Aβ(1-40), IPSL-Cys-Aβ(1-40), and Aβ(1-40)-Cys-IPSL were subjected to aggregation by

solubilisation in fibril growth buffer at 200 µM and incubation for five days at 37 °C. After incubation the aggregates were separated by centrifugation from the free monomers. For comparison, a series of freshly solubilized peptides were prepared and were briefly incubated for one minute and one hour respectively. The samples were mixed with sample buffer and Tris-Tricine PAGE was performed. The gels were stained with a Coomassie Brilliant Blue solution for visualization (Figure 28).

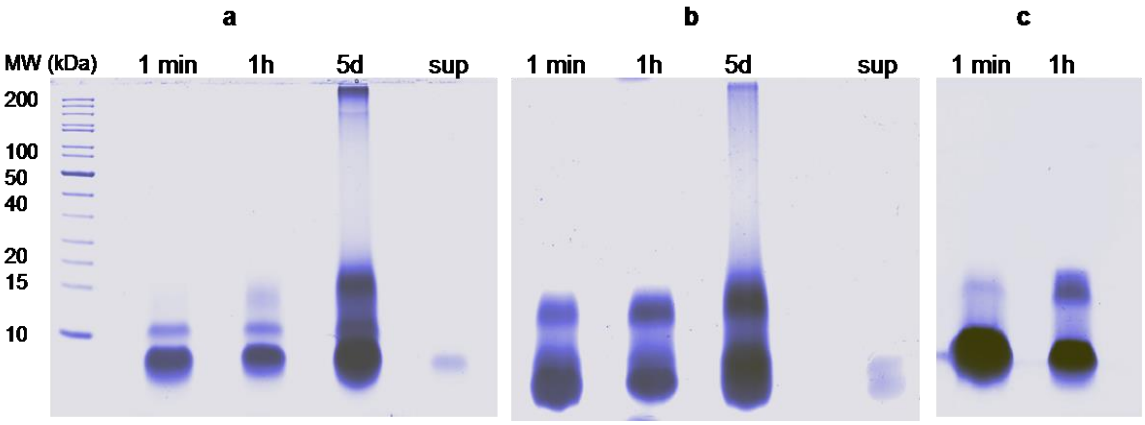

Figure 28. Tris-Tricine PAGE of IPSL-Cys-Aβ(1-40), (a), Aβ(1-40)-Cys-IPSL, (b), and Aβ(1-40), (c), after successive times of incubation: 1 minute, 1 hour and 5 days. After 5 days the samples were centrifuged and the precipitated fibrils separated from the supernatant

The gel electrophoresis showed that the amyloid peptides start to aggregate immediately after solubilisation with no difference between the three peptides. After five days of incubation, however, an effect of the Aβ sequence modification was visible. While the N-terminal modified peptide showed a high yield in high molecular weight aggregates, the C-terminal modified peptide shows a much lower yield. This is an indication that the C-terminal end of the amyloid beta peptide is highly packed inside the fibrils structure and any modification in this region would prevent the transition from oligomers to fibrils.

2.2.6 Aggregation study of modified beta amyloid peptides by Thioflavin T assay

Thiolavin T (ThT) is a specific dye for amyloid beta sheets. It is used to characterize the presence of misfolded proteins in Alzheimers Disease[148]. When this hydrophobic molecule aligns itself along the beta sheets, a red shift appears in its fluorescence[149]. Free ThT absorbs at 342 nm and emits at 430 nm while when bound to fibrils it absorbs at 442 and emits at 482 nm. This ThT property makes the method a good approach to quantify the amyloid plaques present in tissue and to diagnose Alzheimers Disease.

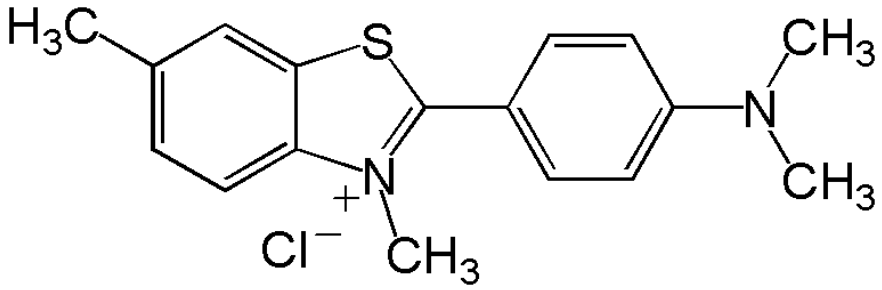

Figure 29. Thioflavin T molecule, chloride salt

To better characterize the difference between N- and C-terminal modified amyloid beta peptides and the influence of the modification upon aggregation, the aggregates were investigated using the Thioflavin T assay. Peptide samples were solubilized at 200 µM in fibrilization buffer and incubated for 5 days at 37 °C. After separation by centrifugation, the fibrils were suspended with 50 µL MilliQ water. Thioflavine T was solubilized in 50 mM Glycine solution (pH 8.5) at 100 µM. Before the measurement 50 µL peptide samples were mixed with 50 µL Thioflavin solution and measured on a Wallac 1420 Victor 2 (PerkinElmer) reader. A 450 nm filter was used for excitation and 486 nm for emission readings for 0.1 seconds.

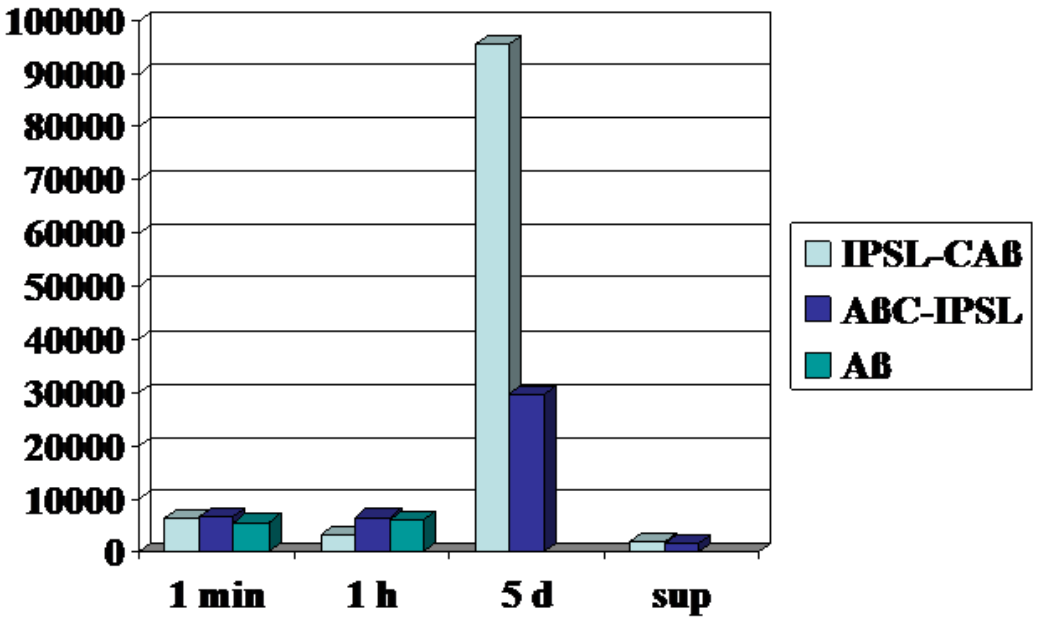

Figure 30. Thioflavin T fluorescence monitoring of spin labeled Aβ peptides during incubation over different periods of time at 37°C

The Thioflavin T fluorescence measurements (Figure 30) showed an increase in signal with time indicating the formation of fibrils. After five days of incubation, the IPSL-Cys-Aβ(1-40) showed a three fold higher emission intensity than the Aβ(1-40)-Cys-IPSL. The supernatant showed lithe to none emission. These experiments show that prolonging the Aβ sequence with a Cysteine residue at the C-terminal and attaching the spin label to it has a direct effect on fibrilization. This conclusion s in full agreement with the Tris-Tricine PAGE experiment.

2.2.7 Electron paramagnetic resonance characterization of N-terminal and C-terminal labeled beta amyloid peptide

The influence of the spin label position on the peptide backbone can be also observed by electron paramagnetic spectroscopy. In this case the mobility of the spin label can determine which of the N- and C-terminal ends of the Aβ(1-40) peptide is more freely moving in the aggregates. Two samples of N- and C-terminal labeled amyloid beta peptides were incubated for 5 days at 37 °C in fibrilization buffer.

The supernatant rich in monomers was separated from the precipitated aggregates and subjected to EPR measurements. The two supernatant samples showed no difference in signals (Figure 31) proving that there are only free moving monomers in the solutions.

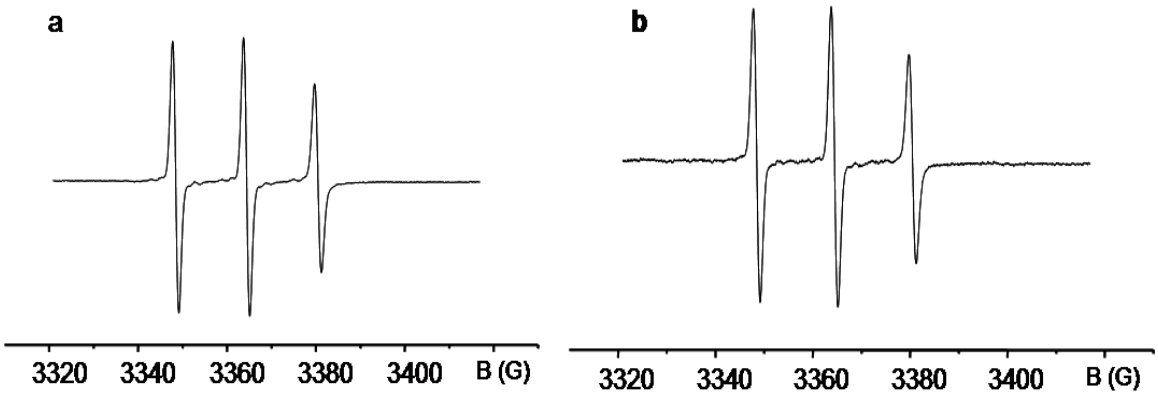

Figure 31. CW-EPR spectra of the centrifuged supernatant solution containing the IPSL-Cys-Aβ(1-40) (a) and Aβ(1-40)-Cys-IPSL (b) monomers after 5 days of incubation at 37°C

EPR signals of the precipitates, on the other hand, were different in shape. The C-terminal labeled Aβ(1-40)-Cys-IPSL peptide showed a more fluctuating EPR signal than the N-terminal labeled IPSL-Cys-Aβ(1-40), as observed in Figure 32. The more distorted a signal is from the three sharp peaks characteristic to the free moving IPSL, the more hindered and fixed into position the label is. This is consistent once again that the C-terminal of Aβ peptide is at the core of the fibrils structure.

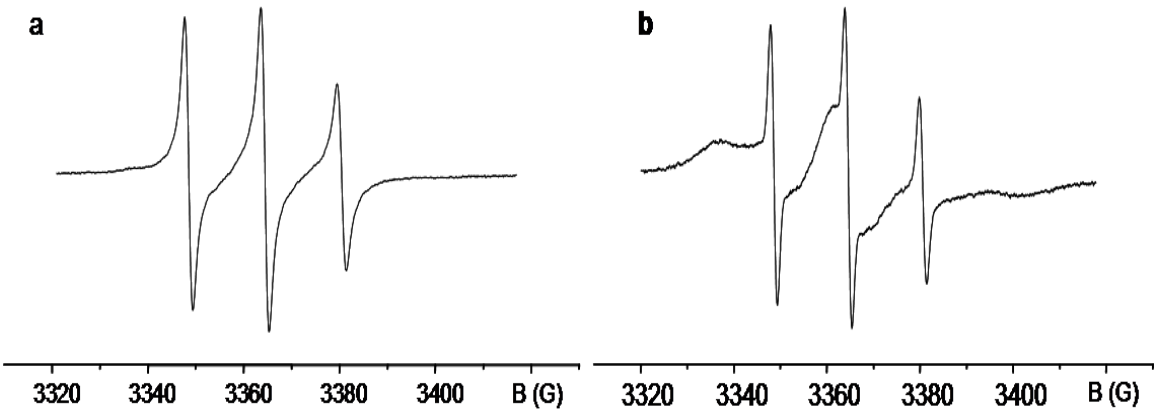

Figure 32. CW-EPR spectra of the centrifuged precipitate containing the IPSL-Cys-Aβ(1-40), (a), and Aβ(1-40)-Cys-IPSL (b) aggregates after 5 days of incubation at 37 °C

2.2.8. Ion mobility spectroscopy mass spectrometry of beta amyloid aggregates

Ion mobility mass spectrometry is a new mass spectrometric method that uses the advantage of a drift tube to separate ions prior to MS measurement. The drift tube uses the drag of a counter flowing neutral gas to slow down the charged analyte ions and to separate them upon their average cross-section. Depending on the technology, the ions can be accelerated at the beginning of the drift tube, or could be pushed along the tube by a caring voltage wave generated by a set of ring electrodes (Figure 33). The later method is a more flexible solution permitting several drift tubes to be coupled together for a tandem IMS-IMS characterization by fragmentation.

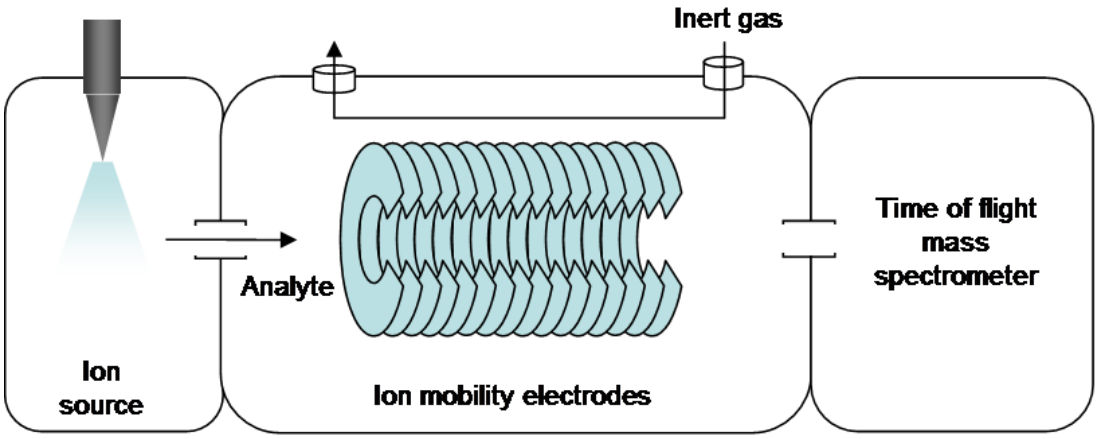

Figure 33. Ion mobility instrument with an ESI ion source, a carrying wave drift tube and a time of flight mass spectrometer.

Before the IMS-MS measurements two Aβ(1-40) solutions were prepared. One Aβ(1–40) peptide solution (220 μM) was incubated for 5 days at 37 °C and soluble oligomers were separated by centrifugation. The other solution was similar in concentration but freshly prepared. The soluble fraction of the Aβ(1–40) fibril preparation and the fresh one were subjected to comparative analysis by ion mobility spectroscopy mass spectrometry (Figure 34) [117, 150].

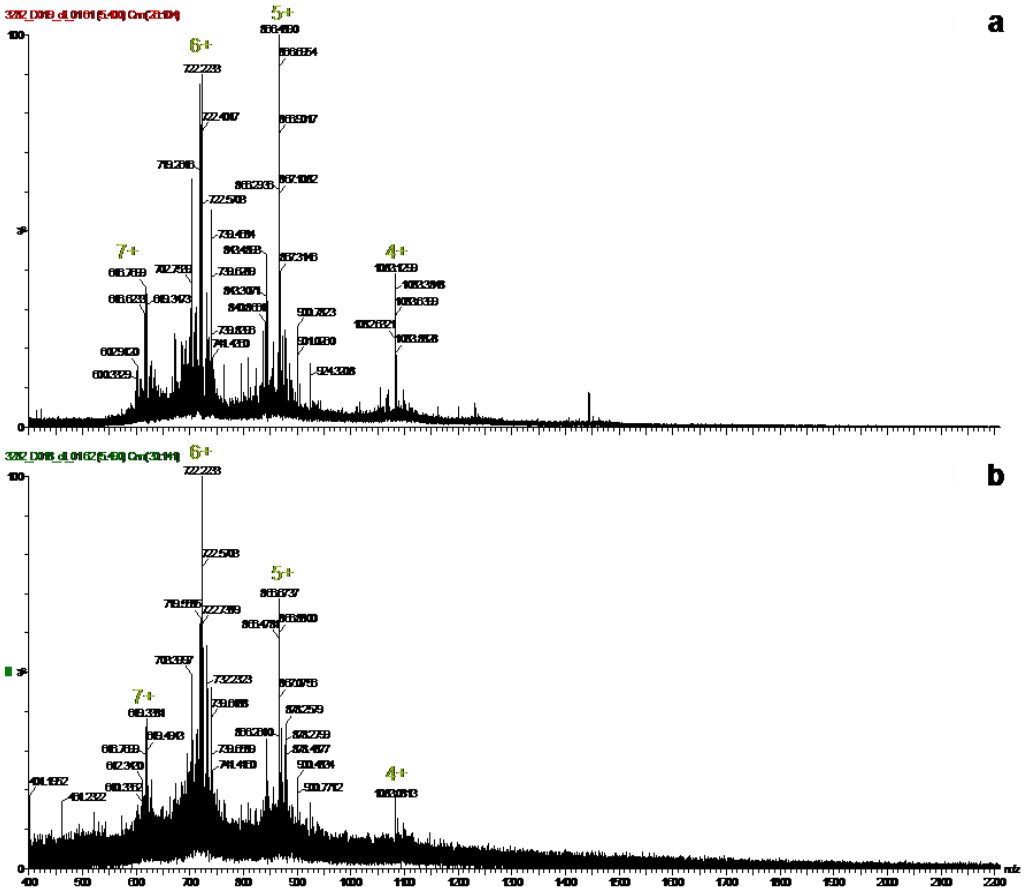

Figure 34. Ion mobility MS analysis of (a), freshly prepared Aβ(1-40); (b), supernatant after 5 days of incubation

In the case of freshly prepared Aβ(1–40) the 5+ charged ion was found to be the most abundant, while in the fibril preparation supernatant the 6+ charged ion was the predominant one. The signal to noise ratio of the $[M+5H]^{5+}$ and $[M+6H]^{6+}$ ions was higher in the freshly prepared Aβ(1–40) sample than in the fibril preparation supernatant, confirming that a consistent amount of Aβ(1–40) monomer formed aggregates in the later sample.

Analyzing the IMS-MS drift scope of the Aβ oligomers supernatant (Figure 35) two conformational states with different mobility drift times could be observed. One conformation had the predominant ion charge 5+ and a second one 6+ which may be indicative of a change in shape due to unfolding during the oligomerization process.

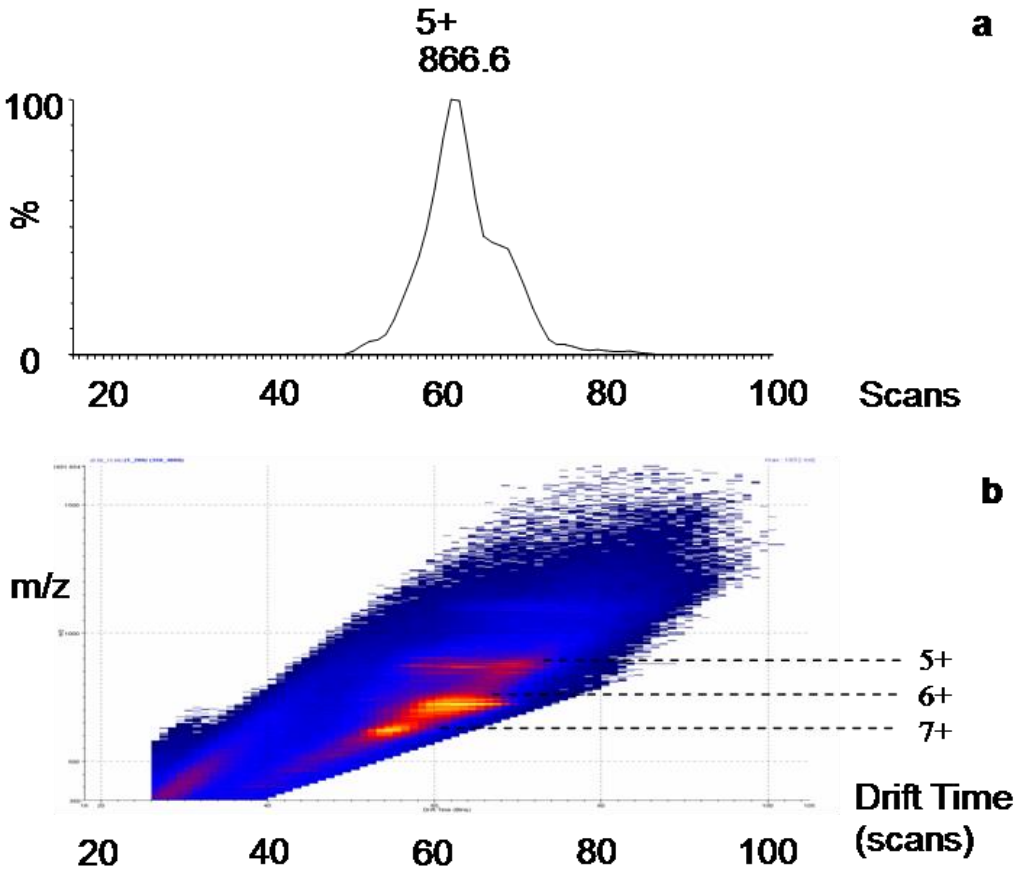

Figure 35. Drift time profile of the Aβ(1-40) supernatant after 5 days of incubation. (a), the ion mobility profile for the $[M+5H]^{5+}$ ion and, (b), the drift scope

To compare the evolution of the two conformational states analyses of the extracted mobility profiles of the Aβ sample were performed before and after incubation. From the peak area of the 5+ charged ion from the freshly prepared Aβ(1-40) (Figure 36.a) and the incubated peptide (Figure 36.b), it was observed that upon incubation the proportion of the first conformation (A) was decreased compared to the second conformational state (B).

From the mass spectrometric data of the ion mobility two modifications of Aβ peptide were observed in the deconvoluted spectrum of the fibril preparation: the oxidation at the Met^{35} residue of Aβ(1-40) and the loss of one water molecule (Figure 37).

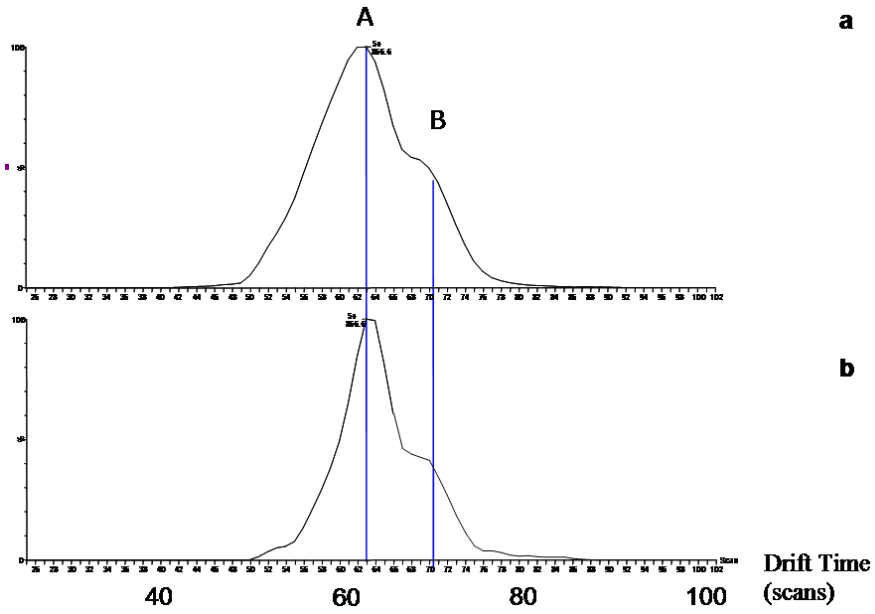

Figure 36. Extracted ion mobility profiles for m/z 866.6, $[M+5H]^{5+}$ from freshly prepared Aβ(1-40) solution (a) and supernatant after 5 days of incubation (b)

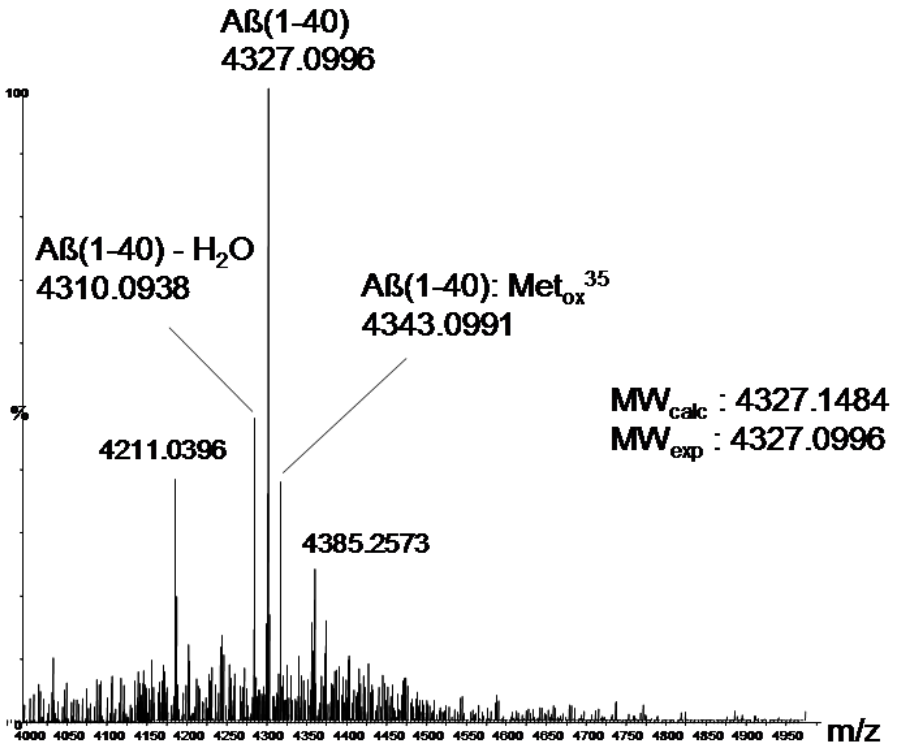

Figure 37. Ion mobility MS analysis of the Aβ(1-40) supernatant after 5 days of incubation. The deconvoluted spectrum showed the presence of the Met 35 – sulfoxide oxidized product.

2.3 Identification of antigen recognition domains by affinity mass spectrometry

2.3.1 Affinity – mass spectrometric approaches for protein epitope identification

Antibody compexes with proteins or peptide antigens are interactions of non-covalent nature. The antibody domain involved in the interaction is called paratope while the antigen binding domain(s) is called epitope. Each antibody recognizes a single epitope. A monoclonal antibody is an Ab produced by identical immune cells (clones). A polyclonal antibody is an antibody produced by different B cells lines and recognizes the same antigen. Proteolytic epitope excision and – extraction are two complementary chemical methods for the identification of antibody-antigen interaction sites () initially developed in our laboratory [68-71, 83].

2.3.2 Affinity mass spectrometric determination of alpha galactosidase epitope

2.3.2.1 Preparation of anti-alpha-galactosidase antibody affinity column

Alpha galactosidase (A-Gla) is an enzyme that hydrolyses the terminal alpha-galactosyl groups from glycoproteins. The genetic information for this enzyme is encoded on the X-chromosome and its absence (e.g., through mutations) can lead to Fabry disease, one of the many members of the lysosomal storage diseases (LSD) family. In order to determine the alpha galactosidase epitope against a monoclonal antibody, the alpha galactosidase enzyme and anti-alpha galactosidase antibody, obtained from Sino Biological (Beijing), were employed. The anti- alpha galactosidase antibody was immobilized on an activated sepharose micro column by incubation for two hours at 37 °C under agitation. After coupling, the excess unbound antibody was washed away and the remaining active binding sites were blocked with ethanolamine.

After preparation, the antibody column was tested with the A-Gla protein antigen. The enzyme was loaded onto the affinity column and incubated for two hours at 37 °C. The unbound protein was removed from the column and the column washed with PBS and water. The bound protein was then eluted from the column by changing the pH from 7 to pH 1 with 0.1% TFA in water. The supernatant, last wash and elution fractions were lyophilized and prepared for SDS polyacrylamide gel electrophoresis analysis. After staining with Coomassie Brilliant Blue a set of bands with molecular weights of 50, 150 and over 200 kDa were observed in the supernatant and elution fractions, but none in the washing fraction (Figure 38).

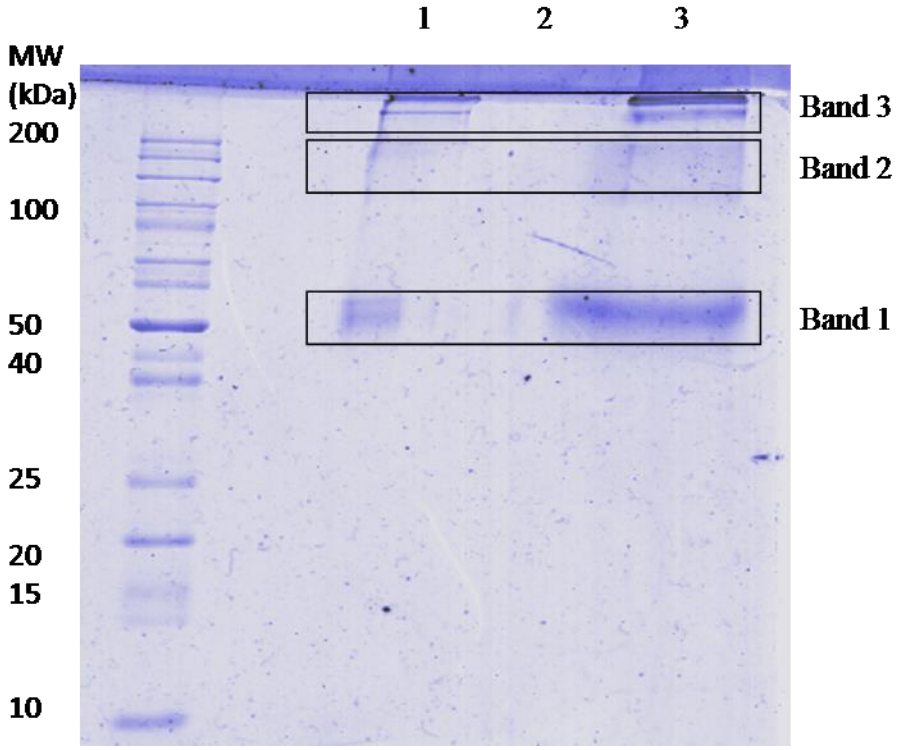

Figure 38. A-Gla affinity column testing: lane 1 supernatant, lane 2 last wash and lane 3 elution, and the three horizontal bands marked for excision and in-gel digestion

To determine the composition of the unknown protein gel bands, they were excized and prepared for digestion. First the bands were destained by a series of alternating steps of de- and re-hydration with acetonitril and trypsin solutions. After destaining the bands were dried and swollen in a cooled solution containing Trypsin. The in-gel digestion was performed for 12 hours at 37 °C. After extracting the digestion mixture from the gel bands, the

samples were subjected to MALDI-ToF mass spectrometric characterization (Figure 39, Figure 40 and Figure 41).

After mass spectrometric analyses the identified masses were searched using the MASCOT peptide mass fingerprint against the NCBInr database,and alpha galactosidase enzyme was identified in all three gel bands as being the only constituent (Figure 42).

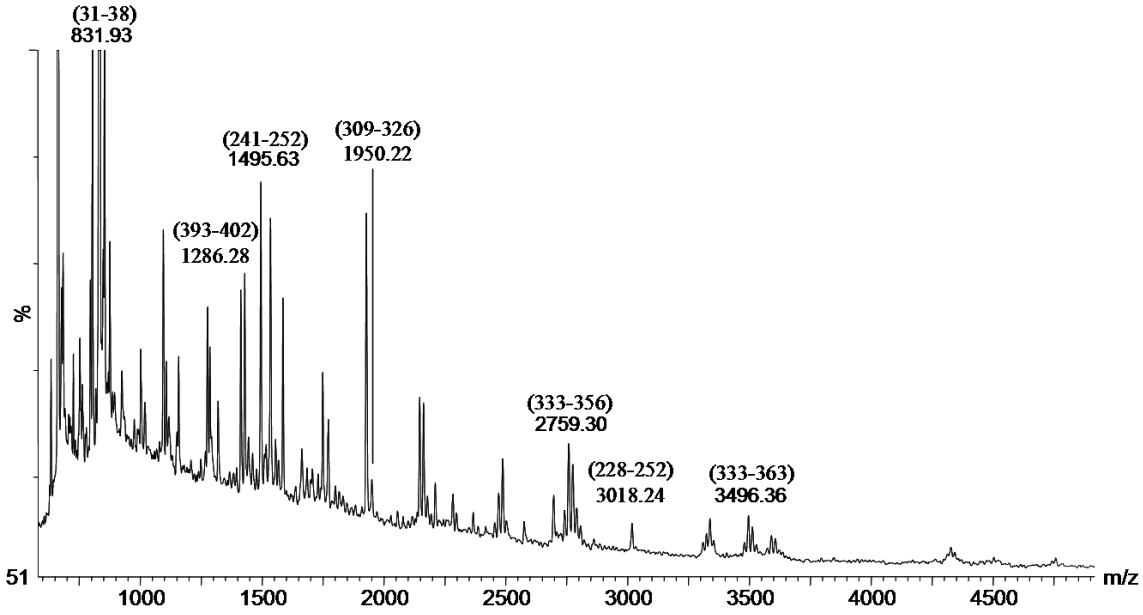

Figure 39. MALDI-ToF mass spectrum of in-gel tryptic digestion of A-Gla SDS band 1

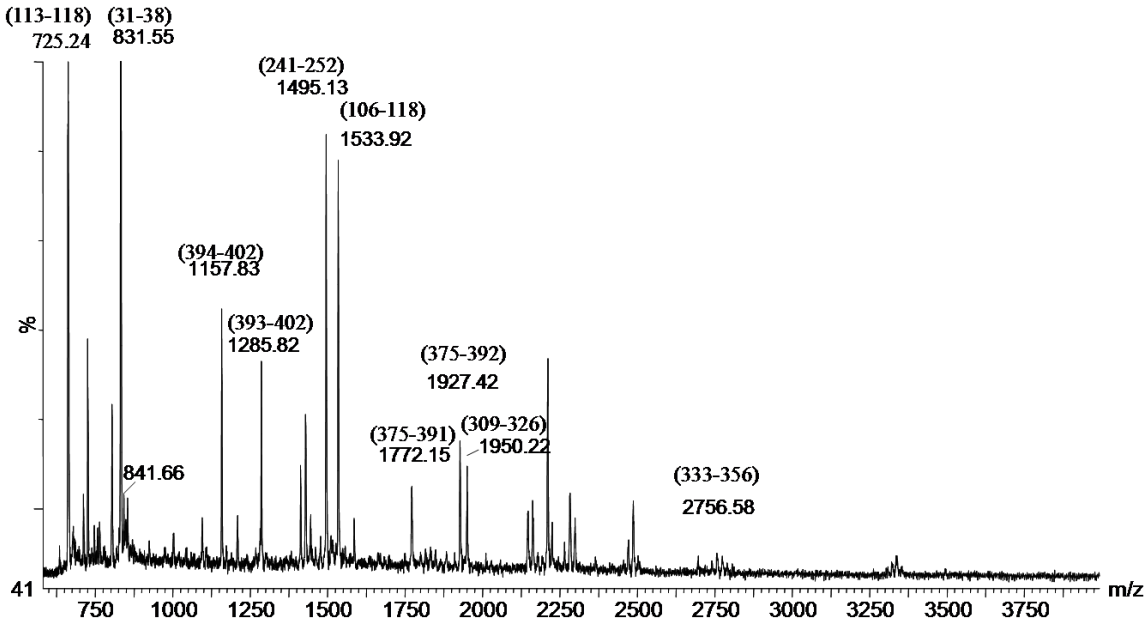

Figure 40. MALDI-ToF mass spectrum of in-gel tryptic digestion of A-Gla SDS band 2

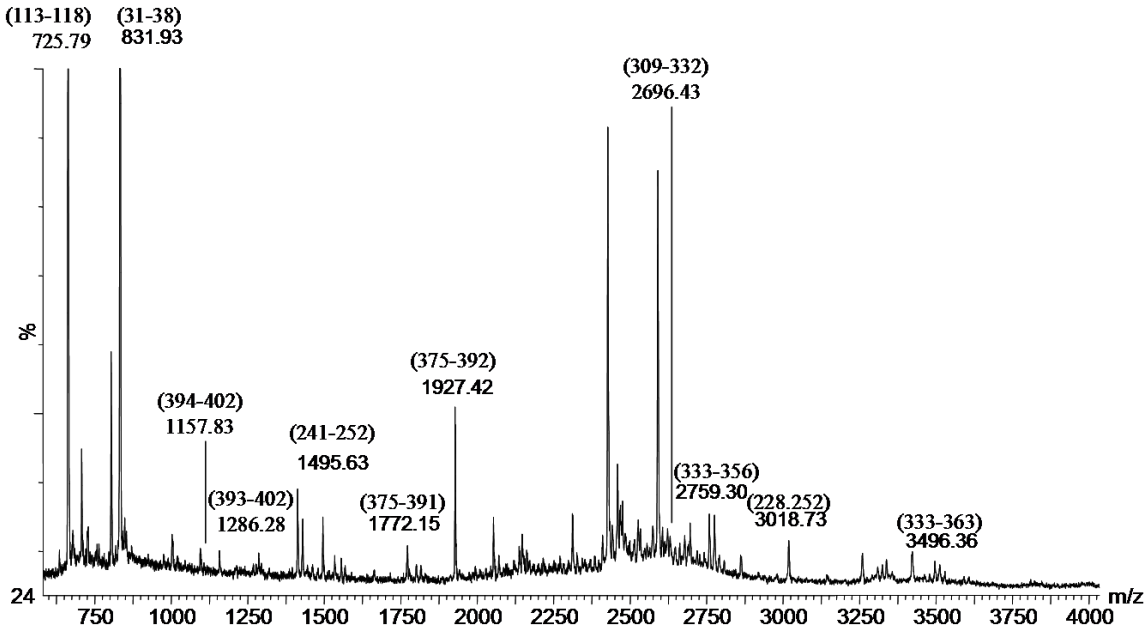

Figure 41. MALDI-ToF mass spectrum of in-gel tryptic digestion of A-Gla SDS band 3

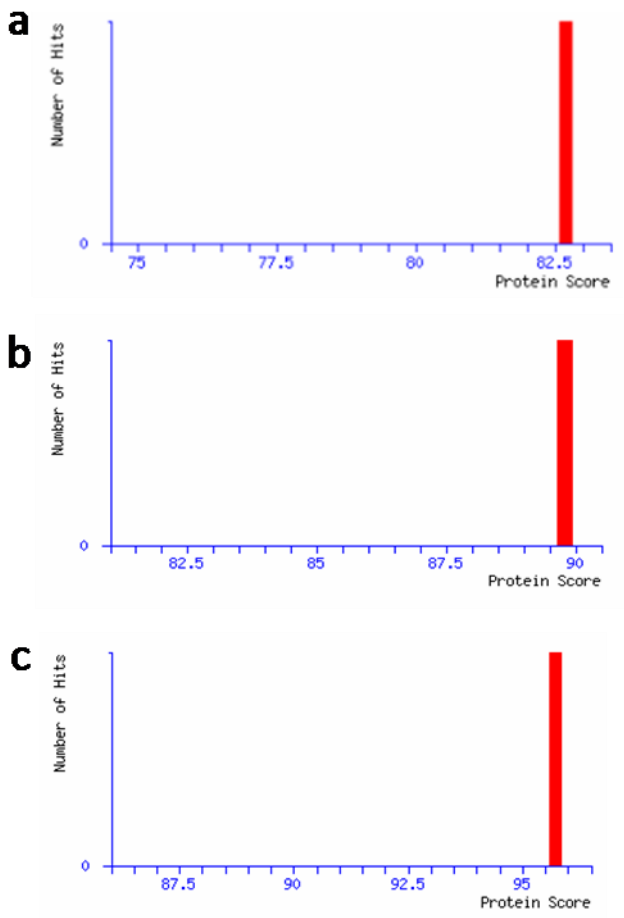

Figure 42. Database search identification scores of A-Gla in-gel digestion band 1 (a), 2 (b) and 3 (c) respectively

2.3.2.2 Epitope determination of alpha-galactosidase by epitope excision mass spectrometry

For the determination of the A-Gla epitope against the anti-A-Gla antibody, 20 µg alpha galactosidase was loaded onto the anti-A-Gla column. The column was incubated for two hours at 37 °C under agitation and the supernatant discarded. After washing, a solution of trypsin in PBS was added to the column. To allow the protease to digest the A-Gla, the column was again incubated for two hours at 37 °C under agitation. The supernatant was collected and lyophilized. Subsequently the supernatant was desalted and concentrated using a desalting pipette tip (ZipTip) in preparation for mass spectrometric characterization (Figure 43).

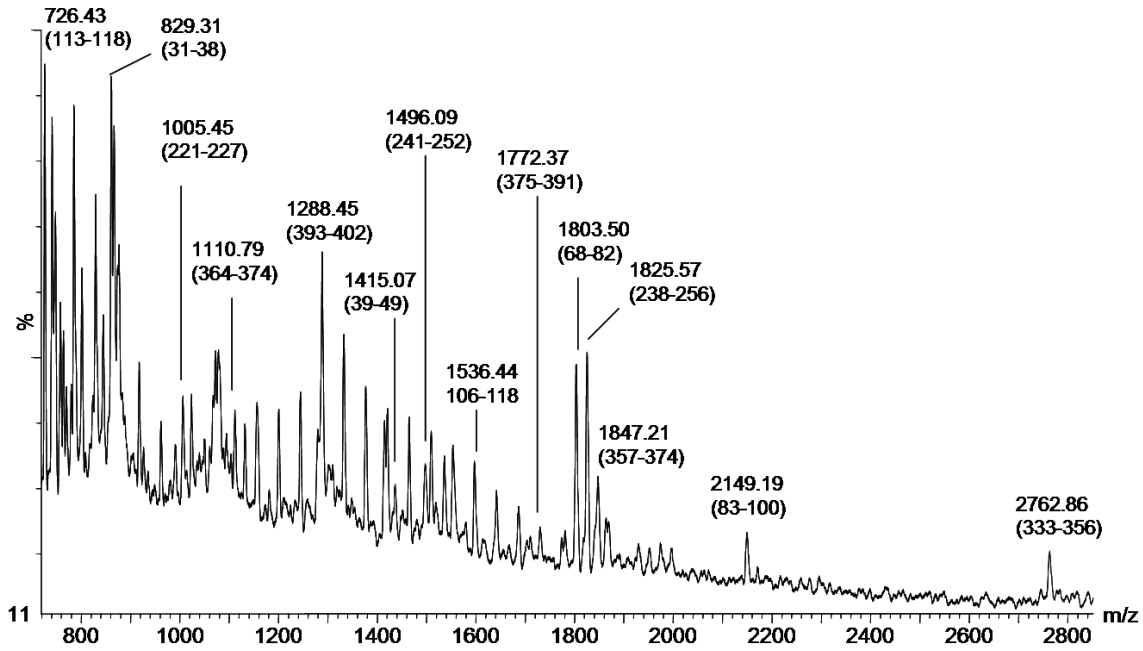

Figure 43. MALDI ToF mass spectrum of A-Gla tryptic digestion epitope excision supernatant fraction

The MALDI-ToF mass spectrum revealed a large number of peaks that were identified as A-Gla tryptic digestion fragments. The identification was confirmed by peptide mass-fingerprinting and database search (Figure 44).

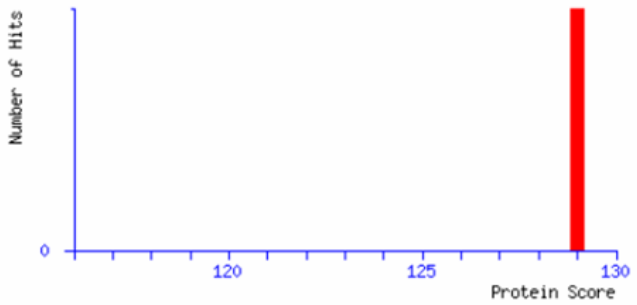

Figure 44. Database search identification score of A-Gla tryptic digestion epitope excision supernatant fraction

After the on-column digestion, the affinity antibody column was washed and the washing fraction analyzed by MS (Figure 45). The spectrum showed only a few signals from the MALDI matrix and no digestion fragments meaning that the column was clean.

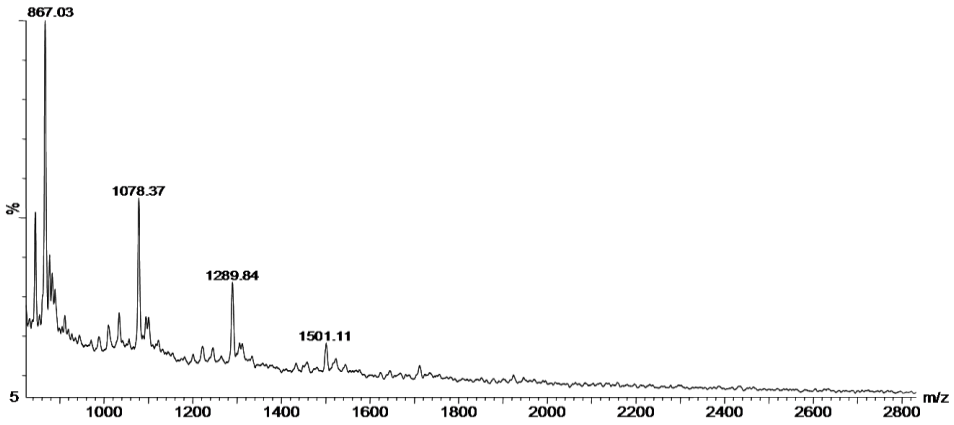

Figure 45. MALDI ToF mass spectrum of A-Gla tryptic epitope excision last washing fraction showing no signals but CHCA matrix

After washing the column, the epitope bound fraction was eluted with 0.1% TFA in MilliQ by incubation for ten minutes under agitation for four times. The collected elution fractions were combined, lyophilized and co-crystallized on a target with CHCA matrix solution for MALDI-ToF mass spectrometry. The MS measurement identified the alpha galactosiase epitope as the A-Gla(309-332) fragment. As shown in Figure 46 the epitope contained two Lysine residues which were not digested, indicating the shielding by the antibody upon digestion.

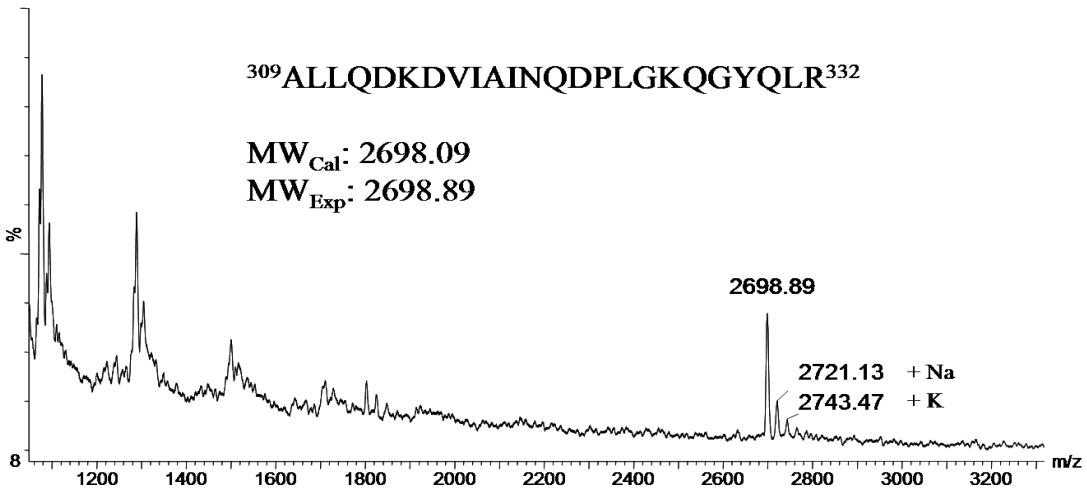

Figure 46. MALDI-ToF-MS of A-Gla tryptic epitope excision elution fraction showing the identified epitope peptide

After identifying the alpha galactosidase epitope, the affinity was characterized by the strength of its binding to the antibody. Since the epitope sequence contains two tryptic cleavage sites which were protected by the antibody (Lys^{314} and Lys^{326}) the epitope was expected to be shorter. Therefore three epitope peptides A-Gla(309-332), A-Gla(317-332) and A-Gla(325-332) were chosen for synthesis and affinity characterization.

2.3.2.3 Synthesis and purification of alpha galactosidase epitope peptides

Automated solid phase peptide synthesis using Fmoc chemistry, was used to synthesize three A-Gla epitope peptides, one full length A-Gla(309-332) and two shorter variants, A-Gla(317-332) and A-Gla(325-332). After synthesis, the peptides were purified by RP-HPLC and their homogeneity verified by mass spectrometric analysis. Alpha galactosidase (309-332) was purified on a Vidaq C8 column with a retention time of 16 minutes (Figure 47), while A-Gla(317-332) and A-Gla(325-332) were purified on an Vidaq C18 column with retention times of 19 minutes (Figure 48) and 12 minutes (Figure 49), respectively.

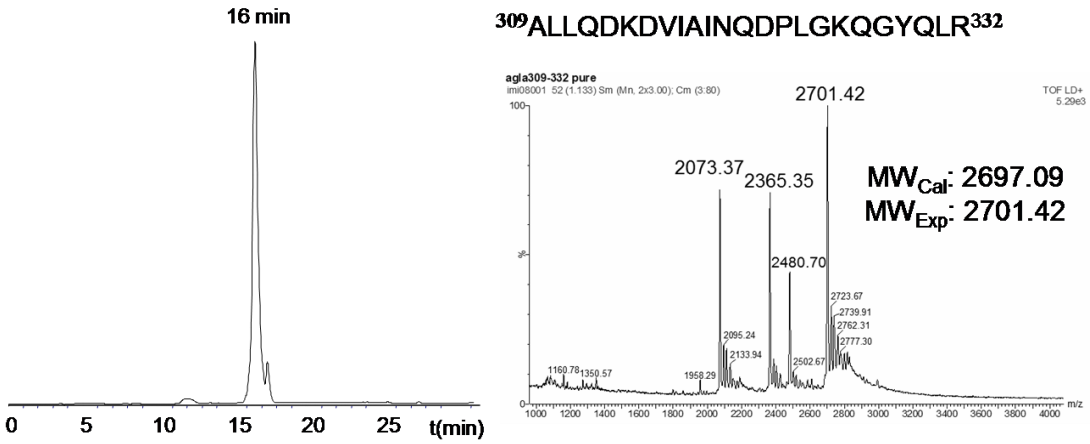

Figure 47. RP-HPLC purification chromatogram profile (left) and the MALDI-TOF mass spectrum (right) of A-Gla(309-332) synthetic peptide

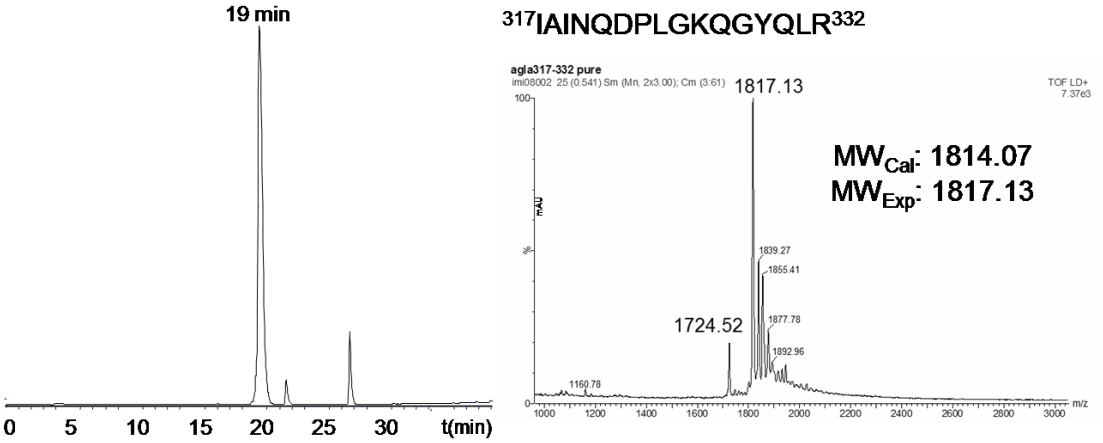

Figure 48. RP-HPLC purification chromatogram profile (left) and the MALDI-TOF mass spectrum (right) of A-Gla(317-332) synthetic peptide

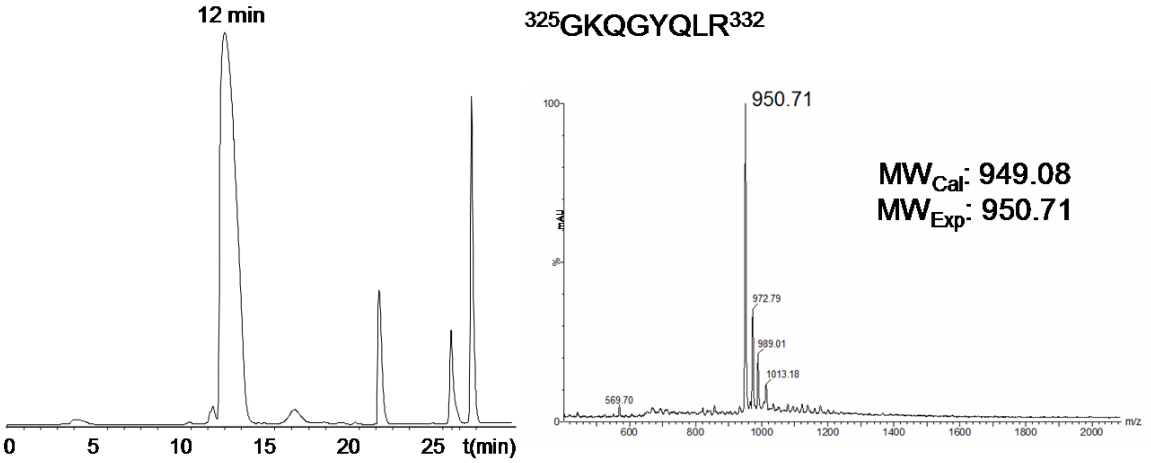

Figure 49. RP-HPLC purification chromatogram profile (left) and the MALDI-TOF mass spectrum (right) of A-Gla(325-332) synthetic peptide

2.3.2.4 Affinity characterization of alpha-galactosidase epitope peptides

After purification, synthetic A-Gla epitope peptides were tested for affinity properties against the anti-A-Gla antibody. 5 µg of each peptide in 50 µL PBS, pH 7.5, were separately loaded on the affinity microcolumn and incubated for 2 hours at 37 °C under agitation. After removing the supernatant the column was washed and the peptide eluted by decreasing the pH. All affinity fractions were characterized by MALDI-ToF mass spectrometry to verify that no unbound peptides were present on the column. The elution

fraction mass spectra showed a clear affinity for the A-Gla(309-332) (Figure 50), as well as for the shorter epitope peptide fragments A-Gla(317-332) (Figure 51), and A-Gla(325-332) (Figure 52).

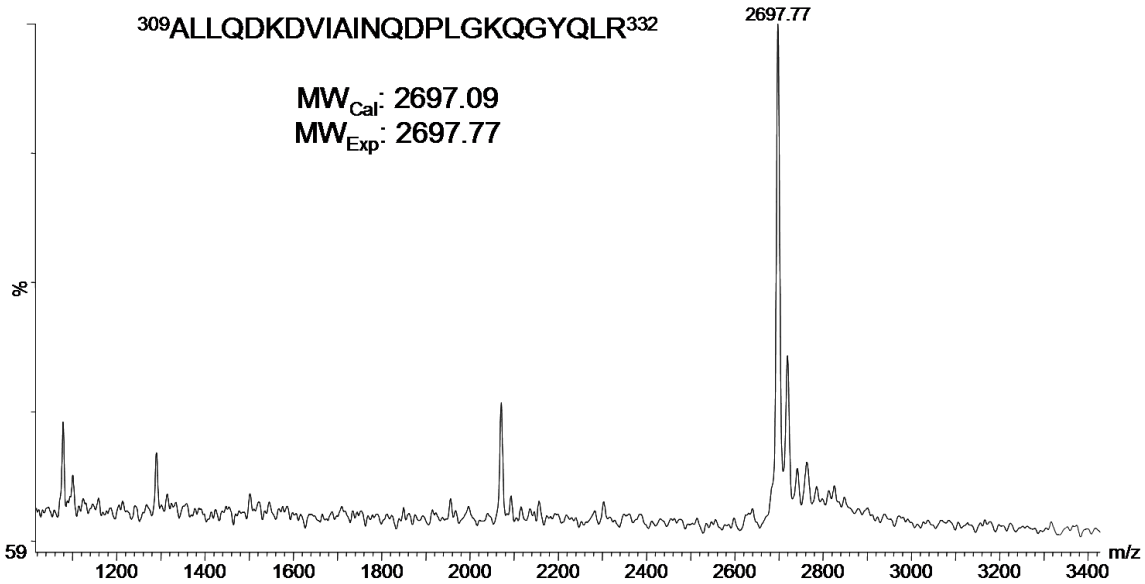

Figure 50. MALDI-TOF mass spectrum of affinity elution of synthetic A-Gla(309-332) peptide

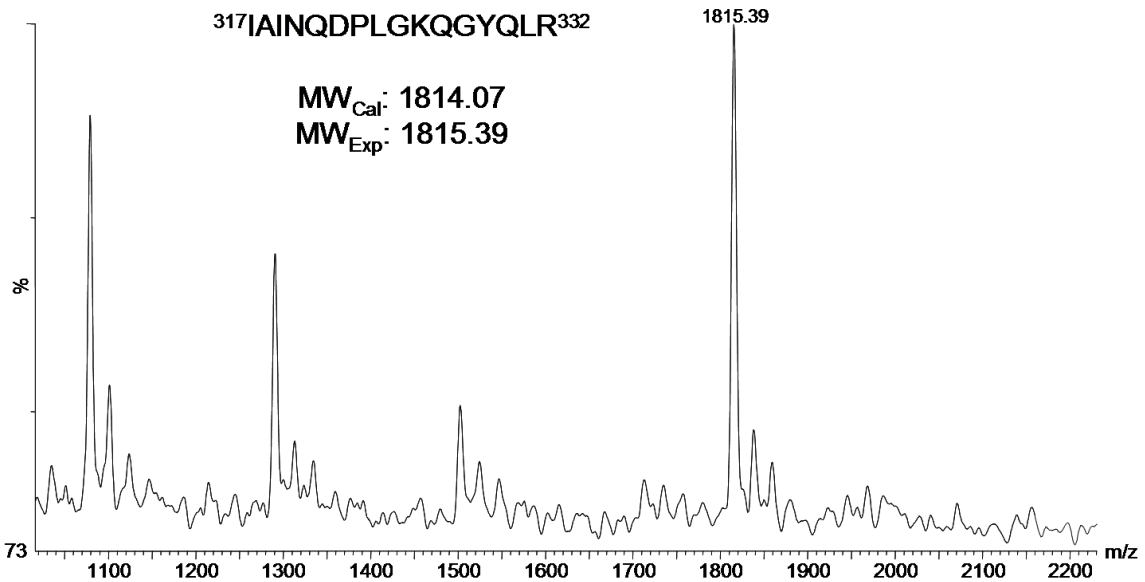

Figure 51. MALDI-TOF mass spectrum of affinity elution of synthetic A-Gla(317-332) peptide (unmarked peaks are of CHCA matrix origin)

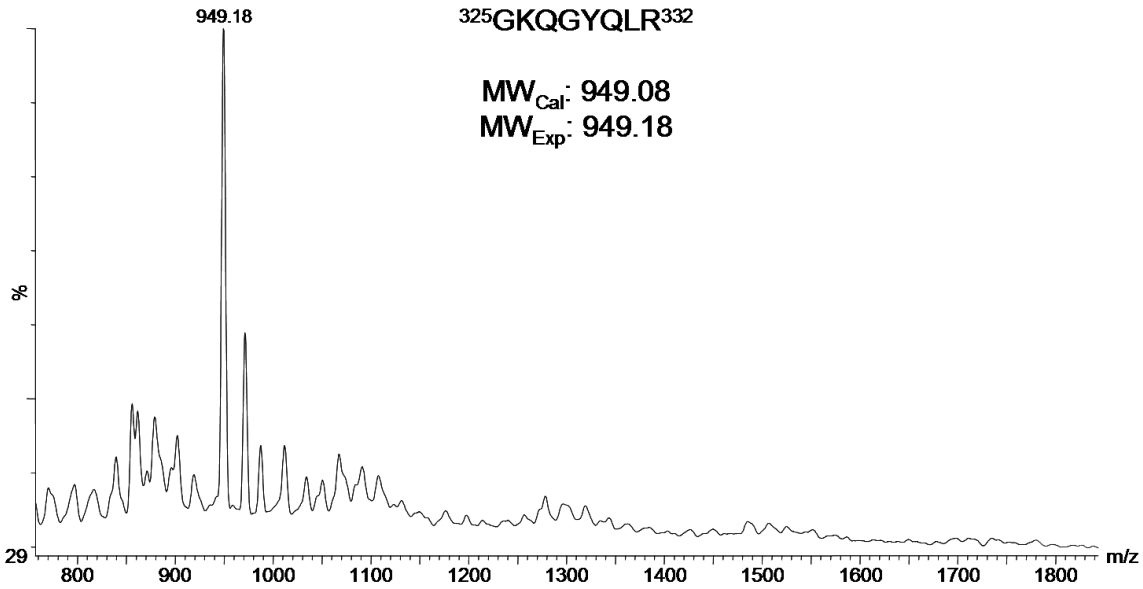

Figure 52. MALDI-TOF mass spectrum of affinity elution of synthetic A-Gla(325-332) peptide

2.3.2.5 Determination of affinity binding constants by SAW biosensor analysis for alphagalactosidase epitope peptides

After establishing the affinity properties of the synthetic A-Gla epitope peptides, the shortest sequence, A-Gla(325-332) was selected for affinity determination of dissociation constant K_D. The K_D value was measured using an Ssens K5 SAW biosensor (SAW Instruments, Bonn, Germany). In preparation of the experiment a gold plated quartz chip was covered with a self assembling monolayer of 12-mercaptododecanoic acid by incubation for 12 h at RT in a 10 mM 12-mercaptododecanoic acid solution in $CHCl_3$. The chip was then introduced in the microfluidic cell and activated by injecting a solution of 200 mM N-(3-dimethylaminopropyl)-N-ethylcarbodiimide (EDC) and 50 mM N-hydroxysuccinimide (NHS). Alpha-Gla(325-332) was then covalently immobilized on the active layer of the chip and the remaining active sites were blocked with ethanolamine (EA). A series of 8 anti-A-Gla antibody solutions with increasing concentrations (5-200 nM) was prepared and injected on the chip (Figure 53).

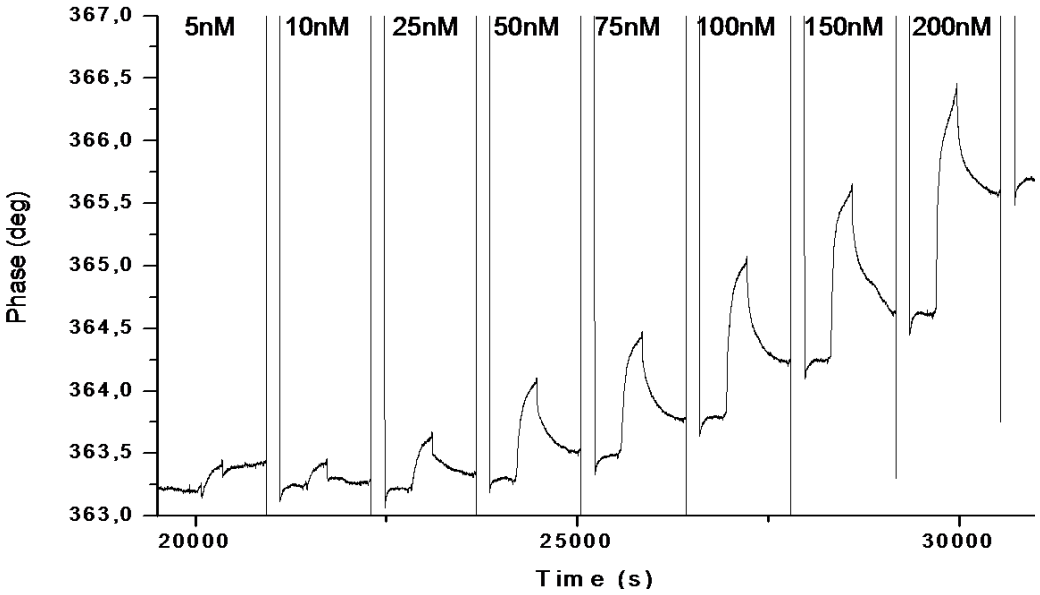

Figure 53. SAW-Biosensor sensorgram of anti A-Gla antibody injectios on A-Gla(325-332) gold plated chip

After measurement, the recorded data were fitted according to the theoretical 1:1 Langmuir binding model (Figure 54). The extracted observed rate constants (k_{Obs}) were plotted against the analyte concentrations and the linear regression (Figure 55) of the data points yielded the association rate constant k_{on} and dissociation rate constant k_{off}. The equilibrium dissociation constant K_D of A-Gla – anti-A-Gla interaction was calculated from the association and dissociation rate constants, $K_D = k_{off} / k_{on}$, and it proved to be 28.5 nM.

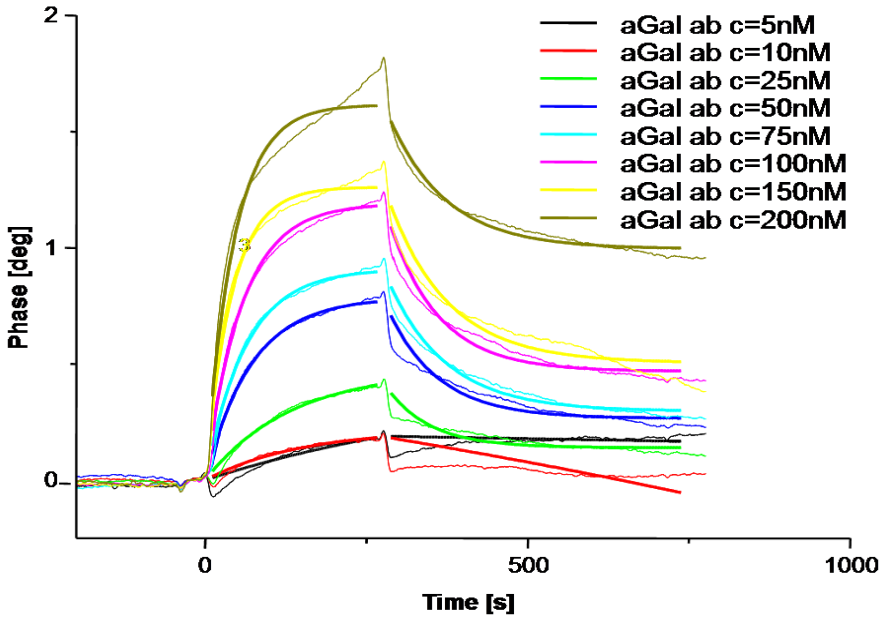

Figure 54. Fitting-curves analysis of the SAW-Biosensor sensorgram of anti A-Gla antibody – A-Gla interaction

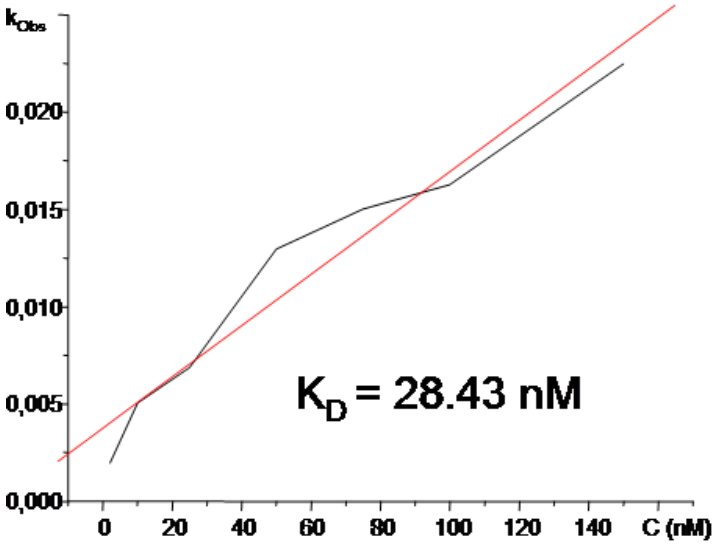

Figure 55. Plot of anti-A-Gla k_{Obs} values versus concentration; $K_D=k_{off}/k_{on}$ (black) and linear regression (red)

2.3.3 Epitope Identification of human leukocyte antigen B27 by affinity mass spectrometry

The major histocompatibility complex (MHC) is a set of proteins capable of binding foreign peptide fragments and to expose them for antibody recognition. The MHC proteins are encoded in the human leukocyte antigen (HLA) genes from which were given their names. There are three major classes of HLA (noted I, II and III) and several subclasses. The class I B27 protein is believed to be a factor for the development of Ankylosing spondylitis (AS) and other Spondyloarthritides [151], which are inflammatory diseases which affects the axial skeleton, and cause pain in the joints and fusion of the spine.

The functional HLA forms a heterotrimer of HLA-B27 (heavy chain) with β2-microglobulin (light chain) and a short foreign or self peptide. This complex migrates to the cell surface where it is recognized by T cells. The HLA-B27 complex may dissociate, resulting in free heavy chains which may lead to heterodimer formation. It is believed that the heterodimers trigger the inflammatory response of the disease. However, while 90% of the ankylosing spondylitis patients express the HLA –B27 [152], not all persons possessing the gene develop the disease.

Two monoclonal antibodies were selected from a phage display[1], the monoclonal HD5 mAb, which binds specifically to HLA-B272 homodimer, and HD6 mAb which recognizes both HAL-B272 and HLA-B27 free heavy chains.

[1] Provided by our collaborators from Prof. Renner's group from University of Zurich

2.3.3.1 Anti- human leukocyte antigen B27 antibodies affinity columns preparation

Two affinity columns were prepared by packing 0.6 g of NHS-activated sepharose on two 1 mL micro-columns. The HD5 and HD6 monoclonal antibodies were loaded onto the columns in sodium phosphate buffer (PBS), pH 7.15, and immobilized by incubation for 2 h at 37 °C. The unbound free active sites of the matrix were blocked with ethanolamine after the incubation and removal of supernatant. The columns were washed with PBS and stored at 4°C.

In preparation for experiments aimed at epitope identification, a sample of the free heavy chain HLA-B272 homodimer was loaded on the HD5 antibody microcolumn and incubated for 2 h at 37 °C. The supernatant was separated and prepared for gel electrophoresis characterization and the column was washed and prepared for further epitope excision experiments. The unbound HLA-B27 from the supernatant was loaded on a SDS polyacrylamide gel and after electrophoretic separation the gel was staind with Coomassie Blue. A large band around 30 kDa and a fainted band about 60 kDa could be observed in the gel (Figure 56) corresponding to the monomeric and dimeric forms of free HLA-B27 heavy chain. This showed that the HLA homodimers from the sample were immobilized on the HD5 antibody column while the free monomers remained in the supernatant.

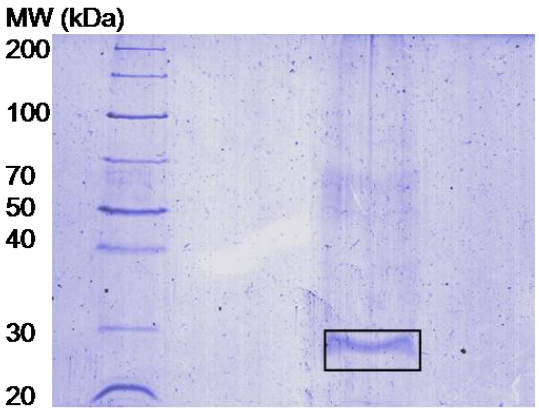

Figure 56. SDS-PAGE of HLA-B27 affinity column testing and the marked band for excision and in-gel digestion

The HLA-B27 monomer band was cut out from the gel, destained and dehydrated. The band was then further swollen in a trypsin containing buffer and incubated for 12 h at 37 °C for digestion. After incubation, the tryptic mixture was extracted from the gel, concentrated and prepared for MALDI-mass spectrometric characterization (Figure 57).

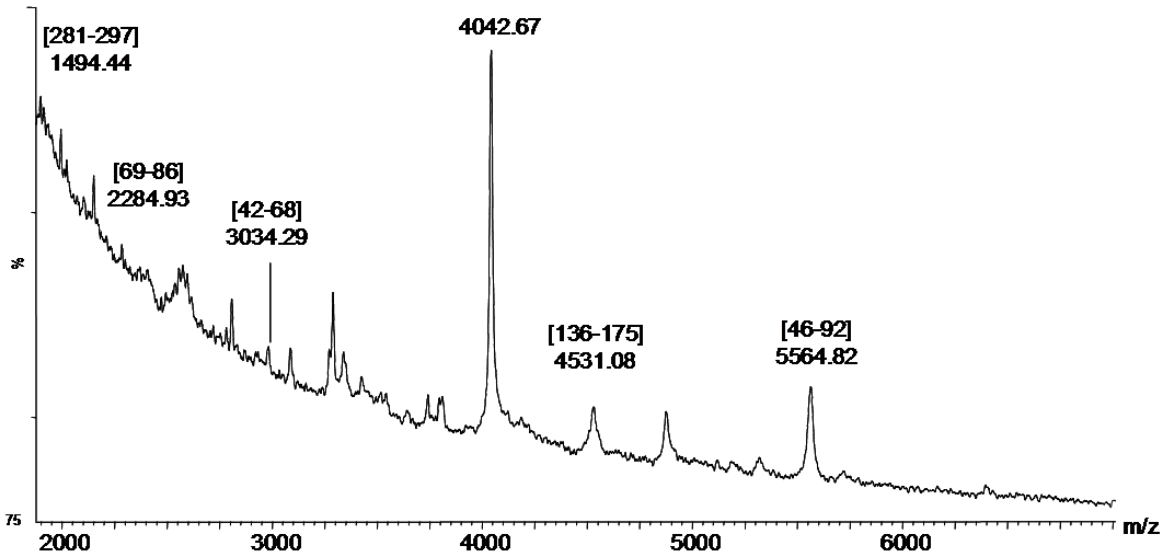

Figure 57. MALDI-ToF mass spectrum of tryptic in-gel digestion of HLA-B27 gel band

The masses identified by MS corresponding to the HLA-B27 digested protein were searched against the NCBInr database using the MASCOT search engine. The search ascertained with a high identification score that the sample was identified as HLA-B27 protein (Figure 58).

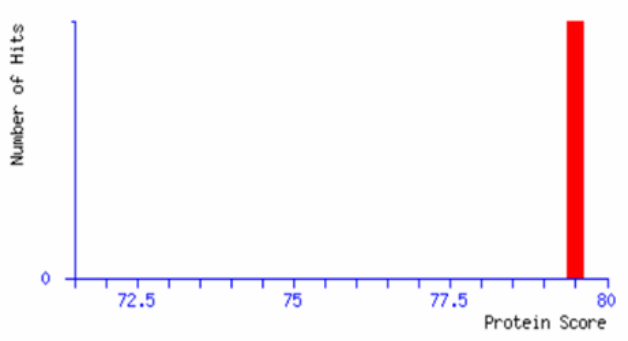

Figure 58. Database search identification score of HLA-B27 tryptic in-gel digestion

2.3.3.2 Epitope identification of Human leukocyte antigen B27 by affinity epitope excision – mass spectrometry

The previously prepared HD5 antibody column with the HLA-B272 protein bound to it was further subjected to tryptic epitope excision. A solution of trypsin in PBS was added to the column and it was incubated for two hours at 37 °C. The supernatant was collected and desalted and concentrated by zip-tip enrichment. After zip-tip, the sample was characterized by MALDI-ToF mass spectrometry (Figure 59) showing the presence of HLA-B27 digestion fragments: [274-309], [274-311], [7-44] and [257-309].

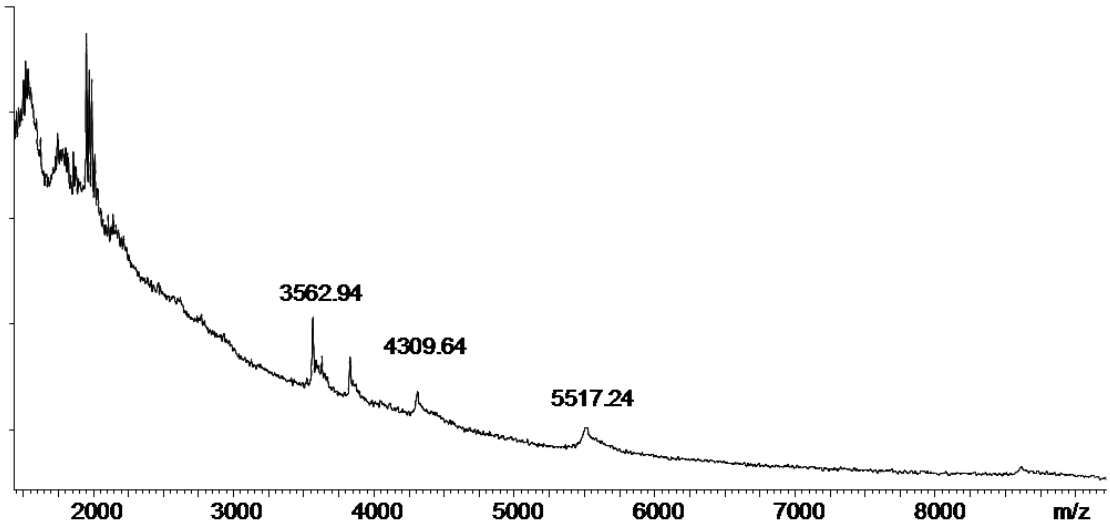

Figure 59. MALDI-ToF-MS of HLA-B27 tryptic epitope excision supernatant fraction

Before epitope elution the column was thoroughly washed with PBS and water. The solution from the last washing step was collected and subjected to mass spectrometric characterization (Figure 60) showing the absence of any fragments on the column.

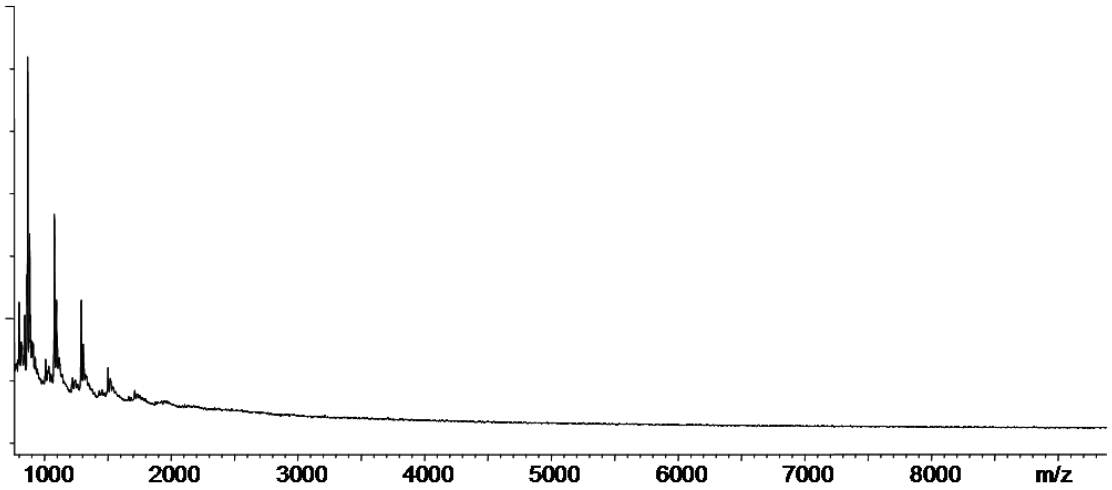

Figure 60. MALDI-ToFMS of HLA-B27 tryptic epitope excision washing fraction

After washing, the epitope peptide was eluted from the affinity micro-column by changing the pH to a lower value. A 0.1% TFA in water solution was used, 250 µL at a time. The elution was performed four times by incubation for 10 minutes at RT under agitation. The combined elution fractions were lyophilized and resolubilized in 10 µL MALDI solvent. Using CHCA matrix the epitope sample was crystallized and prepared for MALDI-ToF analysis. The mass spectrum (Figure 61) is showing the identification of the eluted epitope peptide with a molecular weight of 4042.92 kDa.

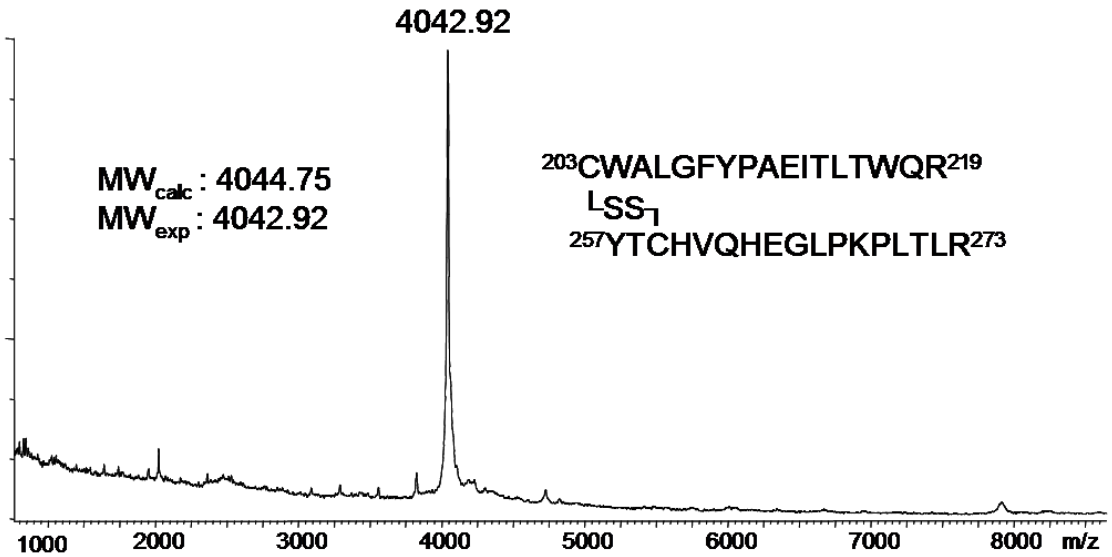

Figure 61. MALDI-ToF-MS of HLA-B27 tryptic epitope excision elution fraction showing the identified disulfide linked epitope peptide

Upon analyzing the results it could be deduced that the epitope is not comprised of a single, continuous sequence. The epitope proved to be formed from two discontinues peptides bound together by disulfide bridge: HLA-B27 (203-219)-SS-(257-273). When visualized on the 3D crystal structure of the HLA-B27 trimer (Figure 62) we can observe that the epitope is situated at the surface of the protein where it can easily be accessed by the antibody.

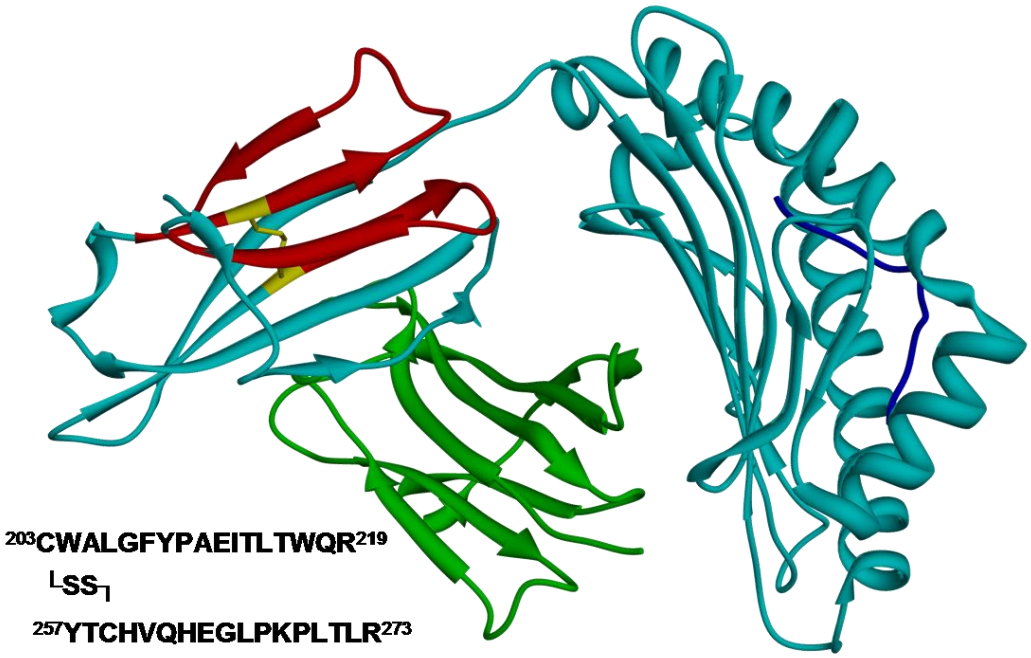

Figure 62. HLA-B27 proteine crystal structure (cyan) with the epitope (red), disulfide bridge (yellow), beta gamma globulin (green) and antigen peptide RPHERNGFTVL (blue) marked on it

2.3.3.3 Synthesis and purification of HLA epitope peptides

HLA-B27 epitope peptides were synthesized on an automated peptide synthesizer, 50 µM scale on Rink amide MBHA resin, Fmoc chemistry. The peptides were purified via RP-HPLC and the purity verified by MALDI-ToF mass spectrometric characterization. HLA-B27 (203-219) was purified on a C18 Vidaq column and had a retention time of 22.5 minutes (Figure 63) while HLA-B27 (257-273) had a retention time of 37 minutes (Figure 64).

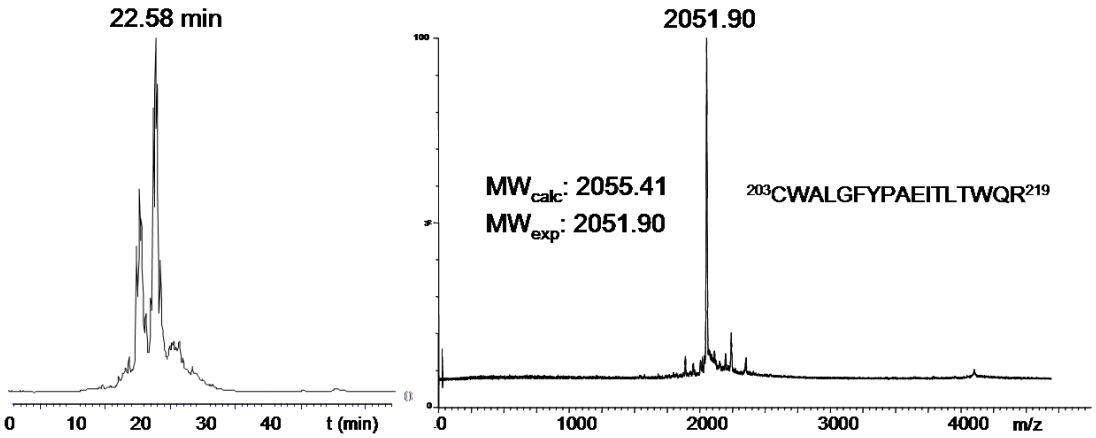

Figure 63. RP-HPLC purification chromatogram profile and the MALDI-TOF mass spectrum of HLA-B27(203-219) synthetic peptide

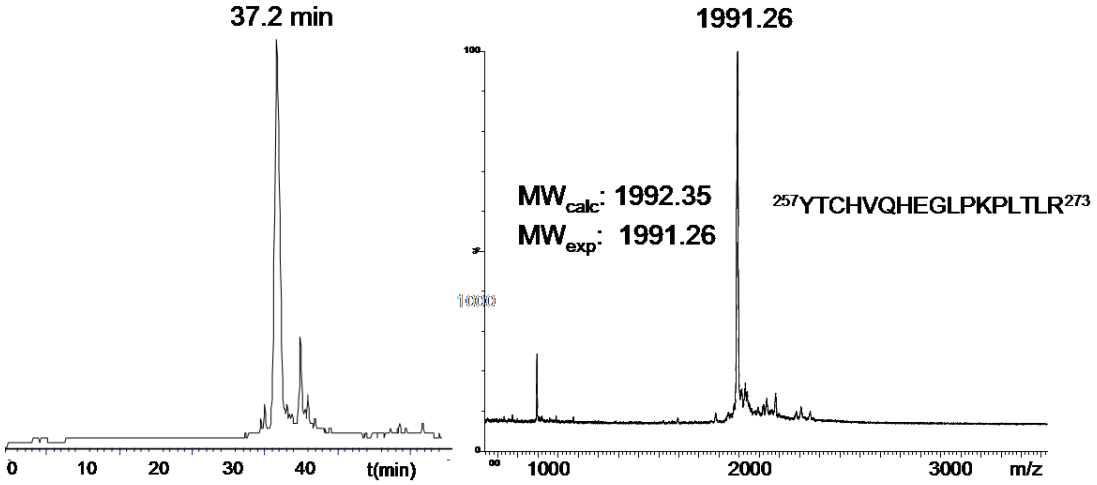

Figure 64. RP-HPLC purification chromatogram profile and the MALDI-TOF mass spectrum of HLA-B27(257-273) synthetic peptide

2.3.3.4 Affinity determination of synthetic epitope peptides

HLA-B27(203-219) and HLA-B27(257-273) peptides were subjected to a preliminary affinity test on the HD5 and HD6 antibody columns. 5 µg peptide were solubilized in 50 µL PBS and loaded on the column. After two hours of incubation at 37 °C under agitation the supernatant was removed and the column washed. The elution was done by lowering the pH with 0.1% TFA solution in deionized water, four times of 250 µL under agitation. All elution fractions were combined and concentrated via lyophilization.

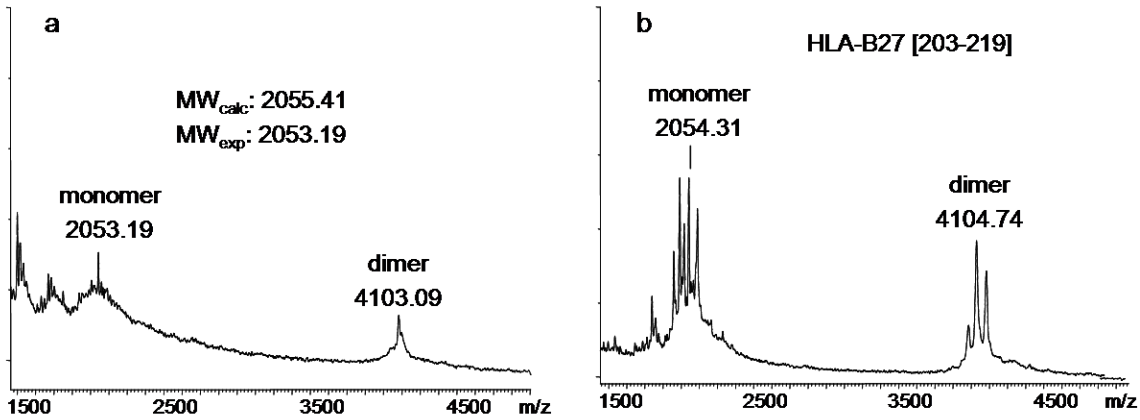

Figure 65. MALDI-ToF mass spectra of affinity testing of HLA-B27(203-219) peptide on HD5 (a) and HD6 (b) antibody columns

The success of the affinity experiment was ascertained by mass spectrometric measurements of the elution fractions. A small amount of sample (0.8 µL) was mixed with 0.8 µL saturated CHCA matrix solution on a MALDI target and left to co-crystallize. After measurement, the spectra showed that both the HLA-B27(203-219) epitope peptide (Figure 65) as well as the HLA-B27(257-273) peptide (Figure 66) presented affinity for the HD5 and HD6 antibodies.

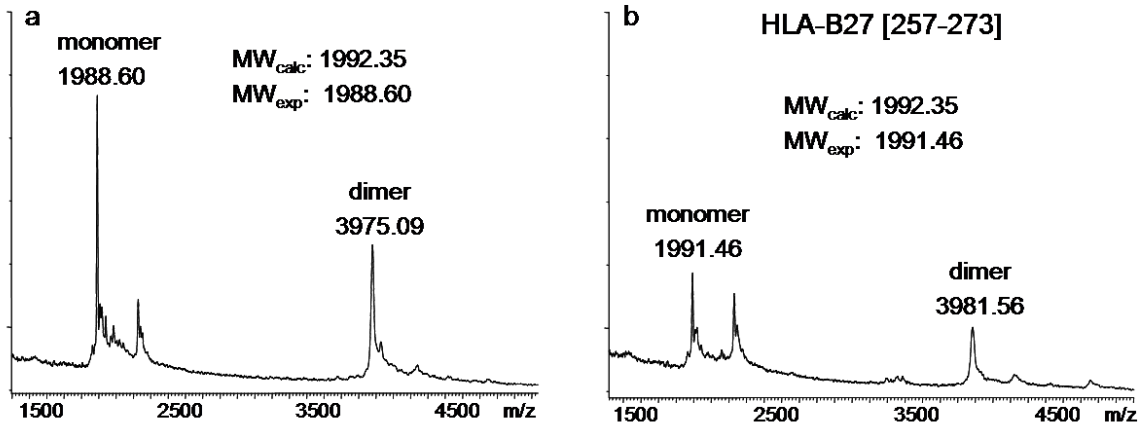

Figure 66. MALDI-ToF mass spectra of affinity testing of HLA-B27(257-273) peptide on HD5 (a) and HD6 (b) antibody columns

Beside the monomeric species, the MALDI-ToF mass spectra revealed that the HLA-B27 epitope peptides tend to form homodimers in solution during the affinity experiments and that these dimers have also affinity for the two antibodies. In order to determine which epitope peptide has a stronger affinity, a competitive affinity experiment was designed using a mixture of the two peptides. The mixture was loaded on the two columns and left to interact with the antibodies. The mass spectrometric analysis of the elution fractions revealed not only the presence of both monomers, but also the presence of the HLA-B27(203-219)-SS-B27(257-273) disulfide linked heterodimer as the major component of the elution fraction (Figure 67).

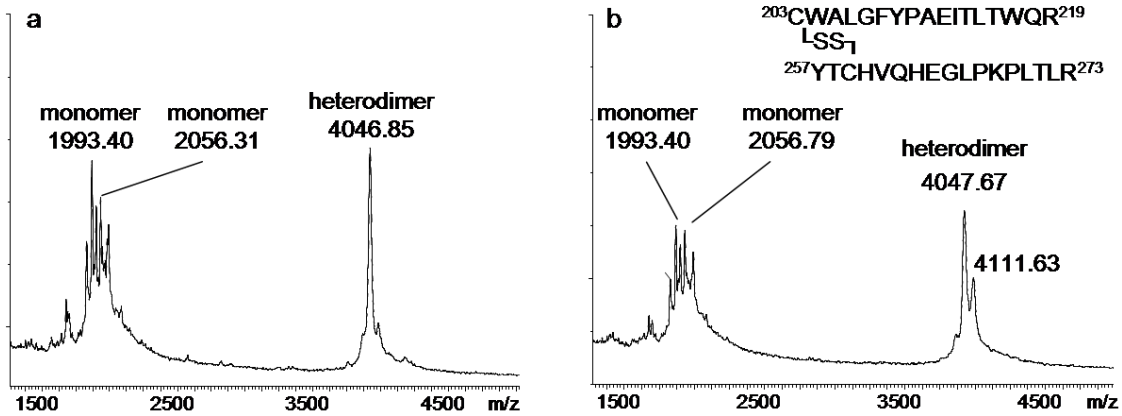

Figure 67. MALDI-ToF mass spectra of affinity testing of HLA-B27 ((203-219) and (273-257) peptide mixture on HD5 (a) and HD6 (b) antibody columns showing the major formation of disulfide linked heterodimer in the presence of the antibodies

The formation of the heterodimer in the presence of the antibodies shows that both peptides are part of the epitope and play a major role in the affinity binding.

2.3.3.5 Synthesis and purification of HLA disulfide linked epitope

Since the epitope peptides showed a high tendency to form the disulfide linked heterodimer upon binding to the antibody, it was decided to synthesize it for further investigations. A mixture of HLA-B27(203-219) and HLA-B27(257-273) peptides 1:1 (molar ratio) were solubilized at 1 mg/mL in a solution of DMSO/ammonium acetate 1:1 (v:v) and incubated at RT for 24 h under agitation. After incubation, the reaction mixture was diluted with 0.1% TFA in water to reduce the DMSO concentration under 20% and to ensure compatibility with reverse phase HPLC. The separation of reaction mixture components was done on a semi-preparative Vidaq C18 column with a gradient increase of 1% per min organic solution (80% acetonitril, 0.1% TFA in water). HLA-B27(257-273) components eluted first, with a retention time of 24 min and HLA-B27(203-219) components eluted last with 44 min retention time. The mixed disulfide linked peptides eluted in the middle with a retention time of 34 min (Figure 68).

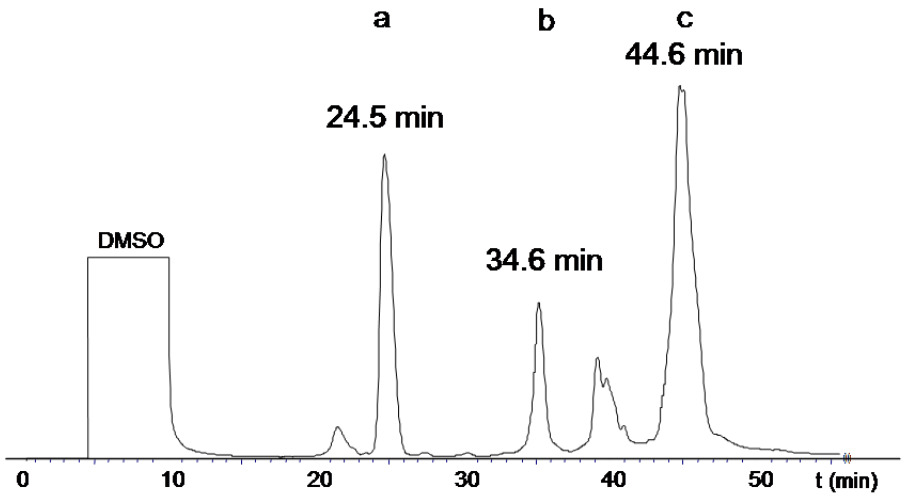

Figure 68. RP-HPLC chromatographic separation of disulfide bridge reaction mixture showing three major reaction products: HLA-B27(257-273) homodimer (a), HLA-B27(203-219)-SS-(257-273) heterodimer (b) and HLA-B27(203-219) homodimer (c) respectively

To ascertain the identity of eluted RP-HPLC fractions, they were immediately analyzed by MALDI-ToF mass spectrometry. For the homodimeric forms it was hard to estimate the conversion rate since the dimer 2+ ions are over imposed on the monomers 1+ ions (Figure 69a and c). The homodimer mass spectrum on the other hand, is able to show, beside the homodimer 2+ ion, the two monomers 1+ ions present in the sample (Figure 69b). The sample however, beside the presence of a few monomeric species, is totally composed of the heterodimeric form of the disulfide linked epitope and no homodimers are present in the sample.

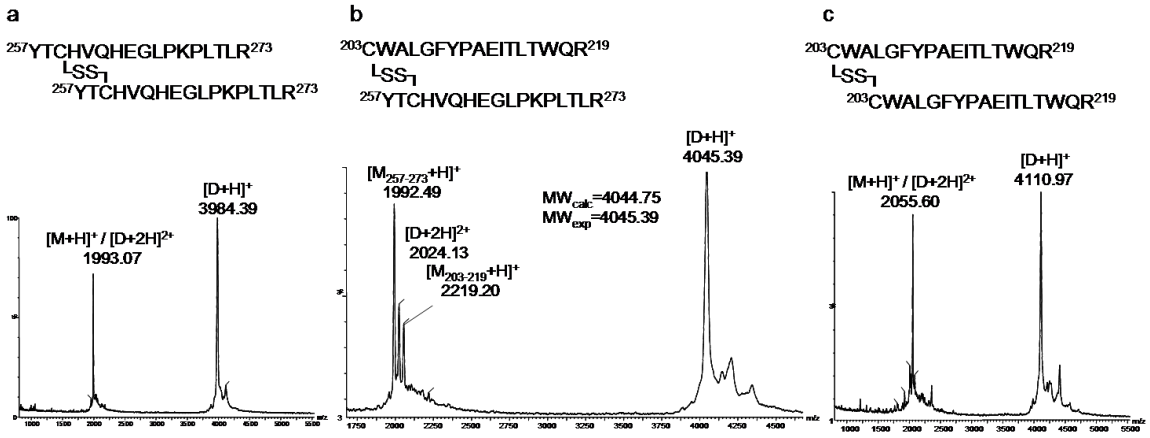

Figure 69. MALDI-ToF mass spectrometric identification of RP-HPLC chromatographic fractions from the disulfide bridge reaction mixture showing the HLA-B27(257-273) homodimer (a), HLA-B27(203-219)-SS-(257-273) heterodimer (b) and HLA-B27(203-219) homodimer (c) respectively

2.3.3.6 Affinity determination of HLA disulfide linked epitope peptides

Before K_D determinations could be done, the HLA-B27(203-219)-SS-(257-273) peptide was tested for affinity against the HD5 and HD6 antibodies. A 20 µg HLA-B27 epitope peptide sample was solubilized in PBS (pH 7.5) and loaded on each affinity column. After incubation at 37 °C for 2 h under agitation, the columns were washed and the epitope was eluted by lowering the pH with a 0.1% TFA aqueous solution. After concentration by lyophilisation, the samples were measured by MALDI-ToF-MS in the presence of CHCA matrix. The spectra showed that both antibodies have affinity for the synthetic HLA-B27(203-219)-SS-(257-273) epitope peptide (Figure 70).

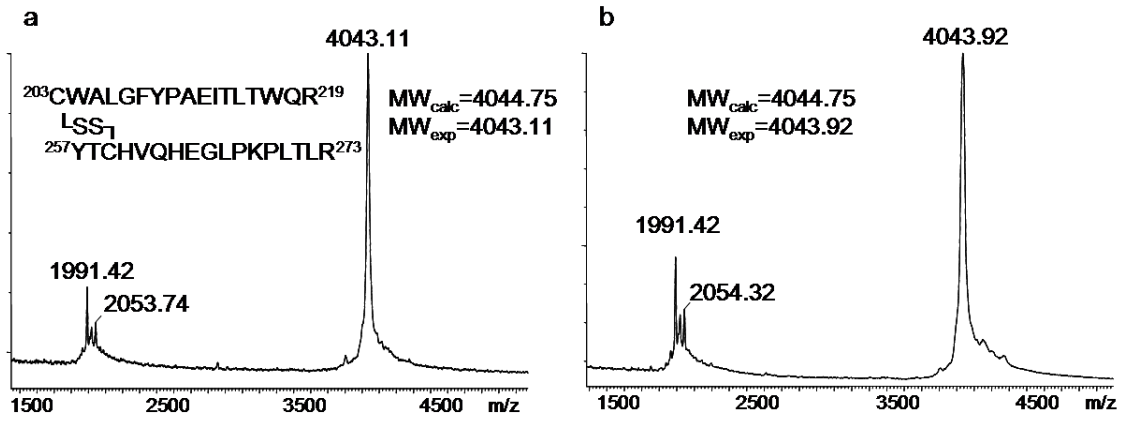

Figure 70. MALDI-ToF mass spectra of affinity testing of HLA-B27 ((203-219)-SS-(273-257) mixed epitope on HD5 (a) and HD6 (b) antibody columns

2.3.3.7 Determination of binding constants using SAW Biosensor analysis

The K_D values of HLA-B27 epitope peptides were determined using an Ssens K5 surface SAW biosensor (SAW Instruments, Bonn, Germany). Five binding partners were chosen for the K_D determination studies: HLA-B27(203-219) and HLA-B27(257-273) monomers, HLA-B27(203-219)-SS-(203-219) and HLA-B27(257-273)-SS-(257-273) homodimers and the HLA-B27(203-219)-SS-(257-273) heterodimeric disulfide linked epitope peptide.

For each peptide, a gold plated quartz chip was covered with a self assembling monolayer of 12-mercaptododecanoic acid and the peptide was covalently immobilized to it. A series of 8 HD6 mAb solutions with ascending concentrations (5-150 nM) were prepared and loaded into the instrument for affinity measurements. After the measurements were completed, the sensorgrams were fitted according to the theoretical 1:1 Langmuir binding model (Figure 71). The extracted observed rate constants (k_{Obs}) were plotted against the analyte concentrations. The K_D values for each antibody-antigen pair was calculated from the linear regression of k_{Obs} versus concentrations (Table 4).

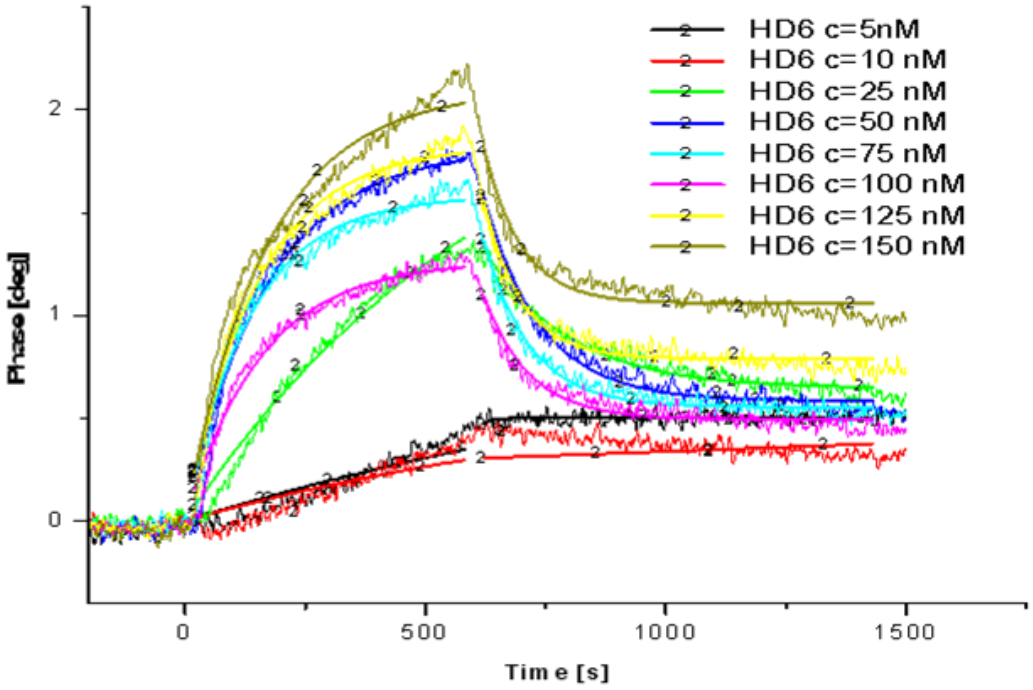

Figure 71. Fitting-curves analysis of the SAW-Biosensor sensorgram of HD6 antibody – HLA-B27(203-219)-SS-(257-273) interaction

Table 4. KD values of HD6 antibody against HLA-B27 epitope peptides

HLA-B27 peptide	K_D HD6 antibody x10^{-9} M (R^2)
(203-219)-SS-(257-273) heterodimer	41.3 (0.98)
(203-219)-SS-(203-219) homodimer	339.2 (0.93)
(257-273)-SS-(257-273) homodimer	-
(203-219) monomer	-
(257-273) monomer	100 (0.85)

3 EXPERIMENTAL PART

3.1 Materials and reagents

3.1.1 Chemical reagents

For this work the following commercially available reagents were used:

Urea, Dithiothreitol (DTT), iodoacetamide (IAA), TEMED, Coomassie Brilliant Blue G250, NHS-activated Sepharose, activated CH-Sepharose 4B, polyoxyethylen-sorbitanmonolaureat (Tween20), 2,2,2-trifluoroethanol (TFE), trichloroacetic acid (TCA), dimethylsulfoxide (DMSO), ammonium persulfate (APS), diethanolamine (min 98%), alpha-cyano-4-hydroxycinamic acid (CHCA), phosphoric acid 85% (H_3PO_4) were purchased from Sigma (St. Louis, MO, USA). Bromophenol Blue, t-butylmethylether, N-methylmorpholine (NMM), piperidine, 1,8-diazabicyclo-[5.4.0]undec-7-ene (DBU), trifluoroacetic acid (TFA), triethylsilane, triisopropylsilane, dihydroxy benzoic acid (DHB) were purchased from Fluka Chemie (Buchs, Switzerland). Ammonium sulfate – (NH4)2SO4), glycerol, glycine, acrylamide/bis solution (30% acrylamide), sodium dodecyl sulfate (SDS), trichloroacetic acid (TCA), acetonitrile (ACN), acetic acid, sodium chloride, silver nitrate, formic acid (FA), tris-hydroxymethyl-aminomethane (2-Amino-2-hydroxymethyl-propane-1,3-diol) (Tris) and ethanol were purchased from Roth. N-α –Fmoc protected amino acids, NovaSyn TGR, TGA, Rink Amide MBHA resins, Benzotriazole-1-yl-oxy-tris-pyrrolidino-phosphonium hexafluoro-phosphate (PyBOP) were purchased from NovaBiochem (Läufelfingen, Switzerland) or GL Biochemicals (Shanghai, China). Disodium hydrogen rypsin t-2-hydrate (Na_2HPO_4 x $2H_2O$) was from Riedel-de Haen. N, N-dimethylformamide (DMF) was purchased from Acros Organics (Geel, Belgium). Hydrochloric acid (37% p.a.), sodium hydroxide (99%), urea, thiourea: Merck (Darmstadt, Germany). Trypsin was purchased from Promega (Madison, WI, USA). OxyBlot 2,5dihydroxybenzoic acid (DHB) was from BrukerDaltonics (Bremen, Germany). Urea and thiourea were from Merck (Darmstadt, Germany). Dichloromethane (DCM): VWR. Deionized water (Millipore, Bedford, MA,

USA) with a minimum electric resistance at 18.2 MΩ (Ω: Ohm) was used for all solutions. 96 well Optiplate black: Perkin Elmer; Low binding test tubes: Sigma Aldrich; OMIX™ Pipette Tips C18 were from Varian (Walnut Creek, CA, USA).

The reagents and solvents used were of analytical grade, or highest available purity.

3.1.2 Buffers and stock solutions

Phosphate buffer saline (PBS): 0.1 M phosphate, 0.15 M NaCl, pH 7.15. Prepare a 8.89 g Na_2HPO_4 x $2H_2O$ and 4.36 g NaCl in 500 mL rypsi solution and a 2.75 g NaH_2PO_4 x H_2O and 1.75 g NaCl in 200 mL rypsi solution and mix the two solutions until reaching a pH of 7.15.

Affinity column preparation buffers: Coupling buffer 0.2 M $NaHCO_3$, 0.5 M NaCl, pH 8.3, Blocking buffer (A) 0.1 M Ethanolamine, 0.5 M NaCl, pH 8.3. Washing buffer (B) 0.2 M NaOAc, 0.5 M NaCl, pH = 4.

Buffers used for SDS PAGE: Sample buffer, 4% SDS, 25% Glycerol, 50 mM Tris, 0.02% Coomassie, 6 M Ureea, pH 6.8; 4x Stacking gel buffer, 0.5 M Tris-HCl, 0.4% SDS (w/v), pH 6.8; 4x Separating gel buffer, 1.5 M Tris-HCl, 0.4% SDS (w/v), pH 8.8; Running buffer, 25 mM Tris, 192 mM Glycine, 0.1% SDS.

Buffers used for Tris Tricine gels: 2x Sample buffer, 100 mM Tris pH 6.8, 24% Glycerol, 8% SDS, 0.02% Coomassie Brilliant Blue G-250; 1x Catode buffer (upper chamber), 100 mM Tris, 100 mM Tricine, 0.1% SDS; 10x Anode buffer (lower chamber) 2 M Tris, pH 8.96; Tris-HCl/SDS 3 M Tris, 0.3% SDS.

Coomassie Brilliant Blue staining: Buffer A, 10% NH_4SO_4, 2% H_3PO_4; Coomassie Blue Solution, 20% methanol, 0.1% Coomassie Brilliant Blue G-250 in buffer A; Fixing solution, 30% ethanol, 10% acetic acid; Incubatin

solution, 11.2% CH_3COONa x 3 H_2O, 30% ethanol, prior to use add 0.2% Na_2SO_3 x $5H_2O$.

For 2 small 15% Tris-tricine gels: Separation gel, 7.5 mL acrilamide, 5 mL Tris-HCl/SDS, 0.9 mL Milli Q water, 1.58 mL Glycerol, 75 µL APS (10%), 10 µL TEMED; Stacking gel, 978 µL acrilamide, 1.86 mL Tris-HCl/SDS, 4.67 mL Milli Q water, 40 µL APS (10%), 7.5 µL TEMED.

ZipTip solutions: wetting solution, 50% ACN in Milli Q; washing solution, 0.1% TFA in Milli Q; elution solution, 50% ACN, 0.1% TFA in MilliQ.

SPPS deprotection solution: 2% DBU, 2% piperidine in DMF, or 20% pipeidine in DMF. Side chain group deprotection and cleavage of peptide from the resin was done in acidic conditions with a 5% TIPS, 5% water, 90% TFA solution.

RP-HPLC solutions: Solvent A, 0.1% TFA in MilliQ water; Solvent B, 80% ACN, 0. 1% TFA in MilliQ water.

MALDI solvent: ACN/0.1% TFA in MilliQ water (2:1, v:v)

3.1.3 Proteins and antibodies

Mouse, anti human alpha galactosidase, monoclonal antibody was purchased from Sino Biological, Beijing, China.

Human alpha galactosidase was purchased from Sino Biological, Beijing, China.

HD5 and HD6 antibodies were obtained by screening a human antibody phage display against the HLA-B27 protein by Ossiris Maroquin at University Spital Zürich.

HLA-B27 heterotrimers and free heavy chains (dimers) were expressed by recombinant DNA in e-Coli.

3.2 Peptide synthesis

Solid phase peptide synthesis (SPPS) is a synthetic method for small proteins and peptides. It involves the use of a resin (solid phase) as the support for the synthetic molecule because it makes it easier to move the product from one reaction to another by washing the resin without the need to separate, purify and resolubilize the peptide. The resin must be insoluble to the solvents and reagents used to carry on the chemical reactions and the washing of byproducts and excess reagents.

NovaSyn TGR resin was used to synthesize the Aβ(1-40) peptide and its variants and RynkAmid RMBH was used for the synthesis of the epitope peptides identified through the tryptic epitope excision experiments. The synthesis was done on a 50 µM scale using Fmoc chemistry. The amino group of the resins and amino acids used are protected by a Fmoc group while the carboxy group is free. Each amino acid was added to the sequence through a complex reaction cycle involving several steps: (i) removal of the Fmoc protecting group from the amino group of the amino acid or resin with 20% piperidine in DMF, (ii) washing of the resin with 8 – 10 mL DMF, (iii) addition of the next Fmoc N-α-protected amino acid with 0.9 M PyBOP (Benzotriazol-1-yl-N-oxy-trispyrrolidino-phosphoniumhexafluorophosphat) and 1.3 M NMM (N Methyl-morpholine) in DMF and incubation for 30 min to allow the formation a new peptidic bond, (iv) washing with DMF. To increase the yield of the peptide synthesis, each amino acid was added twice in two consecutive reactions (double coupling). To verify the completion of each coupling, a bromo-phenole blue test was done after each manually added amino acid.

At the end of the synthesis the resin was washed with DCM and ethanol and dried. The side chain protecting groups were cleaved all together under acidic conditions using a mixture of TIPS (tri-iso-propil-sylane) / water / TFA (2.5: 2.5: 9.5, v: v: v); 2.5 mL / 100 mg resin incubated at RT for 2 h under agitation. In these conditions takes also place the finished peptide cleavage from the resin. The resin was removed by filtration and the peptide

was precipitated by addition of 20 folds cold diethylether. The solid peptide was filtered, resolubilized using 10% acetic acid and lyophilized.

Automated SPPS was carried out on two semiautomated peptide synthesizers, EPS 221 (Abimed/Intavis, Langenfeld, Germany) and ResPepSL (Intavis Bioanalytical Instruments, Koeln, Germany).

3.3 Gel electrophoretic separation

Gel electrophores is the most widespread separation method to analyze high molecular weight complex biological mixtures. It is mostly used in genetics, for DNA and RNA, and proteomics, for proteins and peptides separation. It is a fast, nondestructive method that can be used in tandem with other methods such as electro-bloting or in-gel peptide digestion. The proteins are mixed with an anionic detergent that would give the molecules a negative electric charge directly proportional to their molecular weight. When an electric field was applied, the proteins would migrate through the gel according to their electrophoretic mobility toward the anode. The gels were made between two glass plates (90 x 60 x 1 mm, size of the final gels) and were run using a Mini-Protean II gel electrophoresis system (Biorad, München, Germany).

The molecular weight estimation was done by comparing the migration distance with a molecular weight ladder formed from known molecular weight proteins. A PageRuler ^{TM} unstained protein ladder (Fermentas) with a span of 10 – 200 kDa was used as a molecular weight marker.

3.3.1 Tris/Glycine gel electrophoresis

SDS Tris/Glycine PAGE gels were prepared according to the Laemmli method (Table 5). A 12% running gel was pored between the glass plates, covered with water and allowed to polymerize for 15 minutes. On top of it the stacking gel was poured, a comb was inserted to create the sample pockets and allowed to polymerize for another 15 minutes. The comb was removed and the samples were poured into the pockets. The gel was set to run at 80 V until the samples entered the separating gel and then at 100 V until the end of the run.

Table 5. SDS Tris/Glycine PAGE gel receipe

	10% gel	12% gel	15% gel	Stacking gel
4 x Stacking gel buffer	-	-	-	2.5 mL
4 x Separating gel buffer	6 mL	6 mL	6 mL	-
MilliQ water	10 mL	8.4 mL	6 mL	5.8 mL
Acrylamide/bis	8 mL	9.6 mL	12 mL	1.7 mL
10% APS	125 µL	125 µL	125 µL	85 µL
TEMED	20 µL	20 µL	20 µL	20 µL

3.3.2 Tris/Tricine gel electrophoresis

SDS Tris/Tricine PAGE gels were prepared according to the Schägger and von Jagow method (Table 6). A 15% running gel was pored between the glass plates, covered with water and allowed to polymerize for 15 minutes. On top of it the stacking gel was poured, a comb was inserted to create the sample pockets and allowed to polymerize for another 15 minutes. The comb was removed and the samples were poured into the pockets. The gel was set

to run at 60 V until the samples entered the separating gel and then at 120 V until the end of the run.

Table 6. SDS Tris/Tricine PAGE gel recipe

	10% gel	15% gel	Stacking gel
Acrylamide/bis	4.9 mL	7.5 mL	978 µL
Tris-HCl/SDS	5 mL	5 mL	1.86 mL
MilliQ water	3.8 mL	0.9 mL	4.67 mL
Glycerol	1.58 mL	1.58 mL	-
10% APS	75 µL	75 µL	40 µL
TEMED	10 µL	10 µL	7.5 µL

3.3.3 Colloidal Coomassie staining

Coomassie Brilliant Blue G-250 is a dye that nonspecifically binds to all peptides and proteins. It may be used for visualization, but also for quantification because it binds stoichiometrically to the proteins by interacting with amino acids such as arginine, lysine, tyrosine and histidine. Before staining, the gels were separated from the glass plates and incubated for ½ h at RT in fixing solution (12% TCA). After fixation, the gels were stained by overnight incubation with Coomassie Brilliant Blue solution under gentle agitation. After 12 hours the excess stain was removed by several washing steps and the gels were scanned for data storage and interpretation. The proteins appeared as blue bands against a transparent background.

3.4 Chromatographic methods

3.4.1 Reverse phase high performance liquid chromatography

High performance liquid chromatography (HPLC) is a widely used method for separation and purification of chemical compounds. In the case of peptides and small proteins, a reverse phase is used because of their hydrophobicity. The stationary phase comprises a hydrophobic layer of short saturated hydrocarbons. The proteins are loaded onto the column in a polar solvent and than they were eluted from the stationary phase by decreasing the polarity with the addition of an organic solvent. Two solvents were used: A, 0.1% TFA, and B, 80% acetonitrile, 0.1% TFA (v:v) and an increasing gradient (1 – 2% Solvent B/min) of elution solution was used to elute the peptides from the columns (Table 7). Before purification, synthetic peptides were solubilized in Solvent A or a mixture of Solvents A and B (4:1, v:v) depending of the solubility. The column was equilibrated with the same solution for 10 minutes and than the sample injected. Analytical RP-HPLC was performed with a 1 mL/min flow and semi-preparative RP-HPLC with a 3-5 mL/min. After each run, the column was washed with Solvent B until the signal returned to zero.

Table 7. Gradient used for RP-HPLC purification

Time	%A	%B
0	100	0
5	100	0
55	0	100
60	0	100

The experiments described in this thesis were performed on an UltiMate 3000 system (Dionex, Germering, Germany), equipped with LPG-3400A pumps, and on a Thermo Scientific SpectraSystem (Thermo Scientific, Bremen, Germany) instruments. Depending on the hydrophobicity of the synthetic peptides, Vydac C_4, C_8 and C_{18} columns were used for the

purification of the samples. The chromatograms were registered by UV detection at 220 nm and the sample fractions were collected manually. Before use, the solvents were degassed by sonication under vacuum for 15 min.

3.4.2 ZipTip desalting

ZipTip pipette tips are solid phase micro columns that fit inside a pipette tip. They are widely used as solid support [153] for sample desalting and enrichment when only a very small amount of sample is at disposal. The desalting was performed using ZipTipR® 10 µL pipette tips with a reverse phase media embedded at the end. C_4 and C_{18} tips were used for various peptide sizes. The solutions needed were wetting solution, 50% ACN in Milli Q, washing solution, 0.1% TFA in Milli Q and elution solution, 50% ACN, 0.1% TFA in Milli Q. The sample must be prior solubilized in 0.1% TFA in Milli Q and the ZipTip tip wetted 5 x in wetting solution. The sample was loaded onto the tip by inserting it into the sample solution and aspiring 10-15 times (without air intake). The tip was washed by 10 x aspiration in washing solution and the sample eluted by 10 x aspiration in 5 µL elution solution. The tip was washed before the process is repeated 3-5 times.

3.5 Proteolytic digestion

In order to identify protein bands from SDS-PAGE, in-gel tryptic digestion was done. The bands were manually Trypsin with a scalpel from the gel and washed with MilliQ water. Destaining was performed by alternatively dehydrating the gel pieces with 60% acetonitrile (v:v) and destaining with 50 mM NH_4HCO_3, 3 x 15 min on a shaker. After destaining, the gel pieces were dried in a vacuum centrifuge and rehydrated with digestion buffer (12 ng/µL Trypsin in 50 mM NH_4HCO_3) on ice for 45 minutes. Digestion was carried out by incubation overnight (12 h) at 37 °C. The following day the tryptic mixture was extracted 3 x with ACN/0.1% TFA in MilliQ (3:2, v:v) and lyophilized.

3.6 Thioflavin T measurement

Thioflavin T (ThT) was used to ascertain the presence of β-sheet rich Aβ oligomers and fibrils. A 10 mM aqueous stock solution was used to make one time use aliquots. The aliquots were stored at -20 °C in the dark until use. Fresh 100 µM Thioflavine T solution was made before each measurement by dilution with 50 mM Glycine solution (pH 8.5). Aβ aggregates samples were mixed with ThT solution (1:1, v:v) in a 96 well plate and measured on a Wallac 1420 Victor 2 (PerkinElmer) fluorescence reader. A 450 nm filter was used for excitation and 486 nm for emission readings for 0.1 seconds.

3.7 Affinity methods

The antibody – antigen affinity is a non-covalent interaction of much interest. It plays an important role both *in-vivo*, offering an immune response, and *in-vitro*, immuno-affinity chromatography, circumstances. The investigation of such an interaction can be done using direct measurement methods (ELIZA, Plasmon resonance, SAW) or indirect methods (proteolytic epitope excision and extraction)

3.7.1 Activated sepharose affinity columns

Antibody columns were prepared using NHS-activated 6-aminohexanoic acid-coupled Sepharose 4B (Sigma-Aldrich) as a solid support to covalently attach the antibodies. Free amino groups available on the surface of the antibody react with the Sepharose to form a stabile amide bond and release N-hydroxysuccinimide. 66 mg Sepharose were swollen in 200 µL coupling buffer with 50 µg antibody and incubated for 2 h at RT under agitation. The matrix was than transferred into a 0.8 mL micro-column (Mobitec, Germany) and washed 14 x 6 mL with blocking buffer (0.1 M ethanolamine, 0.5 M NaCl, pH 8.3) and washing buffer (0.2 M NaOAc, 0.5 M NaCl, pH 4) alternatively. The columns can be stored at 4 °C for future use.

Before each affinity experiment the column was washed with 20 mL PBS and incubated with the peptide of interest for 2 h at RT under agitation.

The supernatant was collected and the column washed with 100 mL PBS and 30 mL MilliQ, collecting the last mL of wash. The elution from the column was made incubating 4 x 15 min x 500 µL 0.1% TFA and combining elution fractions for lyophilization. The column regeneration was done by washing with an additional 20 mL 0.1% TFA and 20 mL PBS.

3.7.2 Proteolytic epitope excision

For the proteolytic epitope excision experiment three antibody columns were prepared using Anti-human alpha galactosidase antibody for one column and HD5 and HD6 antibodies for the other two. After preparation, the proteins of interest were loaded onto the columns, alpha galactosidase and HLA-B27 respectively, for affinity bonds formation. Due to the antibody – antigen interactions, the epitope region from the proteins is shielded by the antibody and can be isolated for identification by proteolytic excision. For this, 0.1 µg Trypsin in 200 µL PBS was added to each column and incubated for 2 h at 37 °C under agitation. After collecting the supernatant the columns were washed with PBS and MilliQ. The elution took place with 500 µL 0.1% TFA in MilliQ 4 x 15 min and the combined elution fractions were lyophilized. The epitope fragments obtained were further identified via mass spectrometric characterization.

3.7.3 Surface acoustic wave - determinations of dissociation constant

The bio-affinity family of investigations is able to detect the interaction between single molecules and to measure the strength of that interaction. One of the newest members of this family is the surface acoustic wave (SAW) biosensor. This molecular “scale” is a device that is able to quantify the deposition of material on a gold plated chip. Using a piezo-electric effect an acoustic wave is generated at one end of a quartz chip and registered at the other. The middle of the chip is coated with a layer of gold that acts as the active surface. The preparation of the chip is multi-step process.

1. Before activation, the chip was cleaned by insertion in piranha solution (98% H_2SO_4:30% H_2O_2, 1:1, v:v) for 45 minutes. Afterwards it was washed with MilliQ water and ethanol and dried. The functionalization of the chip was done by generating a self assembling monolayer (SAM) of 16-mercaptohexadecanoic acid on the gold surface. The chip was incubated for 12 h at RT in a 10 mM SAM solution in $CHCl_3$, washed with ethanol and dried. In this stage the chips could be stored at 4 °C before use.

2. The activation of the chip and immobilization of the peptides was done inside the biosensor instrument under automated control. The activation was performed by injecting a freshly prepared mixture of 200 mM EDC:50 mM NHS (1:1, v:v) for 5 minutes with a 20 µL/min flow. The peptides of interest were added as a 10 µM solution and let to covalently bind to the active NHS surface during a 5 min injection. The un-reacted active sites were neutralized by capping with 1 M ethanolamine, ph 8.5. Once the attachment completed, the chips could be stored for later use and reuse.

3. The K_D determinations were done using an Ssens K5 SAW biosensor (SAW Instruments, Bonn, Germany). Dilutions of 10-200 nM antibody were prepared in PBS and injected on the chip. After each injection, a dissociation step was performed using 0.1 M HCl.

4. Data interpretation was done by generating fitting curves with Origin 7.5 and FitMaster plug-in. A residual affinity bound antibody was taken into account during the calculations of k_{Obs}, a pseudo first order kinetic constant. By plotting k_{Obs} against ligand concentrations a linear regression was calculated with the following equation:

$$k_{Obs} = k_{off} + k_{on} * C$$

k_{off} [s^{-1}] is the intercept with the y axis and k_{on} [$c^{-1}s^{-1}$] is the slope of the regression. The K_D was then calculated as being the ratio:

$$K_D = k_{off} / k_{on}$$

3.8 Mass spectrometric methods

Mass spectrometry has proven over the years to be the best method for the identification of peptides and proteins. It is a fast and sensitive method capable to adapt to a variety of circumstances, especially when it is coupled with other biochemical methods such as HPLC and proteolytic degradation. A mass spectrometer consists of three major parts responsible for the generation of ions, separation and/or analysis and detection of ions. The ion source is the place where the analyte is prepared to enter the mass spectrometer, with the matrix assisted laser desorption ionization (MALDI) and electro spray ionization (ESI) being the oldest and most used two methods among an ever increasing number of new ionization methods. The analyzer is the main part of a mass spectrometer and it is responsible with the capture, guidance and separation of ions according to their mass to charge ratio (m/z) while the detector will count the number and register the number of ions for each m/z value.

3.8.1 Matrix assisted laser desorption ionization ion source

MALDI ionization is an ionization method which implies the use of laser as an energy source for the ionization process. In order to transfer the energy to the analyte, the sample must be co-crystallized with a matrix that would absorb at the wavelength of the laser. When hit by the energy beam, the matrix crystals would explode releasing the molecules of analyte inside the vacuum of the mass spectrometer. The matrix also provides the hydrogen ions that give charge to the analyte molecules. The major ion charged species produced by MALDI is singly charged, with doubly charged being the second. A saturated alpha-cyno-4-hydroxi-cinamic acid (CHCA) solution in MALDI solvent (ACN/0.1% TFA, 3:2, v:v) was used for sample preparation. On a stainless steel target 0.8 µL samples were mixed with 0.8 µL matrix and let to air dry for 5 min at RT. The target was subsequently introduced into the mass spectrometer for analysis.

3.8.2 Electrospray ionization source

ESI ionization is a soft ionization method that allows analyte molecules to form multiply charged anions. The samples were solubilized in ESI solvent (10% acetonitrile, 0.1% formic acid, 89.9% MilliQ, pH 2.5) and injected into the ionization chamber. Between the needle and the entrance into the instrument an electric potential is applied to charge and guide the ions. A jet of heated dry gas (Nitrogen) is blown around the needle to help the solvent evaporate. The ionization chamber is at atmospheric pressure and the heated gas can reach temperatures between 200-300 °C. The repulsion between charged droplets leads in the end to the formation of independent ions in a process known as the Taylor cone.

3.8.3 Time of flight analyzer

Time of flight (ToF) is a mass spectrometric analyzer that monitors the time needed for ions to travel a certain distance. It is best suited to work in tandem with a MALDI ion source but can be adapted to work with other methods as well by the use of temporarily ion traps. The ions are accelerated through a series of extraction lenses and the beam is focused with the help of a second series of electric potentials. After this, the ions travel freely through a flight tube under vacuum. The length of the tube can be between a few tens of centimeters up to three meters with one meter being the most common. The ions however may travel a longer distance than the length of the tube if reflector lenses are used. This helps eliminate neutral molecules from the ions beam and increase the resolution by increasing the flight distance. If a circular tube is used, the ions may travel several hundred meters before being directed to the exit. At the end of the tube is a detector that monitors the arrival time of the ions. Based on the mass to charge ratio, heavier ions will travel slower and lighter ion ions will travel faster if the same accelerating impulse is received.

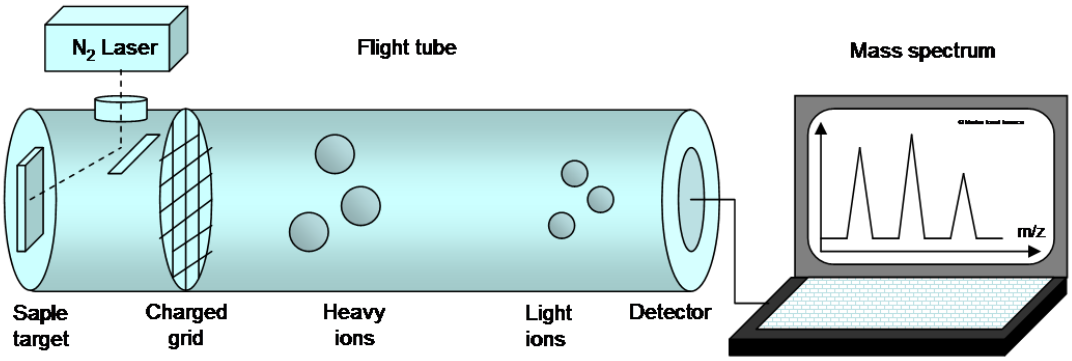

Figure 72. MALDI-ToF instrument: ions are accelerated in an electric field and are separated according to the time of flight inside a one meter vacuum tube.

MALDI-ToF mass spectrometric measurements were carried out on a Micromass Tof Spec 2E (Waters, Eschborne, Germany).

3.8.4 Fourier transform – ion cyclotron resonance analyzer

An ICR cell is a complex analyzer cell that traps and detects ions inside a mass spectrometer. The cell consists of six electrode plates arranged in three opposing pairs to form a cage. Two plates are used for trapping the ions and must be parallel one to another and perpendicular to the direction of the ion beam. The rest of the plates may have different shape and are used for activation of ions and for detection.

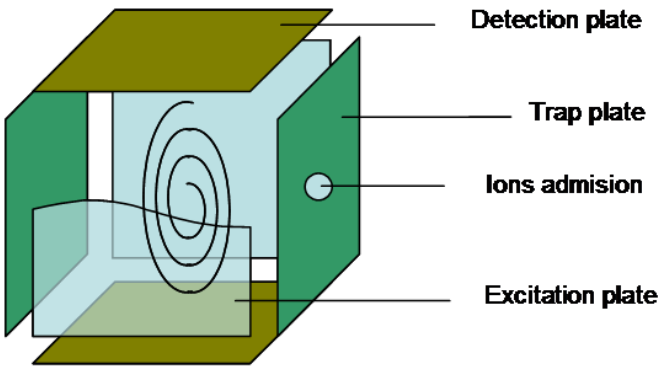

Figure 73. Ion cyclotron resonance (ICR) cell: ions are trapped in a circular motion between the two trap plates; two excitation plates maintain the ions in motion inside the cell while they are scanned by two detection plates

MALDI-FT-ICR mass spectra were recorded on a Bruker APEX II FTICR instrument (Bruker Daltonik, Bremen, Germany). An actively shielded superconducting magnet was used to generate a 7 T magnetic field inside a cylindrical ICR analyzer cell. The ions were generated using an external Scout 100 fully automated X-Y target stage MALDI source and a pulsed nitrogen laser operated at 337 nm. A saturated 100 mg/mL DHB matrix solution in MALDI solvent was used to prepare the sample spots on the MALDI target.

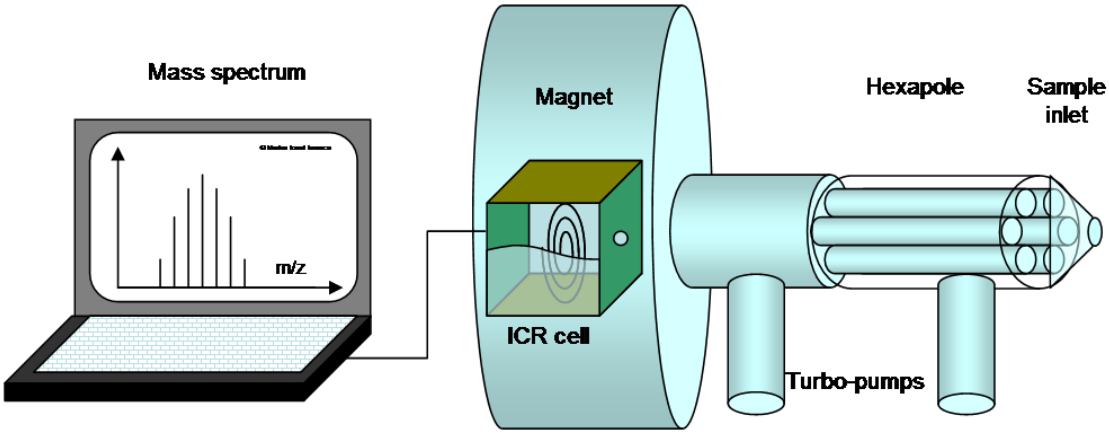

Figure 74. FT-ICR instrument: the ICR cell is placed in a magnetic field inside a 7 T supermagnet cooled with liquid helium; the ions are produced by a MALDI or ESI source and guided through a hexapole to the ICR cell

3.8.5 Ion trap analyzer

An ion trap analyzer consists of a 3D quadrupole trap cell where the RF electric field is applied between one ring electrode and two cap electrodes. The cap electrodes have to offer an entrance for ions to the trap cell and an exit to the detector. The RF field is use to stabilize the ions on a circular orbit and to destabilize them according to their m/z ration and direct them toward the detector. Inside an ion trap tandem MS-MS measurements can be performed using a fragmentation method such as collision induced dissociation (CID). ESI-Ion trap mass spectrometric measurements were performed on an Esquire 3000+ ion trap mass spectrometer (Bruker Daltonik, Bremen, Germany). The samples were introduced by direct infusion with a syringe pump.

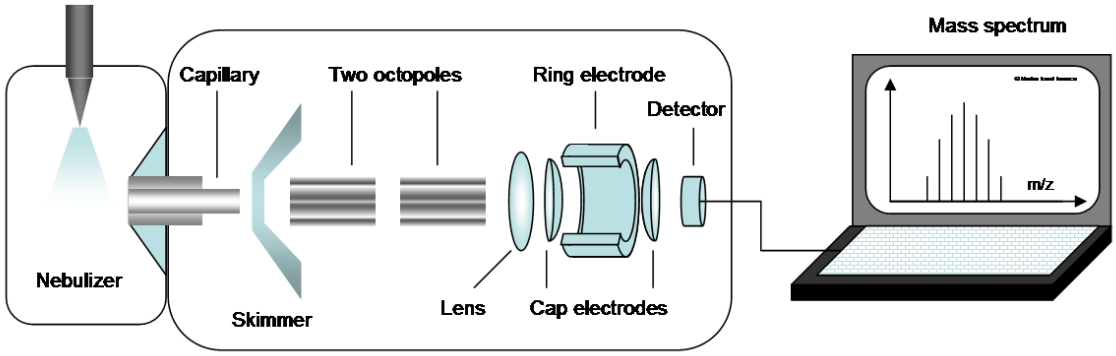

Figure 75. ESI-Ion Trap instrument: ions are formed by an ESI ion source and guided through ion optics to a 3D quadrupole trap

3.8.6 Ion mobility spectroscopy – mass spectrometry analyzer

Ion mobility spectroscopy – mass spectrometry (IMS-MS) is a tandem analysis method that combines an MS analyzer with an IM drift tube. While the mass spectrometer part of the instrument is able to determine the m/z value of an ion, the ion mobility is able to tell more about its shape and collision cross section. An ESI ion source is usually used to produce the ions before entering IMS section of the instrument. The drift tube is a low pressure linear flight tube where the ions must migrate against a current of inert gas. The driving force may be an electric impulse is given at the beginning of the drift tube, or a caring potential wave along the entire length of the drift tube. In both cases the ions will encounter a series of frontal collisions with the inert gas molecules which will slow them down and make them arrive at the end of the tube at different time points. The bigger the size of an ion is, the higher the chances of impact are and the slower the migration through the drift tube will be. After drifting, the ions are pushed into the mass spectrometric analyzer to identify them by m/z.

Ion mobility mass spectrometric measurements were carried out on a Waters SYNAPT G1 HDMS (high definition mass spectrometer) IMS-MS instrument (Waters, Manchester, UK). It consists of a quadrupole, a drift tube

called a Triwave and a ToF analyzer. The Triwave section is a set of three carrying T-waves which gives the instrument the capability of doing ion mobility of the analyte followed by ion fragmentation and ion mobility separation of the resulting fragments. The Aβ samples measurements were performed at Waters Corporation (Manchester, UK) by Waters personnel. Five µL samples (0.5 µg/µL) were injected in a desalting cartridge and eluted with a gradient of 10 to 90% acetonitrile, for 10 min with a flow of 20 µL/min. IMS-MS was performed in the m/z range of 350–4,000 Da at a pressure of 0.45 bars. The cone voltage was 25 V and the drift voltage (T-wave height) was 5 to 15 V.

3.9 Electron paramagnetic resonance

Electron paramagnetic resonance is the electrons equivalent of NMR. It is less common because an unpaired electron is needed to be present, usually inserted by labeling the molecule of interest, but this gives the advantage of less interference and easier to interpret data.

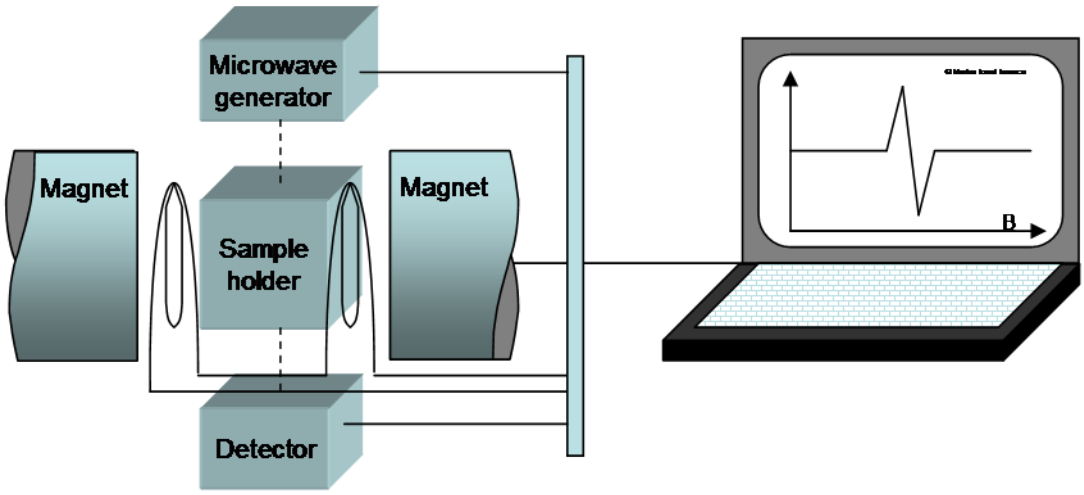

Figure 76. CW-EPR instrument: the sample is situated inside a variable magnetic field while monitoring the absorbance of microwave radiation

The EPR spectra were obtained by measurements on a MiniScope MS200 (Magnettech GmbH, Berlin, Germany) spectrometer at 25°C. Each spectrum consists of an accumulation of 60 x 1 min scans. Modulation

amplitude was set at 400 G and the attenuation at 23 dB. Following acquisition, the spectra were exported to the Matlab (The MathWorks Inc., Natick, Massachusetts, United States) software and fitted by simulations using the EasySpin package. The following simulation parameters were kept constant: g-tensor g=[2.01 2.0068 2.0027], hyperfine tensor A=[13 13 108.4] MHz, and intrinsic line width 0.14 mT.

3.10 Bio-informatics tools

3.10.1 GPMAW

The molecular weight calculation for all proteins and peptides was carried out with the use of GPMAW 5.0 (General Protein – Mass Analysis for Windows) (Lighthouse Data, Denmark) software[154]. The program facilitates the calculation of average and monoisotopic masses for neutral or multiply charged ions. Chemical modifications could be easily added to any amino acid and disulfide bonds could be applied to molecules. The software is also able to predict the hydrophobicity of a protein and the theoretical cleavage sites and digestion mixture for a number of different proteases.

3.10.2 Mascot database search

When an unknown protein is subjected to proteolytic degradation followed by mass spectrometric characterization, the resulting peaks list forms the peptide fingerprint of that protein. In order to identify the protein starting from its peptide fingerprint the Mascot (Matrix Science Inc, Boston, MA, USA) database search engine was used[155].

3.10.3 Matlab with EasySpin plug-in

EPR spectra interpretation and fittings were done using the Matlab (The MathWorks Inc., Natick, Massachusetts, USA) software backed by the EasySpin package. The plug-in is able to generate theoretical fitting curves starting from a set of components.

3.10.4 Origin 7.5 with FitMaster plug-in

For data interpretation of the SAW biosensor measurements the sensorgrams were exported to the Origin 7.5 software (OriginLab, Northampton, Massachusetts, USA). This is a powerful tool for advanced mathematical calculations and wit the help of the FitMaster plug-in it was possible to obtain the K_{on} and K_{off} values from the sensorgrams and to calculate the K_D values.

3.10.5 UCSF Chimera

UCSF Chimera (Resource for Biocomputing, Visualization, and Informatics at the University of California, San Francisco, USA) is a 3D visualization tool for pdb crystal structures [156, 157]. This software was used to highlight sections of the structure and to render graphical images for this thesis.

4 SUMMARY

In present days mass spectrometry (MS) has evolved beyond the status of just an analytical tool. MS is now part of complex interdisciplinary analytical methods. The development of soft ionization methods such as electrospray ionization (ESI) has played a key role in MS expansion, like the coupling with liquid chromatography (LC-MS). The ions of intact molecules obtained by soft ionization have made possible the targeted fragmentation and the development of tandem MS-MS. Recently, a new wave of interconnected methods have appeared around MS. Ion mobility spectrometry - mass spectrometry (IMS-MS) is just one combination, characterized by high resolution and speed of analysis. Even biochemical methods like bio-affinity determination can now be coupled with MS thanks to the development of biosensor instruments.

The first part of this thesis focuses on the development of ion mobility mass spectrometric methods for the characterization of beta Amyloid (1-40) aggregates. The peptide was synthesized by solid phase peptide synthesis and subjected to oligomerization in physiological conditions. The aggregates were identified and characterized successfully by Thioflavin T test, by polyacrylamide gel electrophoresis, in-gel digestion and mass spectrometry.

The second part of the thesis investigates new analytical methods for aggregates characterization based on electron paramagnetic resonance (EPR) spectroscopy. Modified beta amyloid peptides were synthesized by the prolongation of the chain with a cysteinyl residue: Cys-Aβ(1-40) and Aβ(1-40)-Cys. In order to perform EPR measurements, a spin label capable of absorbing electromagnetic radiation was attached to the cysteinyl residue. The modified peptides were subjected to aggregation. The peptide and the aggregates were characterized by EPR measurements.

In the third part of the thesis the epitope of anti-alpha-galactosidase mAb against alpha-galactosidase was determined and characterized by affinity-MS investigations. An affinity micro-column with the mAb was

prepared and the epitope was obtained by affinity proteolytic epitope excision. Mass spectrometry was used to identify the epitope. The epitope peptide was synthesized by SPPS in full length and in truncated versions. The shortest peptide with affinity was selected by running the peptides on the same mAb affinity column. The dissociation constant of this peptide was determined with the use of a surface acoustic wave biosensor instrument.

The last part of the thesis deals with the affinity of HLA-B27 protein against HD5 and HD6 phage display selected antibodies. Two affinity columns were prepared with the two monoclonal antibodies and the HLA-B27 affinity tested. The epitope peptide was determined by affinity proteolytic epitope excision followed by mass spectrometric characterization. The epitope proved to be composed of two separate peptides linked together by a disulphide bridge. The two epitope peptides were synthesized by SPPS and purified by RP-HPLC. To simulate the physiological conditions, the two peptides were linked by a disulphide bridge resulting three possible combinations, two homodimers and one heterodimer. The disulphide linked epitope peptides and the monomeric peptides were tested for affinity against the HD6 mAb column. All dissociation constants of the five peptides were determined by surface acoustic wave biosensor measurements, proving that the specific epitope for the investigated antibodies is the disulphide linked hetero peptide HLA-B27 (203-219)-SS-(257-273).

5 ZUSAMMENFASSUNG

Die Massenspektrometrie (MS) hat sich in den letzten Jahren als ein Höchstleistungsgerät zur Analyse von Biopolymeren entwickelt. Insbesondere ist die MS ist jetzt Teil von komplexen interdisziplinären Analyseverfahren. Die Entwicklung von „sanften“ Ionisationsverfahren, vor allem die Elektrospray-Ionisation (ESI) hat hierbei eine Schlüsselrolle gespielt, wie zB die Kopplung der ESI-MS mit der Flüssigkeitschromatographie in der Entwicklung der LC-MS. Die durch ESI erhaltenen intakten Molekül- Ionen ermöglichen eine selektive Fragmentierung durch die Entwicklung der Tandem-MS-MS. Vor kurzem wurde eine Reihe von kombinierten Methoden der MS entwickelt, von denen die Ionenmobilitäts- Massenspektrometrie (IMS-MS) besonderes Interesse als Gasphasen- Trennmethode mit hoher Auflösung und Geschwindigkeit findet. Auch biochemische und biophysikalische Methoden wie Bioaffinitätsbestimmung mittels Biosensoren wurden vor kurzem mit der MS gekoppelt.

Der erste Teil der vorliegenden Arbeit beschäftigt sich mit der Entwicklung von Ionenmobilitäts- massenspektrometrischen Methoden zur Charakterisierung von Beta-Amyloid (Aß)- Aggregaten, einem Schlüselprotein der Alzheimer- Krankheit. Aß- Peptide wurden durch Festphasenpeptidsynthese synthetisiert und ihre Oligomerisierung unter physiologischen Bedingungen untersucht. Die Aggregation wurden durch Thioflavin-T Test, sowie durch Polyacrylamid-Gelelektrophorese Abbau im Gel und Massenspektrometrie analysiert.

Im zweiten Teil der Arbeit wurden neue analytische Methoden zur Charakterisierung der Aß-Aggregation mit Hilfe der Elektronenspinresonanz (EPR) –Spektroskopie untersucht. Modifizierte Beta-Amyloid-Peptide wurden durch Verlängerung der Peptidkette mit einem Cysteinrest synthetisiert, an den eine geeignete Spinmarkierung (Spinlabel) zur EPR- Analyse gekuppelt wurde. Mit den modifizierten Spinlabel- Peptiden wurden eine Aggregation durchgefuhrt, und das Peptid und die Aß-Aggregate durch EPR-Messungen analysiert.

Im dritten Teil der Arbeit wurde das Epitop eines monoklonalen Antikörpers gegen die Alpha-Galactosidase identifiziert und mittels Affinitäts-MS charakterisiert. Hierzu wurde eine Affinitäts- Mikrosäule des Antikörpers hergestellt, und das Epitop wurde durch proteolytische Epitop- Exzision und Massenspektrometrie identifiziert. Das Epitop-Peptid wurde mittels SPPS mit vollständiger Sequenzlänge und in verschiedenen verkürzten Versionen synthetisiert, und die Minimalsequenz mittels Antikörper- Affinitätssäule identifiziert. Ferner wurde die Dissoziationskonstante des Epitop- Peptids mittels SAW- Biosensoranalyse bestimmt.

Der letzte Teil der Arbeit befasst sich mit der Epitopaufklärung und Affinitätscharakterisierung des HLA-B27-Proteins gegenüber zwei mittels Phagendisplay selektierten Antikörpern, HD5 und HD6. Zwei Affinitätssäulen wurden mit den monoklonalen Antikörpern hergestellt und die Affinität des HLA-B27 Proteins charakterisiert. Das Epitop-Peptid wurde durch proteolytische Epitop-Exzision und anschliessende MALDI-massenspektrometrische Analyse identifiziert. Die Epitopstruktur erwies sich als ein Disulfid- Dimerpeptid, das durch eine Disulfidbrücke verknüpft ist. Die beiden Peptidkomponenten des Epitops wurden durch SPPS synthetisiert und mittels RP-HPLC gereinigt. Um die physiologischen Bedingungen zu simulieren, wurden beide Peptide durch eine Disulfidbrücke oxidativ verknüpft; dabei entstehen drei mögliche Kombinationen, zwei Homodimere und eine Heterodimerstruktur. Die Disulfid- gebunden Epitop- Peptide und die monomeren Peptide wurden auf ihre Affinität gegen den HD6- Antikörper getestet, und die Dissoziationskonstanten der fünf Peptide mittels SAW-Biosensoranalyse bestimmt.

6 BIBLIOGRAPHY

1. Wilkins, M.R., C. Pasquali, R.D. Appel, K. Ou, O. Golaz, J.C. Sanchez, J.X. Yan, A.A. Gooley, G. Hughes, I. Humphery-Smith, K.L. Williams and D.F. Hochstrasser, *From proteins to proteomes: large scale protein identification by two-dimensional electrophoresis and amino acid analysis.* Biotechnology (N Y), 1996. **14**(1): p. 61-5.

2. Tyers, M. and M. Mann, *From genomics to proteomics.* Nature, 2003. **422**(6928): p. 193-7.

3. Semba, R.D., J.J. Enghild, V. Venkatraman, T.F. Dyrlund and J.E. Van Eyk, *The Human Eye Proteome Project: perspectives on an emerging proteome.* Proteomics, 2013. **13**(16): p. 2500-11.

4. Lis, J., M. Orczyk-Pawilowicz and I. Katnik-Prastowska, *[Proteins of human milk involved in immunological processes].* Postepy Hig Med Dosw (Online), 2013. **67**: p. 529-47.

5. Jagr, M., A. Eckhardt, S. Pataridis, Z. Broukal, J. Duskova and I. Miksik, *Proteomics of human teeth and saliva.* Physiol Res, 2014. **63 Suppl 1**: p. S141-54.

6. Karimi, P., A. Shahrokni and M.R. Ranjbar, *Implementation of proteomics for cancer research: past, present, and future.* Asian Pac J Cancer Prev, 2014. **15**(6): p. 2433-8.

7. Deutsch, E.W., J.P. Albar, P.A. Binz, M. Eisenacher, A.R. Jones, G. Mayer, G.S. Omenn, S. Orchard, J.A. Vizcaino and H. Hermjakob, *Development of data representation standards by the human proteome organization proteomics standards initiative.* J Am Med Inform Assoc, 2015.

8. Kim, M.S., S.M. Pinto, D. Getnet, R.S. Nirujogi, S.S. Manda, R. Chaerkady, A.K. Madugundu, D.S. Kelkar, R. Isserlin, S. Jain, J.K. Thomas, B. Muthusamy, P. Leal-Rojas, P. Kumar, N.A. Sahasrabuddhe, L. Balakrishnan, J. Advani, B. George, S. Renuse, L.D. Selvan, A.H. Patil, V. Nanjappa, A. Radhakrishnan, S. Prasad, T. Subbannayya, R. Raju, M. Kumar, S.K. Sreenivasamurthy, A. Marimuthu, G.J. Sathe, S. Chavan, K.K. Datta, Y. Subbannayya, A. Sahu, S.D. Yelamanchi, S. Jayaram, P. Rajagopalan, J. Sharma, K.R. Murthy, N. Syed, R. Goel, A.A. Khan, S. Ahmad, G. Dey, K. Mudgal, A. Chatterjee, T.C. Huang, J. Zhong, X. Wu, P.G. Shaw, D. Freed, M.S. Zahari, K.K. Mukherjee, S. Shankar, A. Mahadevan, H. Lam, C.J.

Mitchell, S.K. Shankar, P. Satishchandra, J.T. Schroeder, R. Sirdeshmukh, A. Maitra, S.D. Leach, C.G. Drake, M.K. Halushka, T.S. Prasad, R.H. Hruban, C.L. Kerr, G.D. Bader, C.A. Iacobuzio-Donahue, H. Gowda, and A. Pandey, *A draft map of the human proteome.* Nature, 2014. **509**(7502): p. 575-81.

9. Rucker, R.B. and F. Wold, *Cofactors in and as posttranslational protein modifications.* FASEB J, 1988. **2**(7): p. 2252-61.

10. Rucker, R.B. and C. McGee, *Chemical modifications of proteins in vivo: selected examples important to cellular regulation.* J Nutr, 1993. **123**(6): p. 977-90.

11. Salzano, A.M. and M. Crescenzi, *Mass spectrometry for protein identification and the study of post translational modifications.* Ann Ist Super Sanita, 2005. **41**(4): p. 443-50.

12. Kwon, S.J., E.Y. Choi, Y.J. Choi, J.H. Ahn and O.K. Park, *Proteomics studies of post-translational modifications in plants.* J Exp Bot, 2006. **57**(7): p. 1547-51.

13. Okeley, N.M. and W.A. van der Donk, *Novel cofactors via post-translational modifications of enzyme active sites.* Chem Biol, 2000. **7**(7): p. R159-71.

14. Perler, F.B., *Protein splicing of inteins and hedgehog autoproteolysis: structure, function, and evolution.* Cell, 1998. **92**(1): p. 1-4.

15. Shao, Y. and S.B. Kent, *Protein splicing: occurrence, mechanisms and related phenomena.* Chem Biol, 1997. **4**(3): p. 187-94.

16. Wallace, C.J., *The curious case of protein splicing: mechanistic insights suggested by protein semisynthesis.* Protein Sci, 1993. **2**(5): p. 697-705.

17. Ball, D., J. Hill and R. Scott, *The Basics of General, Organic, and Biological Chemistry*. 2011: Flat World Knowledge.

18. Uversky, V.N., *Natively unfolded proteins: a point where biology waits for physics.* Protein Sci, 2002. **11**(4): p. 739-56.

19. Feige, M.J. and L.M. Hendershot, *Disulfide bonds in ER protein folding and homeostasis.* Curr Opin Cell Biol, 2011. **23**(2): p. 167-75.

20. Ishimaru, T., K. Ito, M. Tanaka, S. Tanaka and N. Matsudomi, *The role of the disulfide bridge in the stability and structural integrity of*

ovalbumin evaluated by site-directed mutagenesis. Biosci Biotechnol Biochem, 2011. **75**(3): p. 544-9.

21. Castro, J.R., C.A. Fuzo, L. Degreve and A. Caliri, *The role of disulfide bridges in the 3-D structures of the antimicrobial peptides gomesin and protegrin-1: a molecular dynamics study.* Genet Mol Res, 2008. **7**(4): p. 1070-88.

22. Weber, R., R. Preywisch, N. Youhnovski, M. Groettrup and M. Przybylski, *Identification of the molecular composition of the 20S proteasome of mouse intestine by high-resolution mass spectrometric proteome analysis.* Methods Mol Biol, 2009. **564**: p. 173-86.

23. Peters, J.M., W.W. Franke and J.A. Kleinschmidt, *Distinct 19 S and 20 S subcomplexes of the 26 S proteasome and their distribution in the nucleus and the cytoplasm.* J Biol Chem, 1994. **269**(10): p. 7709-18.

24. Glickman, M.H. and N. Adir, *The proteasome and the delicate balance between destruction and rescue.* PLoS Biol, 2004. **2**(1): p. E13.

25. Walker, L.C. and H. LeVine, *The cerebral proteopathies: neurodegenerative disorders of protein conformation and assembly.* Mol Neurobiol, 2000. **21**(1-2): p. 83-95.

26. Luheshi, L.M. and C.M. Dobson, *Bridging the gap: from protein misfolding to protein misfolding diseases.* FEBS Lett, 2009. **583**(16): p. 2581-6.

27. Walker, L.C. and H. LeVine, 3rd, *The cerebral proteopathies.* Neurobiol Aging, 2000. **21**(4): p. 559-61.

28. Mrak, R.E. and W.S. Griffin, *Dementia with Lewy bodies: Definition, diagnosis, and pathogenic relationship to Alzheimer's disease.* Neuropsychiatr Dis Treat, 2007. **3**(5): p. 619-25.

29. Zhu, M.M., D.L. Rempel, Z. Du and M.L. Gross, *Quantification of protein-ligand interactions by mass spectrometry, titration, and H/D exchange: PLIMSTEX.* J Am Chem Soc, 2003. **125**(18): p. 5252-3.

30. Tu, T., M. Dragusanu, B.A. Petre, D.L. Rempel, M. Przybylski and M.L. Gross, *Protein-peptide affinity determination using an h/d exchange dilution strategy: application to antigen-antibody interactions.* J Am Soc Mass Spectrom, 2010. **21**(10): p. 1660-7.

31. Yamada, N., E. Suzuki and K. Hirayama, *Identification of the interface of a large protein-protein complex using H/D exchange and Fourier*

transform ion cyclotron resonance mass spectrometry. Rapid Commun Mass Spectrom, 2002. **16**(4): p. 293-9.

32. Hillenkamp, F. and M. Karas, *Mass spectrometry of peptides and proteins by matrix-assisted ultraviolet laser desorption/ionization.* Methods Enzymol, 1990. **193**: p. 280-95.

33. Hillenkamp, F., M. Karas, R.C. Beavis and B.T. Chait, *Matrix-assisted laser desorption/ionization mass spectrometry of biopolymers.* Anal Chem, 1991. **63**(24): p. 1193A-1203A.

34. Karas, M. and U. Bahr, *Laser desorption ionization mass spectrometry of bioorganic molecules.* Methods Mol Biol, 1993. **17**: p. 215-28.

35. Karas, M. and F. Hillenkamp, *Laser desorption ionization of proteins with molecular masses exceeding 10,000 daltons.* Anal Chem, 1988. **60**(20): p. 2299-301.

36. Fagerer, S.R., S. Nielsen, A. Ibanez and R. Zenobi, *Matrix-assisted laser desorption/ionization matrices for negative mode metabolomics.* Eur J Mass Spectrom (Chichester, Eng), 2013. **19**(1): p. 39-47.

37. Karas, M. and R. Kruger, *Ion formation in MALDI: the cluster ionization mechanism.* Chem Rev, 2003. **103**(2): p. 427-40.

38. Taylor, G., *Disintegration of Water Drops in an Electric Field*. Vol. 280. 1964. 383-397.

39. Fenn, J.B., *Ion formation from charged droplets: Roles of geometry, energy, and time.* J Am Soc Mass Spectrom, 1993. **4**(7): p. 524-35.

40. Fenn, J.B., M. Mann, C.K. Meng, S.F. Wong and C.M. Whitehouse, *Electrospray ionization for mass spectrometry of large biomolecules.* Science, 1989. **246**(4926): p. 64-71.

41. Fenn, J.B., *Electrospray ionization mass spectrometry: How it all began.* J Biomol Tech, 2002. **13**(3): p. 101-18.

42. Bladergroen, M.R. and Y.E. van der Burgt, *Solid-phase extraction strategies to surmount body fluid sample complexity in high-throughput mass spectrometry-based proteomics.* J Anal Methods Chem, 2015. **2015**: p. 250131.

43. Pfaunmiller, E.L., M.L. Paulemond, C.M. Dupper and D.S. Hage, *Affinity monolith chromatography: a review of principles and recent analytical applications.* Anal Bioanal Chem, 2013. **405**(7): p. 2133-45.

44. Thompson, J.W., M.T. Forrester, M.A. Moseley and M.W. Foster, *Solid-phase capture for the detection and relative quantification of S-nitrosoproteins by mass spectrometry.* Methods, 2013. **62**(2): p. 130-7.

45. Sela-Culang, I., V. Kunik and Y. Ofran, *The structural basis of antibody-antigen recognition.* Front Immunol, 2013. **4**: p. 302.

46. Geisberger, R., M. Lamers and G. Achatz, *The riddle of the dual expression of IgM and IgD.* Immunology, 2006. **118**(4): p. 429-37.

47. Mattu, T.S., R.J. Pleass, A.C. Willis, M. Kilian, M.R. Wormald, A.C. Lellouch, P.M. Rudd, J.M. Woof and R.A. Dwek, *The glycosylation and structure of human serum IgA1, Fab, and Fc regions and the role of N-glycosylation on Fcalpha receptor interactions.* J Biol Chem, 1998. **273**(4): p. 2260-72.

48. Delacroix, D.L., C. Dive, J.C. Rambaud and J.P. Vaerman, *IgA subclasses in various secretions and in serum.* Immunology, 1982. **47**(2): p. 383-5.

49. Russell, M.W., J. Reinholdt and M. Kilian, *Anti-inflammatory activity of human IgA antibodies and their Fab alpha fragments: inhibition of IgG-mediated complement activation.* Eur J Immunol, 1989. **19**(12): p. 2243-9.

50. Porter, R.R., *The structure of the heavy chain of immunoglobulin and its relevance to the nature of the antibody-combining site. The Second CIBA Medal Lecture.* Biochem J, 1967. **105**(2): p. 417-26.

51. Al-Lazikani, B., A.M. Lesk and C. Chothia, *Standard conformations for the canonical structures of immunoglobulins.* J Mol Biol, 1997. **273**(4): p. 927-48.

52. North, B., A. Lehmann and R.L. Dunbrack, Jr., *A new clustering of antibody CDR loop conformations.* J Mol Biol, 2011. **406**(2): p. 228-56.

53. Shirai, H., A. Kidera and H. Nakamura, *H3-rules: identification of CDR-H3 structures in antibodies.* FEBS Lett, 1999. **455**(1-2): p. 188-97.

54. Spindler, N., P. Rucker, S. Potzsch, U. Diestel, H. Sticht, L. Martin-Parras, T.H. Winkler and M. Mach, *Characterization of a discontinuous neutralizing epitope on glycoprotein B of human cytomegalovirus.* J Virol, 2013. **87**(16): p. 8927-39.

55. Sivalingam, G.N. and A.J. Shepherd, *An analysis of B-cell epitope discontinuity.* Mol Immunol, 2012. **51**(3-4): p. 304-9.

56. Irving, M.B., L. Craig, A. Menendez, B.P. Gangadhar, M. Montero, N.E. van Houten and J.K. Scott, *Exploring peptide mimics for the production of antibodies against discontinuous protein epitopes.* Mol Immunol, 2010. **47**(5): p. 1137-48.

57. Hager-Braun, C., E.O. Hochleitner, M.K. Gorny, S. Zolla-Pazner, R.J. Bienstock and K.B. Tomer, *Characterization of a discontinuous epitope of the HIV envelope protein gp120 recognized by a human monoclonal antibody using chemical modification and mass spectrometric analysis.* J Am Soc Mass Spectrom, 2010. **21**(10): p. 1687-98.

58. O'Brien, M.A., D.G. Power, A.J. Clover, B. Bird, D.M. Soden and P.F. Forde, *Local tumour ablative therapies: opportunities for maximising immune engagement and activation.* Biochim Biophys Acta, 2014. **1846**(2): p. 510-23.

59. Olinger, G.G., Jr., J. Pettitt, D. Kim, C. Working, O. Bohorov, B. Bratcher, E. Hiatt, S.D. Hume, A.K. Johnson, J. Morton, M. Pauly, K.J. Whaley, C.M. Lear, J.E. Biggins, C. Scully, L. Hensley and L. Zeitlin, *Delayed treatment of Ebola virus infection with plant-derived monoclonal antibodies provides protection in rhesus macaques.* Proc Natl Acad Sci U S A, 2012. **109**(44): p. 18030-5.

60. Li, Y., Y.S. Ning, L. Li, D.D. Peng, W.Q. Dong and M. Li, *[Preparation of a monoclonal antibodies against Plasmodium falciparum glutamate dehydrogenase and establishment of colloidal gold-immunochromatographic assay].* Di Yi Jun Yi Da Xue Xue Bao, 2005. **25**(4): p. 435-8.

61. Sweeley, C.C. and B. Klionsky, *Fabry's Disease: Classification as a Sphingolipidosis and Partial Characterization of a Novel Glycolipid.* J Biol Chem, 1963. **238**: p. 3148-50.

62. Germain, D.P., J. Charrow, R.J. Desnick, N. Guffon, J. Kempf, R.H. Lachmann, R. Lemay, G.E. Linthorst, S. Packman, C.R. Scott, S. Waldek, D.G. Warnock, N.J. Weinreb and W.R. Wilcox, *Ten-year outcome of enzyme replacement therapy with agalsidase beta in patients with Fabry disease.* J Med Genet, 2015.

63. Brewster, M.A., S.A. Whaley and A.C. Kane, *Variables in the laboratory diagnosis of Fabry's disease by measurement of methylumbelliferyl-alpha-galactosidase activity.* Clin Chem, 1974. **20**(3): p. 383-6.

64. Sieper, J., J. Braun, M. Rudwaleit, A. Boonen and A. Zink, *Ankylosing spondylitis: an overview.* Ann Rheum Dis, 2002. **61 Suppl 3**: p. iii8-18.

65. Ramos, M., A. Paradela, M. Vazquez, A. Marina, J. Vazquez and J.A. Lopez de Castro, *Differential association of HLA-B*2705 and B*2709 to ankylosing spondylitis correlates with limited peptide subsets but not with altered cell surface stability.* J Biol Chem, 2002. **277**(32): p. 28749-56.

66. Merino, E., V. Montserrat, A. Paradela and J.A. Lopez de Castro, *Two HLA-B14 subtypes (B*1402 and B*1403) differentially associated with ankylosing spondylitis differ substantially in peptide specificity but have limited peptide and T-cell epitope sharing with HLA-B27.* J Biol Chem, 2005. **280**(43): p. 35868-80.

67. Payeli, S.K., S. Kollnberger, O. Marroquin Belaunzaran, M. Thiel, K. McHugh, J. Giles, J. Shaw, S. Kleber, A. Ridley, I. Wong-Baeza, S. Keidel, K. Kuroki, K. Maenaka, A. Wadle, C. Renner and P. Bowness, *Inhibiting HLA-B27 homodimer-driven immune cell inflammation in spondylarthritis.* Arthritis Rheum, 2012. **64**(10): p. 3139-49.

68. Suckau, D., J. Kohl, G. Karwath, K. Schneider, M. Casaretto, D. Bitter-Suermann and M. Przybylski, *Molecular epitope identification by limited proteolysis of an immobilized antigen-antibody complex and mass spectrometric peptide mapping.* Proc Natl Acad Sci U S A, 1990. **87**(24): p. 9848-52.

69. Glocker, M.O., C. Borchers, W. Fiedler, D. Suckau and M. Przybylski, *Molecular characterization of surface topology in protein tertiary structures by amino-acylation and mass spectrometric peptide mapping.* Bioconjug Chem, 1994. **5**(6): p. 583-90.

70. Van de Water, J., S.O. Deininger, M. Macht, M. Przybylski and M.E. Gershwin, *Detection of molecular determinants and epitope mapping using MALDI-TOF mass spectrometry.* Clin Immunol Immunopathol, 1997. **85**(3): p. 229-35.

71. Fiedler, W., C. Borchers, M. Macht, S.O. Deininger and M. Przybylski, *Molecular characterization of a conformational epitope of hen egg white lysozyme by differential chemical modification of immune complexes and mass spectrometric peptide mapping.* Bioconjug Chem, 1998. **9**(2): p. 236-41.

72. Stefanescu, R., R. Born, A. Moise, B. Ernst and M. Przybylski, *Epitope structure of the carbohydrate recognition domain of asialoglycoprotein receptor to a monoclonal antibody revealed by high-resolution proteolytic excision mass spectrometry.* J Am Soc Mass Spectrom, 2011. **22**(1): p. 148-57.

73. Bilkova, Z., R. Stefanescu, R. Cecal, L. Korecka, S. Ouzka, J. Jezova, J.L. Viovy and M. Przybylski, *Epitope extraction technique using a*

proteolytic magnetic reactor combined with Fourier-transform ion cyclotron resonance mass spectrometry as a tool for the screening of potential vaccine lead peptides. Eur J Mass Spectrom (Chichester, Eng), 2005. **11**(5): p. 489-95.

74. Stefanescu, R., R.E. Iacob, E.N. Damoc, A. Marquardt, E. Amstalden, M. Manea, I. Perdivara, M. Maftei, G. Paraschiv and M. Przybylski, *Mass spectrometric approaches for elucidation of antigenantibody recognition structures in molecular immunology.* Eur J Mass Spectrom (Chichester, Eng), 2007. **13**(1): p. 69-75.

75. Paraschiv, G., C. Vincke, P. Czaplewska, M. Manea, S. Muyldermans and M. Przybylski, *Epitope structure and binding affinity of single chain llama anti-beta-amyloid antibodies revealed by proteolytic excision affinity-mass spectrometry.* J Mol Recognit, 2013. **26**(1): p. 1-9.

76. Macht, M., A. Marquardt, S.O. Deininger, E. Damoc, M. Kohlmann and M. Przybylski, *"Affinity-proteomics": direct protein identification from biological material using mass spectrometric epitope mapping.* Anal Bioanal Chem, 2004. **378**(4): p. 1102-11.

77. Pimenova, T., L. Meier, B. Roschitzki, G. Paraschiv, M. Przybylski and R. Zenobi, *Polystyrene beads as an alternative support material for epitope identification of a prion-antibody interaction using proteolytic excision-mass spectrometry.* Anal Bioanal Chem, 2009. **395**(5): p. 1395-401.

78. Sladewska, A., A. Szymanska, M. Kordalska, A. Lewandowska, A.S. Kolodziejczyk, G. Paraschiv, M. Przybylski and P. Czaplewska, *Identification of the epitope for anti-cystatin C antibody.* J Mol Recognit, 2011. **24**(4): p. 687-99.

79. Juszczyk, P., G. Paraschiv, A. Szymanska, A.S. Kolodziejczyk, S. Rodziewicz-Motowidlo, Z. Grzonka and M. Przybylski, *Binding epitopes and interaction structure of the neuroprotective protease inhibitor cystatin C with beta-amyloid revealed by proteolytic excision mass spectrometry and molecular docking simulation.* J Med Chem, 2009. **52**(8): p. 2420-8.

80. Marquardt, A., B. Bernevic and M. Przybylski, *Identification, affinity characterisation and biological interactions of lectin-like peptide-carbohydrate complexes derived from human TNF-alpha using high-resolution mass spectrometry.* J Pept Sci, 2007. **13**(12): p. 803-10.

81. Moise, A., S. Andre, F. Eggers, M. Krzeminski, M. Przybylski and H.J. Gabius, *Toward bioinspired galectin mimetics: identification of ligand-contacting peptides by proteolytic-excision mass spectrometry.* J Am Chem Soc, 2011. **133**(38): p. 14844-7.

82. Magdeldin, S., S. Enany, Y. Yoshida, B. Xu, Y. Zhang, Z. Zureena, I. Lokamani, E. Yaoita and T. Yamamoto, *Basics and recent advances of two dimensional- polyacrylamide gel electrophoresis.* Clin Proteomics, 2014. **11**(1): p. 16.

83. Macht, M., W. Fiedler, K. Kurzinger and M. Przybylski, *Mass spectrometric mapping of protein epitope structures of myocardial infarct markers myoglobin and troponin T.* Biochemistry, 1996. **35**(49): p. 15633-9.

84. Patching, S.G., *Surface plasmon resonance spectroscopy for characterisation of membrane protein-ligand interactions and its potential for drug discovery.* Biochim Biophys Acta, 2014. **1838**(1 Pt A): p. 43-55.

85. Geschwindner, S., J.F. Carlsson and W. Knecht, *Application of optical biosensors in small-molecule screening activities.* Sensors (Basel), 2012. **12**(4): p. 4311-23.

86. Zheng, Y.B., B. Kiraly, P.S. Weiss and T.J. Huang, *Molecular plasmonics for biology and nanomedicine.* Nanomedicine (Lond), 2012. **7**(5): p. 751-70.

87. Rocha-Gaso, M.I., C. March-Iborra, A. Montoya-Baides and A. Arnau-Vives, *Surface generated acoustic wave biosensors for the detection of pathogens: a review.* Sensors (Basel), 2009. **9**(7): p. 5740-69.

88. Al-Halabi, L., A. Balck, M. Michalzik, D. Frode, S. Buttgenbach, M. Hust, T. Schirrmann and S. Dubel, *Recombinant antibody fragments allow repeated measurements of C-reactive protein with a quartz crystal microbalance immunosensor.* MAbs, 2013. **5**(1): p. 140-9.

89. Wu, J., J.P. Park, K. Dooley, D.M. Cropek, A.C. West and S. Banta, *Rapid development of new protein biosensors utilizing peptides obtained via phage display.* PLoS One, 2011. **6**(10): p. e24948.

90. Wang, S.H., C.Y. Shen, T.C. Weng, P.H. Lin, J.J. Yang, I.F. Chen, S.M. Kuo, S.J. Chang, Y.K. Tu, Y.H. Kao and C.H. Hung, *Detection of cartilage oligomeric matrix protein using a quartz crystal microbalance.* Sensors (Basel), 2010. **10**(12): p. 11633-43.

91. Dragusanu, M., B.A. Petre, S. Slamnoiu, C. Vlad, T. Tu and M. Przybylski, *On-line bioaffinity-electrospray mass spectrometry for simultaneous detection, identification, and quantification of protein-ligand interactions.* J Am Soc Mass Spectrom, 2010. **21**(10): p. 1643-8.

92. Slamnoiu, S., C. Vlad, M. Stumbaum, A. Moise, K. Lindner, N. Engel, M. Vilanova, M. Diaz, C. Karreman, M. Leist, T. Ciossek, B. Hengerer, M. Vilaseca and M. Przybylski, *Identification and affinity-quantification of ss-amyloid and alpha-synuclein polypeptides using on-line SAW-biosensor-mass spectrometry.* J Am Soc Mass Spectrom, 2014. **25**(8): p. 1472-81.

93. Dragusanu, M., B.A. Petre and M. Przybylski, *Epitope motif of an anti-nitrotyrosine antibody specific for tyrosine-nitrated peptides revealed by a combination of affinity approaches and mass spectrometry.* J Pept Sci, 2011. **17**(3): p. 184-91.

94. Alzheimer, A., R.A. Stelzmann, H.N. Schnitzlein and F.R. Murtagh, *An English translation of Alzheimer's 1907 paper, "Uber eine eigenartige Erkankung der Hirnrinde".* Clin Anat, 1995. **8**(6): p. 429-31.

95. Lobo, A., L.J. Launer, L. Fratiglioni, K. Andersen, A. Di Carlo, M.M. Breteler, J.R. Copeland, J.F. Dartigues, C. Jagger, J. Martinez-Lage, H. Soininen and A. Hofman, *Prevalence of dementia and major subtypes in Europe: A collaborative study of population-based cohorts. Neurologic Diseases in the Elderly Research Group.* Neurology, 2000. **54**(11 Suppl 5): p. S4-9.

96. Molsa, P.K., R.J. Marttila and U.K. Rinne, *Survival and cause of death in Alzheimer's disease and multi-infarct dementia.* Acta Neurol Scand, 1986. **74**(2): p. 103-7.

97. Blennow, K., M.J. de Leon and H. Zetterberg, *Alzheimer's disease.* Lancet, 2006. **368**(9533): p. 387-403.

98. Sherrington, R., E.I. Rogaev, Y. Liang, E.A. Rogaeva, G. Levesque, M. Ikeda, H. Chi, C. Lin, G. Li, K. Holman, T. Tsuda, L. Mar, J.F. Foncin, A.C. Bruni, M.P. Montesi, S. Sorbi, I. Rainero, L. Pinessi, L. Nee, I. Chumakov, D. Pollen, A. Brookes, P. Sanseau, R.J. Polinsky, W. Wasco, H.A. Da Silva, J.L. Haines, M.A. Perkicak-Vance, R.E. Tanzi, A.D. Roses, P.E. Fraser, J.M. Rommens, and P.H. St George-Hyslop, *Cloning of a gene bearing missense mutations in early-onset familial Alzheimer's disease.* Nature, 1995. **375**(6534): p. 754-60.

99. Bagyinszky, E., Y.C. Youn, S.S. An and S. Kim, *The genetics of Alzheimer's disease.* Clin Interv Aging, 2014. **9**: p. 535-51.

100. Rongve, A., D. Arsland and C. Graff, *[Alzheimer's disease and genetics].* Tidsskr Nor Laegeforen, 2013. **133**(14): p. 1449-52.

101. Tanzi, R.E., *The genetics of Alzheimer disease.* Cold Spring Harb Perspect Med, 2012. **2**(10).

102. Schellenberg, G.D. and T.J. Montine, *The genetics and neuropathology of Alzheimer's disease.* Acta Neuropathol, 2012. **124**(3): p. 305-23.

103. Francis, P.T., A.M. Palmer, M. Snape and G.K. Wilcock, *The cholinergic hypothesis of Alzheimer's disease: a review of progress.* J Neurol Neurosurg Psychiatry, 1999. **66**(2): p. 137-47.

104. Iqbal, K., C. Alonso Adel, S. Chen, M.O. Chohan, E. El-Akkad, C.X. Gong, S. Khatoon, B. Li, F. Liu, A. Rahman, H. Tanimukai and I. Grundke-Iqbal, *Tau pathology in Alzheimer disease and other tauopathies.* Biochim Biophys Acta, 2005. **1739**(2-3): p. 198-210.

105. Hardy, J. and D. Allsop, *Amyloid deposition as the central event in the aetiology of Alzheimer's disease.* Trends Pharmacol Sci, 1991. **12**(10): p. 383-8.

106. Hardy, J. and D.J. Selkoe, *The amyloid hypothesis of Alzheimer's disease: progress and problems on the road to therapeutics.* Science, 2002. **297**(5580): p. 353-6.

107. Winblad, B., A. Graf, M.E. Riviere, N. Andreasen and J.M. Ryan, *Active immunotherapy options for Alzheimer's disease.* Alzheimers Res Ther, 2014. **6**(1): p. 7.

108. Hayden, E.Y. and D.B. Teplow, *Amyloid beta-protein oligomers and Alzheimer's disease.* Alzheimers Res Ther, 2013. **5**(6): p. 60.

109. Muller, U.C. and H. Zheng, *Physiological functions of APP family proteins.* Cold Spring Harb Perspect Med, 2012. **2**(2): p. a006288.

110. Zhang, X., Y. Li, H. Xu and Y.W. Zhang, *The gamma-secretase complex: from structure to function.* Front Cell Neurosci, 2014. **8**: p. 427.

111. Zhang, X. and W. Song, *The role of APP and BACE1 trafficking in APP processing and amyloid-beta generation.* Alzheimers Res Ther, 2013. **5**(5): p. 46.

112. Lacor, P.N., M.C. Buniel, P.W. Furlow, A.S. Clemente, P.T. Velasco, M. Wood, K.L. Viola and W.L. Klein, *Abeta oligomer-induced aberrations in synapse composition, shape, and density provide a molecular basis for loss of connectivity in Alzheimer's disease.* J Neurosci, 2007. **27**(4): p. 796-807.

113. Shankar, G.M., S. Li, T.H. Mehta, A. Garcia-Munoz, N.E. Shepardson, I. Smith, F.M. Brett, M.A. Farrell, M.J. Rowan, C.A. Lemere, C.M. Regan, D.M. Walsh, B.L. Sabatini and D.J. Selkoe, *Amyloid-beta*

protein dimers isolated directly from Alzheimer's brains impair synaptic plasticity and memory. Nat Med, 2008. **14**(8): p. 837-42.

114. Salminen, A., J. Ojala, A. Kauppinen, K. Kaarniranta and T. Suuronen, *Inflammation in Alzheimer's disease: amyloid-beta oligomers trigger innate immunity defence via pattern recognition receptors.* Prog Neurobiol, 2009. **87**(3): p. 181-94.

115. Broersen, K., F. Rousseau and J. Schymkowitz, *The culprit behind amyloid beta peptide related neurotoxicity in Alzheimer's disease: oligomer size or conformation?* Alzheimers Res Ther, 2010. **2**(4): p. 12.

116. http://www.nia.nih.gov.

117. Iurascu, M., C. Cozma, N. Tomczyk, J. Rontree, M. Desor, M. Drescher and M. Przybylski, *Structural characterization of beta-amyloid oligomer-aggregates by ion mobility mass spectrometry and electron spin resonance spectroscopy.* Anal Bioanal Chem, 2009. **395**(8): p. 2509-19.

118. Vlad, C., K. Lindner, C. Karreman, S. Schildknecht, M. Leist, N. Tomczyk, J. Rontree, J. Langridge, K. Danzer, T. Ciossek, A. Petre, M.L. Gross, B. Hengerer and M. Przybylski, *Autoproteolytic fragments are intermediates in the oligomerization/aggregation of the Parkinson's disease protein alpha-synuclein as revealed by ion mobility mass spectrometry.* Chembiochem, 2011. **12**(18): p. 2740-4.

119. O'Farrell, P.H., *High resolution two-dimensional electrophoresis of proteins.* J Biol Chem, 1975. **250**(10): p. 4007-21.

120. Chen, Z., F.A. Shamsi, K. Li, Q. Huang, A.A. Al-Rajhi, I.A. Chaudhry and K. Wu, *Comparison of camel tear proteins between summer and winter.* Mol Vis, 2011. **17**: p. 323-31.

121. de Laurentiis, A., M. Gaspari, C. Palmieri, C. Falcone, E. Iaccino, G. Fiume, O. Massa, M. Masullo, F.M. Tuccillo, L. Roveda, U. Prati, O. Fierro, I. Cozzolino, G. Troncone, P. Tassone, G. Scala and I. Quinto, *Mass spectrometry-based identification of the tumor antigen UN1 as the transmembrane CD43 sialoglycoprotein.* Mol Cell Proteomics, 2011. **10**(5): p. M111 007898.

122. Kosmides, A.K., K. Kamisoglu, S.E. Calvano, S.A. Corbett and I.P. Androulakis, *Metabolomic fingerprinting: challenges and opportunities.* Crit Rev Biomed Eng, 2013. **41**(3): p. 205-21.

123. Chen, T., J. Zhao, J. Ma and Y. Zhu, *Web Resources for Mass Spectrometry-based Proteomics.* Genomics Proteomics Bioinformatics, 2015.

124. Trimpin, S. and D.E. Clemmer, *Ion mobility spectrometry/mass spectrometry snapshots for assessing the molecular compositions of complex polymeric systems.* Anal Chem, 2008. **80**(23): p. 9073-83.

125. Ruotolo, B.T., J.L. Benesch, A.M. Sandercock, S.J. Hyung and C.V. Robinson, *Ion mobility-mass spectrometry analysis of large protein complexes.* Nat Protoc, 2008. **3**(7): p. 1139-52.

126. Ruotolo, B.T., S.J. Hyung, P.M. Robinson, K. Giles, R.H. Bateman and C.V. Robinson, *Ion mobility-mass spectrometry reveals long-lived, unfolded intermediates in the dissociation of protein complexes.* Angew Chem Int Ed Engl, 2007. **46**(42): p. 8001-4.

127. Woods, L.A., S.E. Radford and A.E. Ashcroft, *Advances in ion mobility spectrometry-mass spectrometry reveal key insights into amyloid assembly.* Biochim Biophys Acta, 2013. **1834**(6): p. 1257-68.

128. Zhong, Y., S.J. Hyung and B.T. Ruotolo, *Ion mobility-mass spectrometry for structural proteomics.* Expert Rev Proteomics, 2012. **9**(1): p. 47-58.

129. Vlad, C., M.I. Iurascu, S. Slamnoiu, B. Hengerer and M. Przybylski, *Characterization of oligomerization-aggregation products of neurodegenerative target proteins by ion mobility mass spectrometry.* Methods Mol Biol, 2012. **896**: p. 399-412.

130. Sahu, I.D., R.M. McCarrick and G.A. Lorigan, *Use of electron paramagnetic resonance to solve biochemical problems.* Biochemistry, 2013. **52**(35): p. 5967-84.

131. Moen, R.J., J.C. Klein and D.D. Thomas, *Electron paramagnetic resonance resolves effects of oxidative stress on muscle proteins.* Exerc Sport Sci Rev, 2014. **42**(1): p. 30-6.

132. Tochio, H. and M. Shirakawa, *[Structural analysis of proteins in living eukaryotic cells using magnetic resonance spectroscopy].* Yakugaku Zasshi, 2012. **132**(2): p. 185-93.

133. McHaourab, H.S., P.R. Steed and K. Kazmier, *Toward the fourth dimension of membrane protein structure: insight into dynamics from spin-labeling EPR spectroscopy.* Structure, 2011. **19**(11): p. 1549-61.

134. Jeschke, G. and S. Schlick, *Continuous-Wave and Pulsed ESR Methods*, in *Advanced ESR Methods in Polymer Research*. 2006, John Wiley & Sons, Inc. p. 1-24.

135. Jeschke, G., *Double Resonance ESR Methods*, in *Advanced ESR Methods in Polymer Research*. 2006, John Wiley & Sons, Inc. p. 25-51.

136. Robotta, M., C. Hintze, S. Schildknecht, N. Zijlstra, C. Jungst, C. Karreman, M. Huber, M. Leist, V. Subramaniam and M. Drescher, *Locally resolved membrane binding affinity of the N-terminus of alpha-synuclein.* Biochemistry, 2012. **51**(19): p. 3960-2.

137. Drescher, M., F. Godschalk, G. Veldhuis, B.D. van Rooijen, V. Subramaniam and M. Huber, *Spin-label EPR on alpha-synuclein reveals differences in the membrane binding affinity of the two antiparallel helices.* Chembiochem, 2008. **9**(15): p. 2411-6.

138. Susnea, I., B. Bernevic, M. Wicke, L. Ma, S. Liu, K. Schellander and M. Przybylski, *Application of MALDI-TOF-mass spectrometry to proteome analysis using stain-free gel electrophoresis.* Top Curr Chem, 2013. **331**: p. 37-54.

139. Walsh, D.M., A. Lomakin, G.B. Benedek, M.M. Condron and D.B. Teplow, *Amyloid beta-protein fibrillogenesis. Detection of a protofibrillar intermediate.* J Biol Chem, 1997. **272**(35): p. 22364-72.

140. Walsh, D.M. and D.J. Selkoe, *A beta oligomers - a decade of discovery.* J Neurochem, 2007. **101**(5): p. 1172-84.

141. Merrifield, R.B., *Solid-Phase Peptide Synthesis. 3. An Improved Synthesis of Bradykinin.* Biochemistry, 1964. **3**: p. 1385-90.

142. Made, V., S. Els-Heindl and A.G. Beck-Sickinger, *Automated solid-phase peptide synthesis to obtain therapeutic peptides.* Beilstein J Org Chem, 2014. **10**: p. 1197-212.

143. Masters, C.L., G. Simms, N.A. Weinman, G. Multhaup, B.L. McDonald and K. Beyreuther, *Amyloid plaque core protein in Alzheimer disease and Down syndrome.* Proc Natl Acad Sci U S A, 1985. **82**(12): p. 4245-9.

144. Weidemann, A., G. Konig, D. Bunke, P. Fischer, J.M. Salbaum, C.L. Masters and K. Beyreuther, *Identification, biogenesis, and localization of precursors of Alzheimer's disease A4 amyloid protein.* Cell, 1989. **57**(1): p. 115-26.

145. Glenner, G.G. and C.W. Wong, *Alzheimer's disease: initial report of the purification and characterization of a novel cerebrovascular amyloid protein.* Biochem Biophys Res Commun, 1984. **120**(3): p. 885-90.

146. Gettins, P., A.H. Beth and L.W. Cunningham, *Proximity of thiol esters and bait region in human alpha 2-macroglobulin: paramagnetic mapping.* Biochemistry, 1988. **27**(8): p. 2905-11.

147. Stoll, S. and A. Schweiger, *EasySpin, a comprehensive software package for spectral simulation and analysis in EPR.* J Magn Reson, 2006. **178**(1): p. 42-55.

148. Jameson, L.P., N.W. Smith and S.V. Dzyuba, *Dye-binding assays for evaluation of the effects of small molecule inhibitors on amyloid (abeta) self-assembly.* ACS Chem Neurosci, 2012. **3**(11): p. 807-19.

149. Biancalana, M. and S. Koide, *Molecular mechanism of Thioflavin-T binding to amyloid fibrils.* Biochim Biophys Acta, 2010. **1804**(7): p. 1405-12.

150. Iurascu, M.-I., C. Cozma, J. Langridge, N. Tomczyk, M. Desor and M. Przybylski, *Structural Characterization of Oligomer-Aggregates of _-Amyloid Polypeptide Using Ion Mobility Mass Spectrometry*, in *Ion Mobility Spectrometry - Mass Spectrometry*. 2010, CRC Press. p. 313-325.

151. Brown, M.A., K.D. Pile, L.G. Kennedy, A. Calin, C. Darke, J. Bell, B.P. Wordsworth and F. Cornelis, *HLA class I associations of ankylosing spondylitis in the white population in the United Kingdom.* Ann Rheum Dis, 1996. **55**(4): p. 268-70.

152. Reveille, J.D., *The genetic basis of ankylosing spondylitis.* Curr Opin Rheumatol, 2006. **18**(4): p. 332-41.

153. Nika, H., J. Lee, I.M. Willis, R.H. Angeletti and D.H. Hawke, *Phosphopeptide characterization by mass spectrometry using reversed-phase supports for solid-phase beta-elimination/Michael addition.* J Biomol Tech, 2012. **23**(2): p. 51-68.

154. Peri, S., H. Steen and A. Pandey, *GPMAW--a software tool for analyzing proteins and peptides.* Trends Biochem Sci, 2001. **26**(11): p. 687-9.

155. http://www.matrixscience.com. Available from: http://www.matrixscience.com/cgi/search_form.pl?FORMVER=2&SEARCH=PMF.

156. http://www.cgl.ucsf.edu/chimera. Available from: http://www.cgl.ucsf.edu/chimera.

157. Pettersen, E.F., T.D. Goddard, C.C. Huang, G.S. Couch, D.M. Greenblatt, E.C. Meng and T.E. Ferrin, *UCSF Chimera--a visualization system for exploratory research and analysis.* J Comput Chem, 2004. **25**(13): p. 1605-12.

7 APPENDIX

7.1 Abbreviations

°C	centigrade
3D	three-dimensional
Aβ	amyloid beta peptide
aa	aminoacid
AA	Alois Alzheimer
Ab	antibody
can	acetonitrile
AD	Alzheimer’s Disease
A-Gla	Alpha-galactosidase
APP	amyloid precursor protein
APS	ammoniumperoxodisulfat
CDR	complementarity determining region
CHCA	alpha-cyano-4-hydroxycinamic acid
CID	collision induced dissociation
CW	continuous wave
Da	dalton
DHB	dihydroxybenzoic acid
DMF	dimethylformamide
DTT	dithiothreitol
EA	ethanolamine

EDC	N-(3-dimethylaminopropyl)-N-ethylcarbodiimide (EDC)
EF	electrophoresis
e.g.	exempli gratia (for example)
ELISA	enzyme linked immunosorbent assay
EPR	electron paramagnetic resonance
ESR	electron spin resonance
ETD	electron transfer dissociation
ESI	electro-spray ionization
FA	formic acid
FD	Fabry Disease
Fmoc	9-Fluorenylmethoxycarbonyl
FT-ICR	fourier transform ion cyclotron resonance
G	gauss
h	hour
HLA	human leukocyte antigen
HPLC	high performance liquid chromatography
IAA	iodoacetamide
IMS	Ion mobility spectroscopy
M	molar (concentration)
mAb	monoclonal antibody
MALDI	Matrix assisted laser desorption ionization
MHC	major histocompatibility complex
min	minute
mM	milimolar
MS	mass spectrometry

MW	molecular weight
µM	micromolar
NCBInr	National Center for Biotechnology Information non-redundant (protein database)
NHS	N-hydroxysuccinimide
NMM	N-Methyl-morpholine
nm	nanometer
nM	nanomolar
ns	nanosecond
PAGE	polyacrylamide gel electrophoresis
PBS	phosphate buffer saline
pH	negative logarithm of H_3O^+ ions concentration
pI	isoelectric point
PyBOP	benzotriazol-1-yloxy-tris-pyrrolidinophosphonium-PF6
QCM	quartz crystal microbalance
RF	radio frequency
RP	reverse phase
s	second
SAW	surface acoustic wave
SDS	sodium dodecyl sulfate
SPPS	solid phase peptide synthesis
SPR	surface plasmon resonance
TCA	trichloroacetic acid
TEMED	N,N,N',N'-Tetramethylethylendiamine
TFA	trifluoroacetic acid

TFE	2,2,2-trifluoroethanol
ToF	time of flight
Tris	tris-(hydroxymethyl-) aminomethane
UV	ultra violet

7.2 Amino acids abbreviations

Name	Oen letter code	Three letter code	Monoisotopic mass (Da)
Alanine	A	Ala	71.037
Arginine	R	Arg	156.101
Asparagine	N	Asn	114.042
Aspartic acid	D	Asp	115.026
Cysteine	C	Cys	103.009
Glutamine	Q	Gln	128.058
Glutamic acid	E	Glu	129.042
Glycine	G	Gly	57.021
Histidine	H	His	137.058
Isoleucine	I	Ile	113.084
Leucine	L	Leu	113.084
Lysine	K	Lys	128.094
Methionine	M	Met	131.040
Phenylalanine	F	Phe	147.068
Proline	P	Pro	97.052
Serine	S	Ser	87.032
Threonine	T	Thr	101.047
Tryptophan	W	Trp	186.079
Tyrosine	Y	Tyr	163.063
Valine	V	Val	99.068